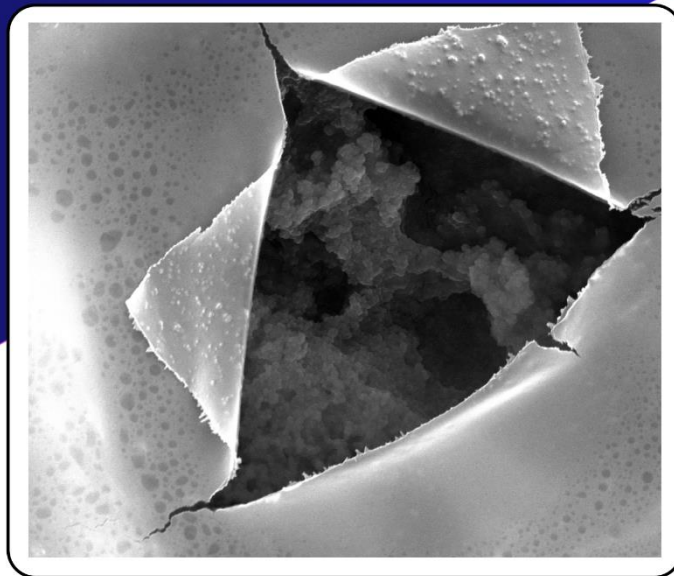


**Doctoral Thesis
2017**

**Photo-responsive
polymer nanocapsules**



Valentina Marturano

Photo-responsive Polymer Nanocapsules

Valentina Marturano

Academic Tutor:

Prof. Veronica Ambrogi

Co-tutor:

Dr. Pierfrancesco Cerruti

This dissertation is submitted for the degree of
Doctor in Philosophy

In

Materials and Structures Engineering

XXVIII cycle



University of Napoli "Federico II"

Department of Chemical, Materials and Production Engineering

April 2017

A Nadia

Fall in love with some activity, and do it! Nobody ever figures out what life is all about, and it doesn't matter. Explore the world. Nearly everything is really interesting if you go into it deeply enough. Work as hard and as much as you want to on the things you like to do the best. Don't think about what you want to be, but what you want to do.

Richard Feynman

Acknowledgements:

First of all, my deepest gratitude goes to my PhD supervisors, Prof. Veronica Ambrogi and Dr. Pierfrancesco Cerruti. They allowed me to embark on this journey, they guided me and pushed me to give the best of me, teaching me to face every challenge with enthusiasm and resolution. I am very grateful for the trust they placed in me and I feel very lucky to have shared with them these wonderful years.

I would like to acknowledge Prof. Marta Giamberini and Dr. Bartosz Tylkowski for their priceless collaboration and for the support and advice that they gave me in these years.

My sincere gratitude goes to Prof. Cosimo Carfagna, that allowed me to attend the laboratories of the Institute for Polymers, Composites and Biomaterials (IPCB-CNR) for my scientific activities. My sincere appreciation goes to all the researchers and students of IPCB-CNR for their friendship and scientific support. Special thanks go to Cristina del Barone, for her patience and dedication to her job and for her friendship.

For the past few years, the Synthesis Lab has become my second home and, among all the brilliant people that attend it, I cannot fail to mention Salvatore Mallardo, for his support and his warmth, Dr. Gabriella Santagata for her kindness and passion, and Dr. Giovanna Gomez D'Ayala for the strength she inspires in all people around her.

My gratitude goes to Dr. Mario Malinconico, Dr. Pietro Amodeo and to all members of MoSeF for introducing me to the wonderful world of scientific dissemination and for teaching me that scientific research does not make sense unless you share it.

I also want to thank my family: my parents that support me in all my choices, my grandmother Antonietta that is a steady example of dedication to our family, to my husband Pavel that knows how to brighten the darkest of days and most of all to my daughter, Nadia, because she is able to teach me something new every day.

My purest gratitude goes to those friends that over the years have become key part of my family: Milly, a friend and a sister, in each of my accomplishments there is a part of hers. Vincente, Francesco, Sara, Michele and Ludovica, for being present with your laughter and affection. Rachele and Peppe Lama, two of the most wonderful people in the world, with whom I shared this journey and so much more. Federico, who is able to be beside me in the darkest days as well as during the loudest laughter. Martin e Krzysztof, whom I consider brothers, they hold a very special place in my heart and are able support me even from far apart. Saritta for her kindness and cheerfulness, which make her irreplaceable.

Finally, for financial support I acknowledge the Italian Ministry for University and Research (in the frame of the projects: Safe & Smart - CTN01_00230_248064 and PRIN 201288JKYY) and University of Napoli Federico II for founding my PhD scholarship.

Table of contents:

CHAPTER 1 – General Introduction and Objectives

1.1.	The Era of Colloidal Particles and Nanotechnology	2
1.2.	History of Encapsulation	4
1.2.1.	Carbonless copy-paper	5
1.2.2.	Electronic-ink	6
1.2.3.	Self-healing materials	6
1.3.	Controlled Release	8
1.4.	Objectives	9
1.5.	References	11

CHAPTER 2 – Light-responsive Polymer Micro and Nano-capsules

<i>Abstract</i>	15
2.1. Introduction	16
2.2. Interfacial Methods for Capsules Formation	18
2.2.1. Emulsion Polymerization	19
2.2.2. Phase Inversion Precipitation	22
2.3. Templating Methods	22
2.3.1. Layer-by-Layer (LbL) Using Polyelectrolytes	23
2.3.2. Layer-by-Layer (LbL) Using Host-Guest Systems	27
2.3.3. Other Templating Methods	29
2.4. Self-Assembly Methods	32
2.4.1. Block Copolymers Self-Assembly	32
2.4.2. Liposomes	34
2.5. Characterization Methods of Photo-Responsive Capsules	38

2.6. Conclusions	39
2.7. References	41

CHAPTER 3 – Photo-responsive Polymer Nanocapsules

<i>Abstract</i>	53
3.1. Introduction	54
3.2. Experimental	56
3.2.1. Materials	56
3.2.2. Preparation of o/w miniemulsions	57
3.2.3. Synthesis of polyamide nanosized capsules	57
3.2.4. Methods of characterization	59
3.3. Results and discussion	60
3.3.1. Emulsion characterization	60
3.3.2. Nanocapsules characterization	64
3.3.3. Photo-responsiveness and release kinetics of the nanocapsules	67
3.4. Conclusions	71
3.5. References	73

CHAPTER 4 – Light-induced Release of Essential Oils from Polymer Nanocapsules

<i>Abstract</i>	81
4.1. Introduction	82
4.2. Experimental	84
4.2.1. Materials	84
4.2.2. Choice of natural oils as organic phase	85

4.2.3. Preparation of Nanocapsules from o/w emulsion	86
4.2.4. Methods of characterization	88
4.2.4.1. Size and morphology	88
4.2.4.3. EOs release kinetics	90
4.2.4.4. C6 release kinetics	91
4.2.4.5. Cytotoxicity and Uptake tests	91
4.3. Results and discussion	92
4.3.1. Selection of essential oils	92
4.3.2. Nanocapsules characterization	93
4.3.2.1 Nanocapsules size and morphology	93
4.3.2.2 Encapsulation efficiency	95
4.3.3. Photo-responsiveness and release kinetics	96
4.3.3. Cellular uptake and cytotoxicity	100
4.4. Conclusions	101
4.5. References	103

**CHAPTER 5 – Photo-triggered Polymer Capsules Loaded with Antimicrobial Essential Oils:
An Application in Active Food Packaging.**

<i>Abstract</i>	110
5.1. Introduction	111
5.2. Experimental	113
5.2.1. Materials	113
5.2.2. Preparation and surface treatments of PE and PLA films	113
5.2.3. Coating of PE and PLA films with nanocapsules	114
5.2.4. Release of EO from nanocapsules-coated films	114
5.3. Results and discussion	115

5.3.2. Characterization of the treated polymer films	115
5.3.4. Characterization of nanocapsules-coated films	116
5.3.5. Release from nanocapsules-coated films	118
5.3.6. Antibacterial properties.	119
5.4. Conclusions	121
 CHAPTER 6 –Visible-light Responsive Azobenzene and Future Applications	
6.1. Introduction	127
6.2. Experimental	128
6.2.1. Material	128
6.2.2. Synthesis of 4,4'-bis(carboxy)-2,2'-dimethoxyazobenzene	128
6.2.3. Characterization of visible light-sensitive azobenzene monomer	129
6.3. Results and Discussion	129
6.4. Conclusions and future applications	132
6.5. References	134
 CHAPTER 7 –General Conclusions	
 Appendix A –List of Figures and Tables	
Figures	140
Tables	144
 Appendix B –List of Publications	
Directly related with the thesis	145
 Appendix C –Congresses and Contributions	
Congresses	147
Chapters in Books	148



CHAPTER 1

General Introduction and Objectives

1.1. The Era of Colloidal Particles and Nanotechnology

Colloid science is the study of dispersions of one phase in another (e.g. oil in water or water in oil), the dispersed phase is typically characterized by dimensions ranging from few nanometers to a few tens of micrometers. In the last five decades, industrial and academic research has achieved a tremendous progress in colloid science and its practical applications show no signs of waning. Colloidal particles can be found in many consumer goods and high-technology products: such as milk, mayonnaise, paints, inks and some lubricants [1]. Colloidal science often breeds with nanotechnology to produce highly performing delivery systems: nanoparticles (NPs), that usually serve as either reservoirs or carriers for an active material. NPs are typically divided in two classes: organic and inorganic NPs as schematized in Figure 1.1.

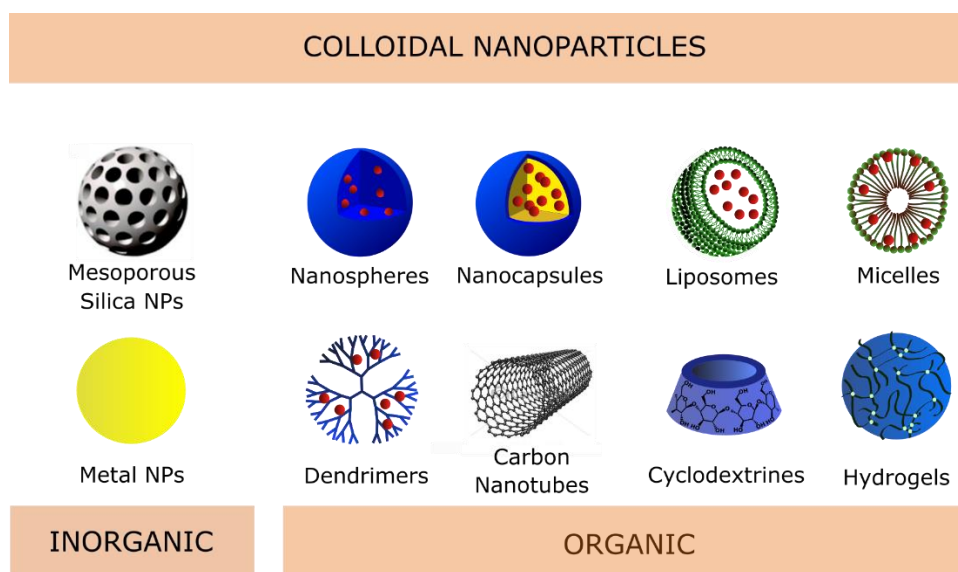


Figure 1.1. – Schematic representation of different types of colloidal nanoparticles.

Thanks to their reduced particle size, inorganic nanoparticles possess previously unexplored chemical, physical and biological properties [2]. Metallic NPs and mesoporous silica systems are classified as inorganic NPs. The former are made of metal elements in the nanometer range and are usually used for magnetic resonance imaging or as contrast agents, the latter are by far the most

promising, having a tunable particle size (50-300 nm), a high surface area and uniform pore size distribution [3].

The class of organic NPs includes: nanospheres, nanocapsules, polymeric micelles, liposomes, dendrimers, carbon nanotubes, cyclodextrins and hydrogels [4, 5].

- 1) Polymeric nanospheres are matrix-type solid colloidal particles. Active ingredients can be dissolved, entrapped, encapsulated, chemically bound or absorbed by the polymer matrix [6]
- 2) Nanocapsules are *nanovesicular* systems in which drugs are enclosed to a cavity, surrounded by a polymer membrane or coating. Active substance can be in solid or liquid form as well as a molecular dispersion in the cavity [6].
- 3) Liposomes are spherical shaped artificial vesicles which are produced by natural non-toxic phospholipids and cholesterol. Liposome properties may be changed depending on their lipid composition, size, surface charge and preparation method.
- 4) Polymeric micelles result from the self-assembly in water of amphiphilic copolymers into a core-shell structure. The hydrophobic core can act as a reservoir of hydrophobic drugs while the hydrophilic corona provides water solubility and colloidal stability [7]
- 5) Dendrimers are monodisperse symmetric macromolecules with highly branched structures around an inner core. Their structures are comprised of three components: a focal core, several layered building blocks which are formed by repeating units, and functional groups on the periphery. Because of their non-polar cavities, they can encapsulate hydrophobic molecules. In addition, they have many positively and negatively charged functional groups on their surface which offer the opportunity to easily attach to oppositely charged molecules. [8]
- 6) Carbon nanotubes (CNTs) are attractive systems because of their excellent mechanical, electrical and surface properties. Surface properties, size and shapes of CNTs are the main factors which affect interactions with cells. They need to be functionalised due their

insolubility in most solvents and their cytotoxic properties, thereby increasing CNTs' solubility and biocompatibility [9].

- 7) Cyclodextrins (CD) are cyclic oligosaccharides characterized by a hydrophilic outer surface, and able to load guest molecules in their lipophilic inner cavity via non-covalent inclusion interactions. As well as other nanocarriers, the use of CD can increase drug solubility, bioavailability, safety, and stability of drug formulations [10].
- 8) Hydrogels can be defined as three-dimensional hydrophilic structure networks which are formed chemically or physically. Active molecules can be loaded in their porous structure which can be controlled by the density of cross-links [11].

Among several promising nanoparticle systems listed above, polymers usually offer the most versatile and custom designed applications. Polymers, in fact, can carry different functional groups which can fulfill a function on the molecular level. Additionally, unlike ceramics and metals, polymers are permeable [12]. This property can be employed to achieve the transport of molecules between two environments divided by a polymer membrane. In colloid science, one of the most successful systems is the construction of core-shell compartments in the form of micro- to nano- capsules in which an inner core is entrapped in a polymer shell. [13].

1.2. History of Encapsulation

Like some of the most brilliant inventions in history, the process of encapsulating a cargo material inside a solid shell was inspired by nature. Eggs, for instances, are the most common example of encapsulation in our every-day life: a calcium carbonate hard shell, stabilized by a protein matrix, confines yolk and albumen, and when the egg has been fertilized it protects the embryo until it is able to survive on its own. Nowadays, micro and nano-capsules are employed in many commodity and

specialty applications, such as medicine, healthcare and household products, bioreactors, etc, as represented in Figure 1.2.

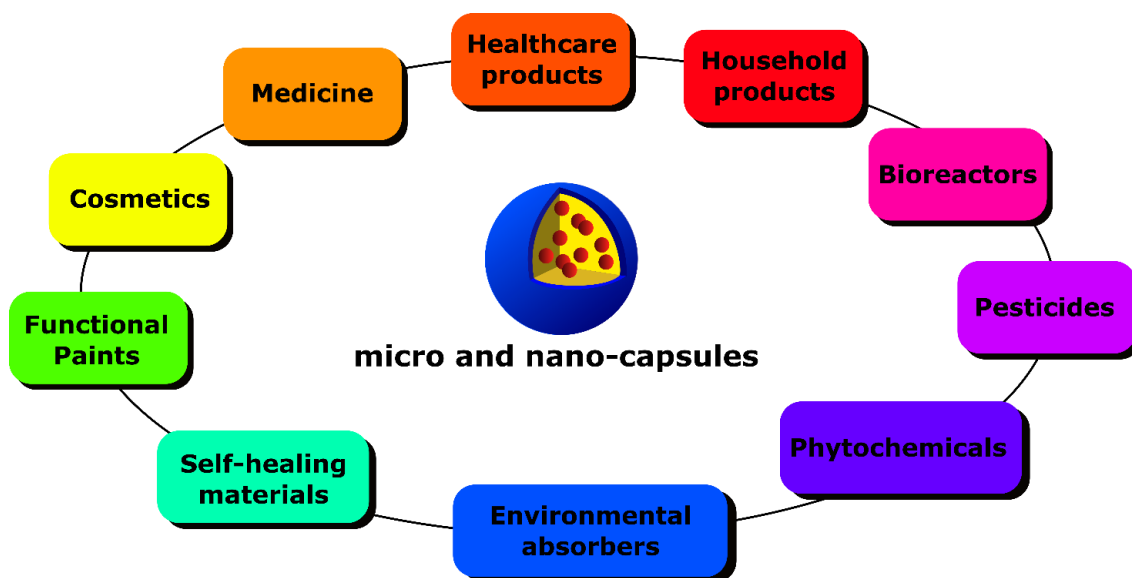


Figure 1.2. – Schematization of the application of micro and nanocapsules.

In the following, several successful applications of micro and nanoencapsulation are described.

1.2.1. Carbonless copy-paper

One of the first documented example of application of microencapsulation dates to the mid-1960s when microcapsules-based copy paper was commercialized by 3M company [14]. As represented in Figure 1.3, a layer of microcapsules, containing an invisible ink, was deposited on the *coated back* (CB) sheet, while *coated front* (CF) sheet was coated with a developer. The shear force applied on the CB when writing, provokes the disruption of the capsules and the release of the colorless-ink that, reacting with the developer, produces color.

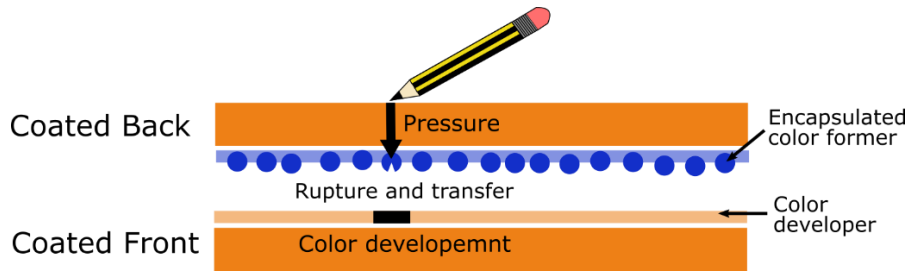


Figure 1.3. – Schematization of a two-sheet copying paper.

1.2.2. *Electronic-ink*

In a more recent application, microcapsules are employed in electronic-inks (E-inks) for a novel class of displays where switchable contrast is achieved by the electro-migration of highly scattering or absorbing microparticles (in the size range 0.1–5 μm) [15]. The display is constituted of a layer of transparent microcapsules (Figure 1.4) which contain positively charged white pigments and negatively charged black pigments dispersed in a transparent oil. The contrast on the display is produced by punctual changes in the polarity on the bottom electrodes layer by changing the polarity.

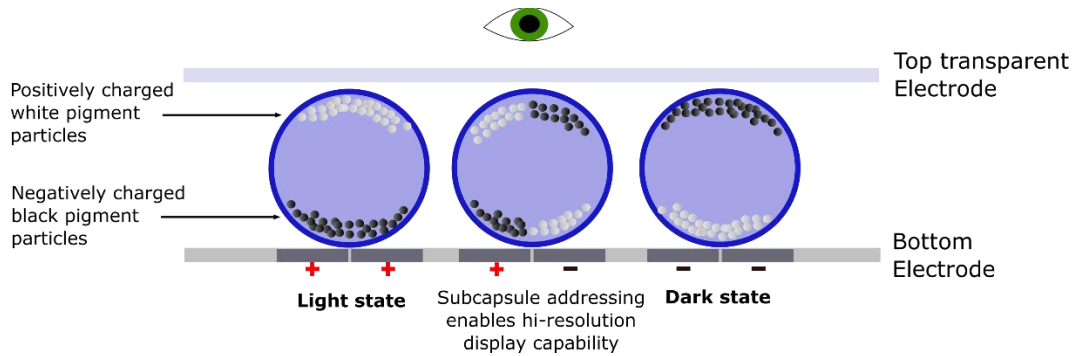


Figure 1.4. – Schematization of microcapsules-based e-ink.

1.2.3. *Self-healing materials*

Self-healing materials are a relatively new class of smart materials that possess the ability to fully or partially recover a functionality that had been adversely effected by operational use [16]. Such materials are capable of assessing their internal damage and performing self-repair leading to

extended service life with good mechanical properties. Polymeric materials are especially susceptible to weathering phenomena, caused by moisture, temperature variations and solar radiations, and leading to degradation and weakening of the artifact. A self-healing material undergoing mechanical failure, for example a crack propagation, is able to relieve geometrical stress concentrations initiated by the crack. These features are typically achieved by crack closure, performed using shape memory alloys or shape memory polymers, or crack-filling processes, potentially achieved by re-bonding the material using cross-linkable polymers. The process of crack-filling involves a method for the storage of a healing agent, a process for the transport of the healing agent and a suitable method for initiation of repair. As depicted in Figure 1.5 the storage of the healing agent may be accomplished by the use of spherical microcapsules. The transport is envisioned to occur by local stresses, which would initiate the rupture and release of the healing agent and flow owing to capillary action. The repair would occur by the polymerization of the healing agent utilizing an embedded catalyst in the matrix.

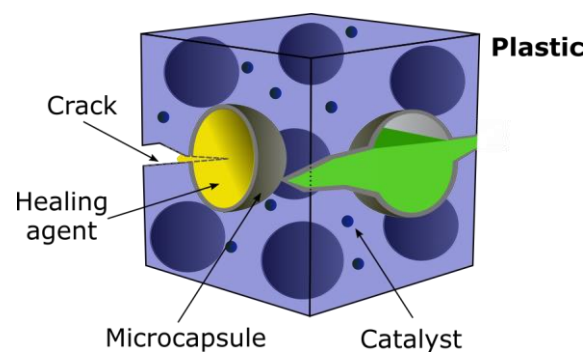


Figure 1.5. – Internal structure of a microcapsules based self-healing material.

Considering the few applications described above it results evident that the encapsulation of the core material provides several advantages if compared to the use of bulk material. In fact, encapsulation:

- physically confines the core material in a solid reservoir,
- reduces the core material reactivity towards the external environment,

- hinders the degradation of the core material (most typically caused by moisture, light and oxygen,
- decreases its evaporation rate to minimize losses,
- improves the workability and processing of core materials, i.e. liquids can be treated as solids, promoting mixing,
- promotes safety of the encapsulated material,
- masks its taste and odor,
- and releases the encapsulation material upon an external stimulus.

1.3. Controlled Release

Regardless of the application, controlled release of payloads is the dominating function of micro and nanocapsules. The term “controlled release” includes a range of different release profiles and mechanisms such as targeted release, triggered release, and sustained (or extended) release. In general, to achieve efficient and reliable controlled release the capsules must meet two requirements

- 1) to prevent the non-controlled leakage of the cargo material in release medium, and
- 2) to ensure that the shell materials adequately promote the release of the payload in response to an external stimulus.

In Figure 1.6. the two main release mechanisms for an encapsulated core material are schematized. An immediate release is achieved when capsule shell is disrupted by melting, chemical dissolution or application of compressive or shear forces. For example, egg shell can break and the encapsulated yolk and albumen are immediately released. However, the final application may require the delivery of an active agent in a specific site and over a precise amount of time, for example, in the dosage of an anticancer encapsulated drug. In this case, encapsulation technologies greatly benefit from the use of a special class of materials, called *smart*, that are able to change their intrinsic properties as a

consequence of a particular triggering factor. Capsule shell can be designed to provide a time-controlled and site-specific release of the core material. The release is obtained exploiting the porosity and permeability of the shell or triggering modifications in the shell morphology by application of external *stimuli* (electric or magnetic fields, pH, heat, radiation, etc.) [17].

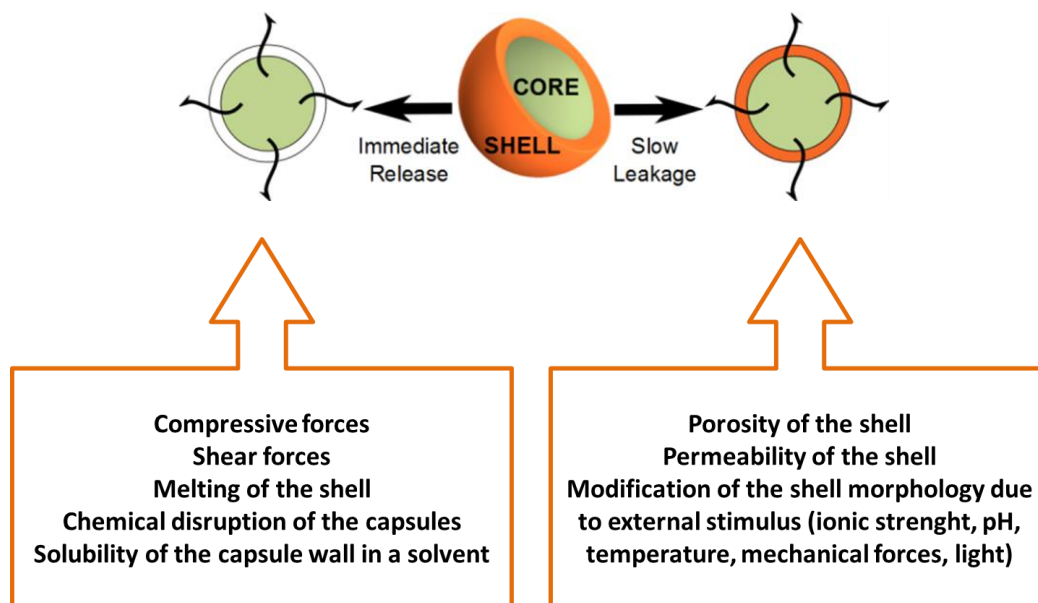


Figure 1.6. – Release mechanisms of core-shell capsules.

1.4. Objectives

The main objective of this dissertation was to report on the feasibility and the reliability of light-responsive polymeric nanocapsules for the delivery of active natural molecules. A miniemulsion polycondensation procedure was employed to perform the *in-situ* synthesis of the capsules shell: a polyamide containing azobenzene moieties in the main chain. The presence of azobenzene moieties in the polyamide backbone contributes the photo-responsive behavior of the *smart* shell. In fact, when irradiated with UV light ($\lambda_{\text{max}} = 360 \text{ nm}$) azobenzene undergoes a *trans-cis* isomerization that results

in adjustments in the polymer conformation and consequent release of the encapsulated material. The work is divided as follows:

Chapter 2 provides a wide review on light-responsive micro and nanocapsules systems, with a special focus on their preparation techniques and characterization.

Chapter 3 reports on the preparation and characterization of photo-responsive polyamide nanocapsules obtained *via* interfacial polycondensation in o/w miniemulsion. These systems provide the proof of concept for the feasibility and reliability of the nanoencapsulation and the release mechanism.

Chapter 4 reports on the selection of suitable natural oil as substitute for toluene in the nanocapsules preparation. Moreover, the morphology and release behavior of photo-responsive nanocapsules loaded with basil and thyme essential oil is also addressed.

Chapter 5 reports on the application of photo-responsive nanocapsules in active food packaging systems. Traditional packaging plastic materials, PLA and PE, were coated with essential oil-loaded nanocapsules and tested as active antimicrobial packaging.

Chapter 6 describes the synthesis and characterization of a modified azobenzene in which the isomerization wavelength is shifted in the visible range (red), opening the road to a wide range of new applications for this class of nanocapsules.

1.5. References:

1. Cosgrove, T., *Colloid Science: Principles, Methods, and Applications*. 2 ed.; Wiley-VCH: 2010.
2. Safari J, Zarnegar Z. Advanced drug delivery systems: nanotechnology of health design: a review. *J Saudi Cheml Soc* 2014 Apr (18):85-99.
3. Jadhav, S.A., 2014. Incredible pace of research on mesoporous silica nanoparticles. *Inorganic Chemistry Frontiers*, 1(10), pp.735-739.
4. Singh, R. and Lillard, J.W., 2009. Nanoparticle-based targeted drug delivery. *Experimental and molecular pathology*, 86(3), pp.215-223.
5. Sahoo SK, Labhasetwar V. Nanotech approaches to drug delivery and imaging. *Drug Discov Today* 2003 Dec;8(24):1112-20.
6. Letchford, K. and Burt, H., 2007. A review of the formation and classification of amphiphilic block copolymer nanoparticulate structures: micelles, nanospheres, nanocapsules and polymersomes. *European journal of pharmaceutics and biopharmaceutics*, 65(3), pp.259-269.
7. Dong, J., Wang, Y., Zhang, J., Zhan, X., Zhu, S., Yang, H. and Wang, G., 2013. Multiple stimuli-responsive polymeric micelles for controlled release. *Soft Matter*, 9(2), pp.370-373.
8. Ambade, A.V., Savariar, E.N. and Thayumanavan, S., 2005. Dendrimeric micelles for controlled drug release and targeted delivery. *Molecular pharmaceutics*, 2(4), p.264.
9. Hilder, T.A. and Hill, J.M., 2008. Carbon nanotubes as drug delivery nanocapsules. *Current Applied Physics*, 8(3), pp.258-261.
10. Challa, R.; Ahuja, A.; Ali, J.; Khar, R.K. Cyclodextrins in drug delivery: An updated review. *AAPS Pharm. Sci. Technol.* 2005, 6, E329–E357.
11. Lee SC, Kwon IK, Park K. Hydrogels for delivery of bioactive agents: a historical perspective. *Adv Drug Deliv Rev* 2013 Jan;65(1):17-20
12. Comyn, J., *Polymer permeability*. Springer Science & Business Media: 1985.

13. Mora-Huertas, C.E., Fessi, H. and Elaissari, A., 2010. Polymer-based nanocapsules for drug delivery. *International journal of pharmaceutics*, 385(1), pp.113-142.
14. Matson, G.W., Minnesota Mining & Mfg, 1970. Microcapsule-containing paper. U.S. Patent 3,516,846.
15. Comiskey, B., Albert, J.D., Yoshizawa, H. and Jacobson, J., 1998. An electrophoretic ink for all-printed reflective electronic displays. *Nature*, 394(6690), pp.253-255.
16. Bekas, D.G., Tsirka, K., Baltzis, D. and Paipetis, A.S., 2016. Self-healing materials: a review of advances in materials, evaluation, characterization and monitoring techniques. *Composites Part B: Engineering*, 87, pp.92-119.
17. Alvarez-Lorenzo, C. and Concheiro, A. eds., 2013. *Smart materials for drug delivery (Vol. 1)*. Royal Society of Chemistry.



CHAPTER 2

Light-responsive Polymer Micro and Nano-capsules

Valentina Marturano, Pierfrancesco Cerruti, Marta Giamberini,

Bartosz Tylkowski and Veronica Ambrogi

Polymers 2017, 9(1), 8

Abstract:

A significant amount of academic and industrial research efforts are devoted to the encapsulation of active substances within micro- or nanocarriers. The ultimate goal of core-shell systems is the protection of the encapsulated substance from the environment, and its controlled and targeted release. This can be accomplished by employing “stimuli-responsive” materials as constituents of the capsule shell. Among a wide range of factors that induce the release of the core material, we focus herein on the light stimulus. In polymers, this feature can be achieved introducing a photo-sensitive segment, whose activation leads to either rupture or modification of the diffusive properties of the capsule shell, allowing the delivery of the encapsulated material. Micro- and nano-encapsulation techniques are constantly spreading towards wider application fields, and many different active molecules have been encapsulated, such as additives for food-packaging, pesticides, dyes, pharmaceuticals, fragrances and flavors or cosmetics. Herein, a review on the latest and most challenging polymer-based micro- and nano-sized hollow carriers exhibiting a light-responsive release behavior is presented. A special focus is put on systems activated by wavelengths less harmful for living organisms (mainly in the ultraviolet, visible and infrared range), as well as on different preparation techniques, namely liposomes, self-assembly, layer-by-layer, and interfacial polymerization.

2.1. Introduction

In recent years, a growing interest has been focused on micro- and nano encapsulation due to their fruitful applications in controlled release of drugs [1], active agents [2], catalysts [3], and paints [4], as well as in synthetic nano-reactors engineering [5]. Academic and industrial research is particularly interested in so-called “environmentally responsive” materials, able to respond to an external stimulus (e.g., temperature, pH, light, electric or magnetic field) by modifying one or more of their intrinsic properties. For their adaptive features, these materials are often called smart [6,7]. One of the most challenging aspects of micro- and nano-encapsulation is the obtainment of a controlled and modulated release of the encapsulated—or core—material that can be achieved using smart materials as components of the capsule shell [8].

The design and development of high-sensitive systems, able to smartly recognize an external triggering factor and to respond by modifying their own structure, is the ultimate purpose of scientists all over the world. For this purpose, polymeric materials are particularly suitable for technical applications because they are versatile and their properties can be easily tailored depending on the final use. Many external stimuli, such as pH [9], temperature [10,11], biological molecules [12], and redox reactions [13] have been employed to effect capsule permeability or induce capsule disruption, enabling the release of the encapsulated material. Light (infrared, UV radiation or simply sunlight) is certainly the most compelling external stimulus, because it can be delivered without direct contact, thus representing one of the few remote-control triggering factors available [14]. Like many promising technologies, photo-responsive systems have been inspired by nature, which has evolved many complex biological systems able to exploit light as an external source of energy and information. For example, the light-induced cis–trans isomerization of the retinal molecule triggers a number of events, including a change in the conformation of the opsin protein to which is bound, leading to a neural signal and ultimately

to the perception of light [15]. Mimicking natural structures, photo-responsive polymers can be obtained introducing photo-sensitive moieties in the polymeric backbone or in the side chains.

Among the best performing photo-sensitive molecules, azobenzene [16], stilbene [17], and spiropyrans [18] stand out. The photoactivity of each of these functional groups is based on the existence of two interconvertible isomers. Upon light irradiation, typically in the ultraviolet range, the molecules undergo a conformational rearrangement. In the case of azobenzene and stilbene, this alteration is expressed by variations in the molecular symmetry from a thermally stable trans (E) orientation to a less favorable cis (Z) orientation (Figure 2.1.a,b) [19]. In spiropyrans, the irradiation induces a ring-opening reaction that leads to the formation of the isomeric merocyanine form, as shown in Figure 2.1.c [18].

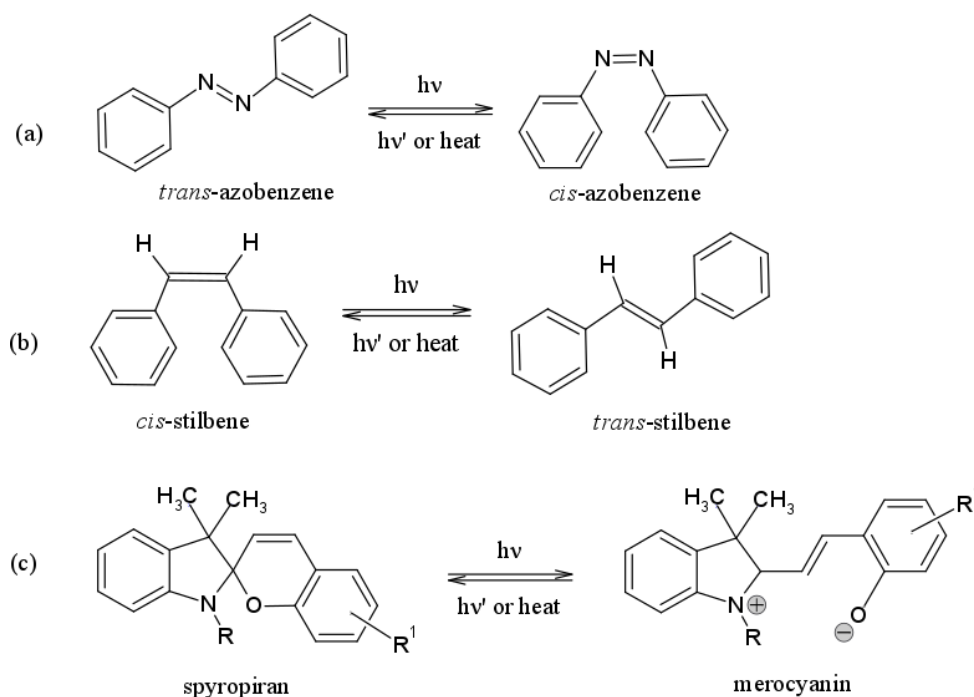


Figure 2.1. – Photo-isomerization mechanism of photochromic molecules: (a) azobenzene; (b) stilbene; and (c) spiropyrane.

One of the most interesting features of such photochromic materials is that isomerization is usually accompanied by molecular changes in physical properties such as polarity, viscosity and absorbance as well as macroscopic changes in material properties such as thickness, wettability and stability

[20]. The presence of photo-responsive moieties in the capsule shell can therefore affect permeability of capsules or even lead to their disruption [21].

A key factor to take into account when designing photo-responsive micro- and nanocapsule systems is the wavelength of the light used to trigger the release. For outdoor use or other applications in which direct contact between light and capsules is granted, it is theoretically possible to employ any wavelength required by the photochromic materials that constitute the capsules shell. However, with regard to biomedical applications, the skin penetration depth of the light source involved in the release is the factor that determines the appropriate use of the capsules. The optical behavior of human skin upon light irradiation has been vastly studied and reviewed [22]. UV and visible light are reported having short penetration (few micrometers) depth and are most suitable for topical uses; on the contrary, near infrared light has a higher skin penetration depth of few millimeters and it could therefore be employed in internal delivery applications.

This review intends to give an overview on recent advances in the preparation of light-responsive polymeric capsules. Different preparation technologies will be discussed in detail, including interfacial methods (interfacial polymerization and phase inversion precipitation), template methods, and self-assembly methods. Capsules properties such as size, morphology and release behavior will also be described, with a view on the envisaged target applications.

2.2. Interfacial Methods for Capsules Formation

In interfacial methods, polymer capsules shell forms at the interface between two immiscible liquids. The first reaction at a liquid-liquid interface was performed in 1883 by Schotten and Baumann [23,24]. Since then, simple and versatile interfacial reactions, such as polycondensation, have been employed to overcome the challenging procedures in bulk or melt [25]. Interfacial polycondensation method is nowadays one of the most performing for in-situ formation of capsule shell [26]. Further, the interface between two immiscible liquids can also be used to precipitate a

preformed polymer that will constitute the capsule shell [27]. In the following, the encapsulation at liquid–liquid interface with both polymerization and polymer precipitation will be discussed.

2.2.1. Emulsion Polymerization

Interfacial polymerization has been widely described in literature, and used for the realization of thin films [28] and particles [29]. This technique can also be employed for the preparation of micro- and nanocapsules [30,31] when supported by an emulsification step. An emulsion is defined as a dispersed system of liquid droplets (dispersed phase) in another, non-miscible liquid (continuous phase), stabilized by means of one or more surfactant agents. In the preparation of core–shell structures, the most performing interfacial reactions are polycondensation and polyaddition due to their simple mechanism, fast kinetics and high yields [26,32]. The polycondensation reaction occurs between different multifunctional monomers, either dissolved in the droplet suspension or in the continuous phase. The monomers react at the interface of the emulsion droplets forming the primary membrane, and the polymerization reaction advances until the depletion of one of the monomers. The typical hollow structure is obtained when the formed polymer is not soluble in the core material [31]. The common approach to obtain a photo-responsive shell membrane is employing photochromic monomers in the polycondensation reaction. For example, Tytkowski et al. [33] proposed a new approach for the preparation of liquid crystalline polyamide microcapsules containing azobenzene mesogens in the main chain. The triggered release of the encapsulated β -carotene was successfully performed by irradiating the capsules with 365 nm UV-light. At this wavelength, trans–cis photo-isomerization of azobenzene occurs, leading to major rearrangements in the macromolecules conformation that eventually result in the release of the encapsulated material.

In order to scale the dimensions of the capsules down to the nanometer range, the polycondensation reaction described above has been combined with a miniemulsification step.

Miniemulsions are a special class of emulsions, produced via high-energy homogenization (e.g., high shear stirring or ultrasonication), stabilized against coalescence and molecular diffusion degradation, and characterized by a narrow droplet distribution [32]. Marturano et al. [34] successfully reported the preparation of photo-responsive polyamide nano-sized capsules. The authors described how simple miniemulsion parameters, such as surfactant type and concentration affect key final properties, such as capsules dimension and release behavior. Release experiments of fluorescent probe molecule coumarin-6 (C6) confirmed the successful light-triggered release. Interestingly, dynamic light scattering (DLS) measurements demonstrated that the average diameter of the capsules significantly increased on UV exposure due to the rearrangement of the polyamide shell from a “closed” to a more “open” conformation, as depicted in Figure 2.2.2

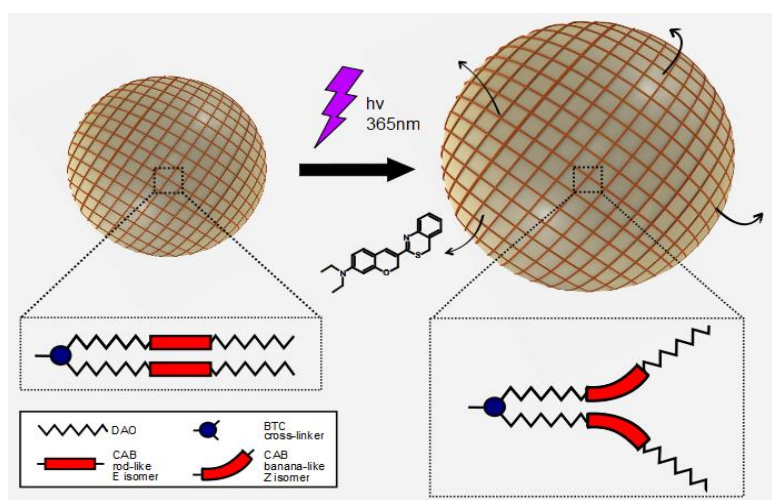


Figure 2.2 – Schematization of the C6 release from photo-responsive polymer nanocapsules as depicted by Marturano et al. [34]. Reproduced with permission from Elsevier.

Micro- and nanocapsules described above can meet the target of many specific applications, depending on their size and release profile, and serve as carriers for the encapsulation and release of different active agents. For example, Bizzarro et al. [35] reported the successful encapsulation and release of cumin and basil essential oils.

One of the great advantages of the described systems is the formation of robust capsules. The release of the core material occurs by leakage as a consequence of changes in shell permeability, without compromising shell integrity. This mechanism makes capsules safer for biological and medical applications, differently from systems where fragments derived from shell disruption can possibly contaminate target environment. On the other hand, one of the main drawbacks is the use of UV light, since this wavelength range has limited use in biological in vivo applications [36] and its concentration in sunlight is too scarce to be employed in agricultural or packaging applications. Beharry et al. [37] and Wegner [38] demonstrated how the incorporation of electron-donating groups in ortho or para position on the azo moiety can dramatically red-shift the photoswitching wavelength. Taking advantage of this work, Tylkowski et al. [39] were able to synthesize modified polyamide microcapsules shell containing ortho-substituted azobenzene moieties. It was shown that this modification led to an increase in shell permeability and release of core material under visible light irradiation.

A new frontier in the preparation of polymeric capsules is the use of microfluidic systems in which low volumes of fluids are processed through automatic and high-yield mechanism to obtain narrowly distributed droplets [40]. For example, interfacial polymerization reactions have been successfully performed in microfluidic devices [41]. Recently, Zeng et al. [42] reported the self-assembly of photo-responsive reversibly cross-linked hydrophilic and hydrophobic copolymers that can be controllably brought together at the water-chloroform interface of a microfluidic droplet. The cross-linking agent consists in a ternary host-guest complex containing azobenzene, whose UV-triggered trans-cis isomerization leads to the reversible disruption of the supramolecular assembly and consequent release of the cargo material.

An alternative approach to obtain photo-responsive microcapsules is employing metal or metal oxide nanoparticles acting as light absorbers. Chen et al. [43] obtained polystyrene microcapsules via Pickering emulsion polymerization using modified SiO₂ and TiO₂ nanoparticles

as Pickering agents. The release of the encapsulated material was achieved by degradation of the polymeric shell caused by the photocatalytic activity of TiO₂ nanoparticles [44].

2.2.2. Phase Inversion Precipitation

As mentioned before, an alternative approach to the synthesis of polymeric carriers is the use of preformed polymers for the capsules shell. Bogdanowicz et al. [45] successfully employed a novel photo-responsive polymer, containing photochromic stilbene moieties in the main chain, poly(α -methylstilbenesebacate-co- α -methylstilbeneisophthalate) (P4), as shell material for vanillin loaded microcapsules. The capsules preparation was based on phase-inversion precipitation procedure, previously optimized by Peña et al. [46]. Using a nozzle device connected to compressed air flow, a homogeneous polymer solution was broken into microdroplets and sprayed in a coagulation bath containing a non-solvent. Precipitation of the polymer at the interface of each droplet was caused by exchange of solvent and non-solvent molecules in contact with the polymer. The authors hypothesized that the overall change in the shell permeability may be due to cooperative rearrangements of the polymeric chains induced by the photo-isomerization of the photo-responsive α -methylstilbene.

2.3. Templating Methods

This section intends to include different examples of micro- and nanocapsules formed via deposition of polymer material on colloidal sacrificial particles serving as template for the formation of hollow structures. The most acknowledged templating method is the layer-by-layer (LbL) approach, based on the consecutive deposition of interacting polymers on a sacrificial template particle which can be removed at the end of the process [47].

2.3.1. Layer-by-Layer (LbL) Using Polyelectrolytes

A wide variety of LbL capsules can be found in literature [48,49], however the vast majority of LbL capsules has been prepared using polyelectrolytes. The procedure, schematized in Figure 2.3, involves alternating deposition of positively and negatively charged polyelectrolytes onto the template, where the driving force for the assembly is the electrostatic interaction. After deposition, polymers can be cross-linked and, finally, hollow capsules are obtained by selective etching of the inorganic template [50].

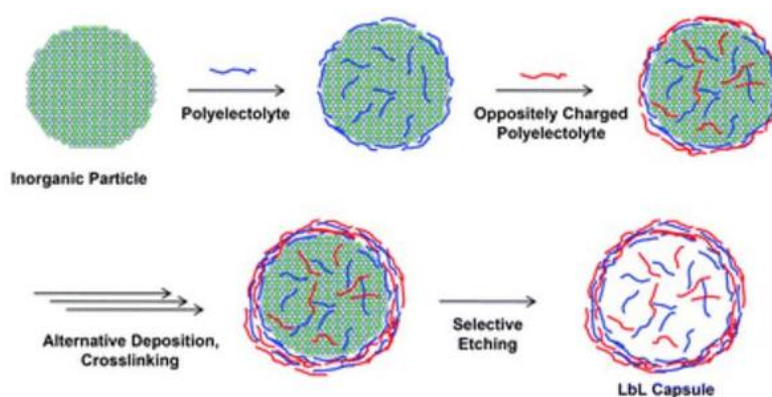


Figure 2.3. – Formation of polyelectrolyte based layer-by-layer nanocapsule as schematized by Yoon et al. [50]. Reprinted with permission from [50]. Copyright 2010 Royal Society of Chemistry.

A wide range of materials, both synthetic and bio-based, are suitable candidates to form the shell, and the range of particle sizes spans from the nanometer to several micrometers, mostly depending on the size of the template. The main challenges concerning the preparation of nano-sized LbL capsules are related to aggregation phenomena. However, this size range cannot be neglected since is particularly important for in vivo applications. On the other hand, micro-sized capsules are very attractive objects because of the simplicity of their characterization and imaging, facile prevention of aggregation and superior loading capacity [51]. The surface of the capsules has been frequently modified in order to tailor the capsules properties to the final application requirements,

such as improved colloidal stability, enhanced confinement of the encapsulated core substances or incorporation in the polymer shell of active materials for imaging and sensing [52].

Tao et al. [53] published in 2004 an early example of a LbL capsule system containing an azo dye in the shell. Negatively charged Congo red (CR), bearing two negative charges and a chromophore moiety, was deposited on a melamine-formaldehyde sacrificial template alternated with positively charged polyelectrolyte. The presence of CR in the capsules shell imprinted brand new properties to the polymer capsules. In particular, the permeability of the shells could be remotely controlled irradiating the capsules with visible light. A similar example of photo-responsive LbL capsules, based on azobenzene moieties, was proposed by Bédard et al. [54]. In this case, the LbL procedure involved alternate absorption of sodium salt of azobenzene, poly(vinylsulfonate) and poly(allyamine hydrochloride) layers. The permeability changes were caused by the trans-cis photo-isomerization of azobenzene. Experimental results showed that exposure of microcapsules to light led to significant shrinking, increased roughness and enhanced permeability of the capsule shell. Moreover, the authors reported the successful encapsulation of a fluorescent probe macromolecule and its release upon light irradiation.

In 2014, Yi and Sukhorukov [55] reported on LbL UV-responsive microcapsules made of alternating layers of negatively charged poly[1-[4-(3-carboxy-4-hydroxyphenylazo) benzenesulfonamido]-1,2-ethanediyl sodium salt (PAZO) and poly(diallyldimethyl ammonium chloride (PDADMAC). In this case, the photo-responsive behavior was attributed to the presence of PAZO segments, that upon UV-light irradiation rearrange forming J aggregates. The schematic illustration of PDADMAC/PAZO microcapsule disruption is reported in Figure 2.4. Extensively investigated in the literature [56], J aggregates are small aggregates, constituted by three or four monomeric units having the same orientation and created via strong non-covalent aromatic-aromatic interaction. These formations are not flexible enough to retain the spherical structure of the shell, so that the capsule gradually breaks, swelling and leaking the core material, until final disruption.

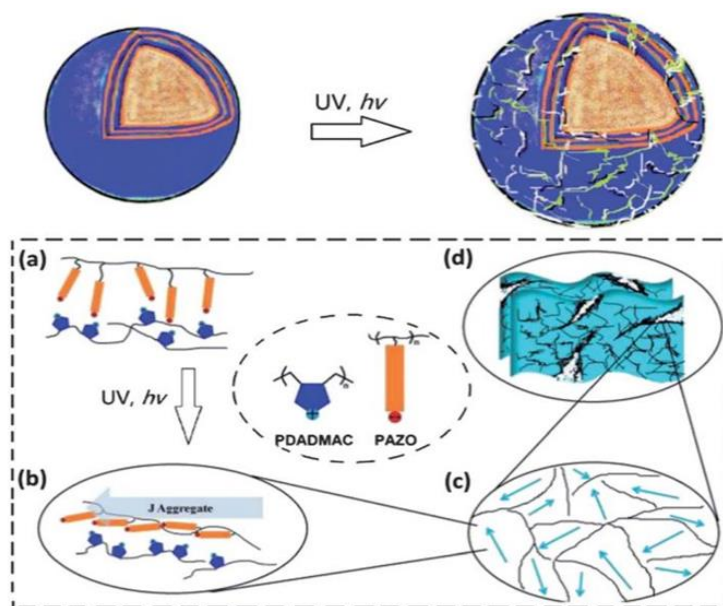


Figure 2.4. – Schematic illustration of (PDADMAC/PAZO) microcapsule disruption induced by UV irradiation [55]: (a) LbL assembly of the polyelectrolytes on the capsule shell surface; (b) formation of J aggregates under UV irradiation; (c,d) extended aggregates act as stress raisers, triggering capsule breakage. Reprinted with permission from [55]. Copyright 2014 Royal Society of Chemistry.

Release experiments were performed on the capsules loaded with a model core substance, bovine serum albumin (BSA). The results showed how the capsules disruption process could be modulated to control the release of the encapsulated BSA by adjusting the UV intensity and microcapsule architecture. However, it was noticed that BSA molecules were able to leak through the porous multilayer shell even without the support of UV-light. To overcome this problem, the same authors developed a very interesting multifunctional capsule system in which UV response was time-dependent and involved both encapsulation and release processes [57]. This approach was specifically designed to promote the confinement of low molecular weight water-soluble substances that usually are very prone to leak from the capsule due to its intrinsic porosity. Instead of increasing the density of the multilayer to obtain a decrease of permeability, Yi and Sukhorukov proposed a chemical sealing of diazoresin (DAR)-containing microcapsules. In both Nafion/DAR and DAR single component [58] microcapsules, irradiation with UV light at 380 nm led to photolysis of the interacting ion pairs, causing the decomposition of the diazonium group, and the formation of a

sulfonate covalent bond, as shown in Figure 2.5. The photo-induced conversion from ionic to covalent chemical bonds via DAR photolysis offers an externally controlled method to seal the multilayer capsules and guarantee minimal diffusion of the encapsulated molecules. Interestingly, UV-sealed capsules showed a more efficient preservation of Rhodamine B, over storage time, than their un-irradiated counterparts.

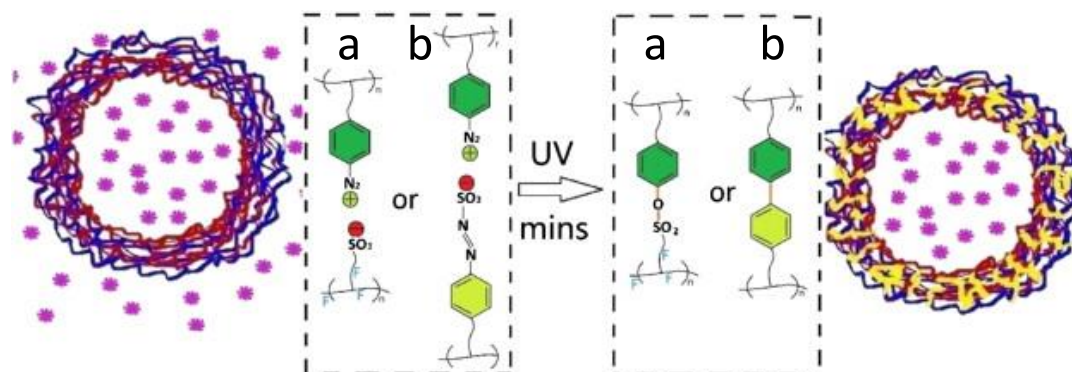


Figure 2.5. – Photolysis-induced small molecule encapsulation in: (a) Nafion/DAR; and (b) DAR single component multilayer capsules as depicted in [57]. Reprinted with permission from [57]. Copyright 2013 American Chemical Society.

The great advantage of this method is that more interesting low molecular weight substances could be encapsulated in the DAR capsules without changing environmental conditions, such as ionic charge [59] or pH [60]. Moreover, the UV-induced rapid capsule sealing would be extraordinarily useful in terms of catching and analyzing small molecules in a biological environment.

2.3.2. Layer-by-Layer (LbL) Using Host-Guest Systems

For a long time, the only driving force of the LbL technique has been the electrostatic interaction between polyelectrolyte pairs, therefore the limited amount of oppositely charged and water soluble polymers available for the process constituted the main drawback of this technique. A

possible alternative to electrostatic-driven LbL structures are supramolecular assemblies, a set of molecules held together by non-covalent bonds. These structures can be formed by just two molecules (e.g., DNA double helix) or, more often, by a great amount of molecules able to form complex structures such as spheres, rods or sheets (e.g., micelles, liposomes and biological membranes). In the domains of supramolecular chemistry, the development of host-guest systems, in which a host molecule can recognize and bind a certain guest molecule, was considered as an important contribution.

A host-guest system refers to a chemical system that is made up of two or more molecular subunits self-assembled together to form a supramolecular complex. Normally, the formation of a host-guest system involves more than one type of noncovalent interaction, for example, hydrophobic association, hydrogen bonding, electrostatic interactions, metal coordination, van der Waals forces, and π - π stacking interactions [61]. In this frame, Xiao et al. [62] successfully obtained photo switchable microcapsules based on host-guest interaction, using a host layer containing α -cyclodextrin (α -CD) and a guest layer based on azobenzene (Azo) assembled on sacrificial CaCO_3 particles via LbL deposition. α -CD-rhodamine B (α -CD-RhB), used as a model drug, was loaded on Azo layers by host-guest interaction. Interestingly, under UV irradiation ($\lambda = 365 \text{ nm}$) a modification of the host guest interaction occurred, mainly due to Azo isomerization, leading to the disruption of the capsules shell and the release of the encapsulated drug. The capsules structure and the release mechanism are depicted in Figure 2.6. The release of the modified α -CD was successfully monitored through spectrofluorometric analysis thanks to the modification of the model drug with the fluorescent rhodamine B. The experiment showed how the drug release from the sample irradiated with UV light was dramatically faster compared to the un-irradiated sample.

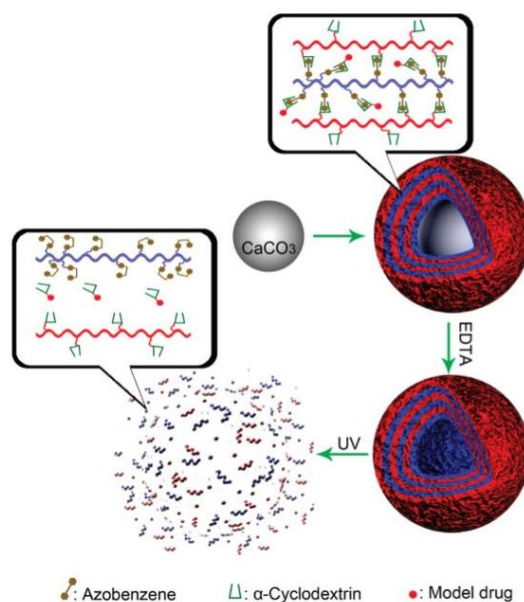


Figure 2.6. – Capsules structure and release mechanism of α -CD/Azo LbL microcapsules as depicted by Xiao et al. [62]. Reprinted with permission from [62]. Copyright 2011 American Chemical Society.

A further implementation of the supramolecular LbL approach was provided by Lin et al. [63]. The LbL assembly was driven by two different host–guest interactions, one between adamantane (AD) and β -cyclodextrin (β -CD) and one between azobenzene (Azo) and β -CD. The versatility of β -CD allows it to accept both AD or Azo as a guest molecule into the inner hydrophobic chamber [64,65]. In particular, the trans-Azo isomer is suitable for entering the inner chamber of β -CD while the cis-Azo isomer shows no supramolecular interaction because of steric hindrance. As a result, UV photo-irradiation could cause the dissociation of β -CD/Azo complex. The microcapsules designed by Lin et al. are able to controllably switch between the “on” and “off” state. As shown in Figure 2.7, the stable host–guest interaction between β -CD and AD maintains the structural integrity of the shell, while the reversible UV-sensitive interactions between Azo and β -CD could form a dense membrane to confine the drug. Under UV light irradiation ($\lambda = 365$ nm) the photo-switching of Azo from trans to cis implies a weakening of the Azo/ β -CD interactions and a decrease in the density of the layers, and the consequent diffusive release of the encapsulated molecule. Release experiments

of the encapsulated fluorescent PEG5000-FITC probe drug confirmed the reversible switching between “on” and “off” state as a proof of concept of the “release-cessate-recommence” mechanism.

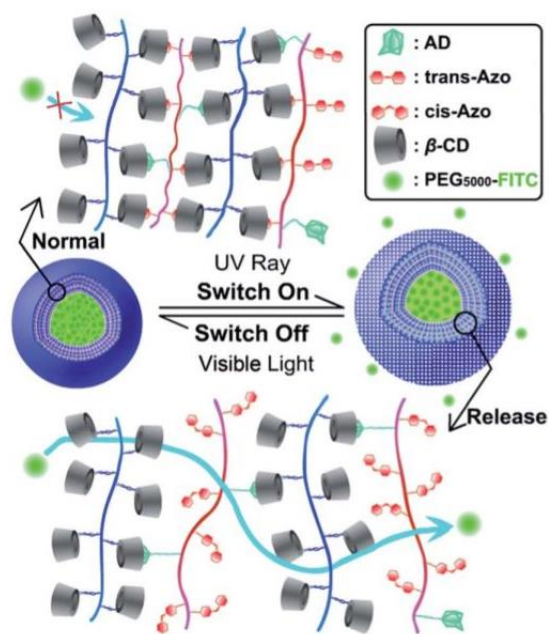


Figure 2.7. – On/off photo-responsive switch in the LbL microcapsules designed by Lin et al. [63]. Reprinted with permission from [63]. Copyright 2014 Royal Society of Chemistry.

2.3.3. Other Templating Methods

It is worth mentioning another example of LbL capsules based on photo-responsive moieties different from azobenzene. Achilleos et al. [66] engineered LbL nanocapsules based on photosensitive spiropyrans (SPs) moieties. Upon UV irradiation, non-polar SPs isomerize to merocyanines (MCs); the process is reversible, since under visible-light irradiation MC regenerates the SP form [67]. The supramolecular design of these capsules was based on the intrinsic feature of MCs to aggregate into either H- or J-type stack-like arrangements through noncovalent π - π interactions.

In the class of templating methods, LbL is by far the most technologically advanced. However, other methods for the formation of hollow capsules based on a sacrificial particle as template can be found in literature. For example host-guest interactions between cyclodextrin-appended polymers

(host) and complementary ferrocene or azobenzene carriers (guest) was employed by Wajs et al. to obtain stimuli-responsive nanocapsules using sacrificial golden colloidal templates [68]. Li et al. [69] introduced a facile method to fabricate photo-responsive capsules, using an ortho-nitrobenzyl derivative as cross-linking agent for polyethyleneimine (PEI) and CaCO₃ templating particles. The release of the encapsulated model cargo under UV light irradiation occurs because of the photo-cleavable nature of the cross-linking points [70,71], leading to capsules dissociation.

For biomedical applications that involve laser-nanoparticle interaction, the light needs to guarantee both minimum absorption by cells/tissue and maximum absorption by nanoparticles. The ideal light source is the so-called biologically “friendly” wavelength window [72]—the near-infrared (NIR) part of the spectrum. Light-responsive capsules have the potential for *in vivo* drug delivery because NIR light is much less harmful and has a much deeper penetration depth in tissues compared with UV or visible light. However, photo-responsive polymer moieties that typically constitute the polymeric capsules shell are inert to IR light, so functionalization of the capsules shell with noble metal nanoparticles becomes necessary [73]. These particles are able to efficiently absorb laser energy and convert it into heat, which locally and transiently dissipates to a polyelectrolyte network. For example, Skirtach et al. proposed polyelectrolyte-multilayer microcapsules carrying silver nanoparticles embedded in their shell. It was possible to remotely activate the capsule, injected in living cells, by irradiation with near-IR light [74,75].

Similarly, Angelatos et al. [76] reported the preparation of NIR-responsive capsules prepared via LbL-assembly of polyelectrolytes using melamine formaldehyde particles as sacrificial templates. Exploiting the pH-dependence of the shell permeability, modified dextran was successfully loaded into preformed capsules. Subsequently, infiltration of light-absorbing gold nanoparticles into the capsule shell was performed to render the capsules optically addressable. A schematization of the process is reported in Figure 2.8.

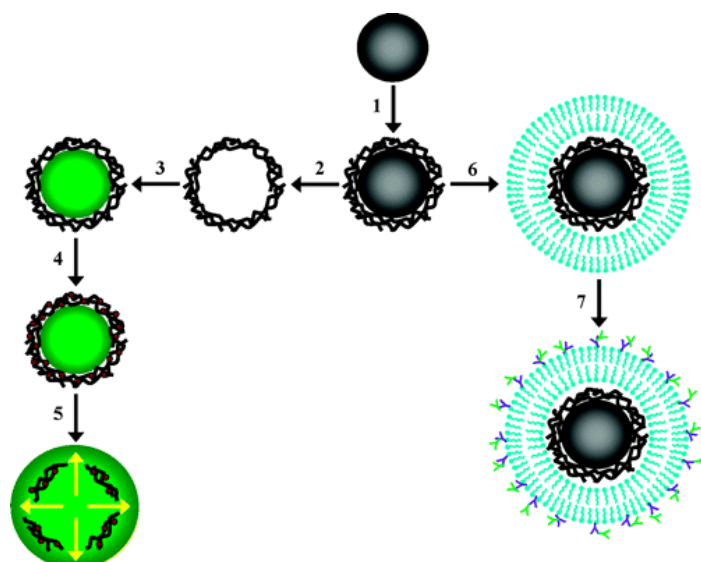


Figure 2.8 - Schematic illustration of the various colloidal systems investigated by Angelatos et al. [76]. Reprinted with permission from [76]. Copyright 2005 American Chemical Society.

The authors demonstrated that it is possible to tune the release of the encapsulated material irradiating the capsule with a short-pulse (10 ns) NIR laser light ($\lambda = 1064$ nm). Moreover, the polyelectrolyte shell was coated with a lipid bilayer, increasing capsules bio-recognition capabilities [77]. Such capsules are likely to have potential as delivery vehicles for drug administration, microreactor applications, and even cell manipulation. Ambrosone et al. [78] reported an interesting application of NIR-responsive LbL capsules for advanced in vivo delivery of an intracellular modulator of Wnt/ β -catenin signaling pathway. The relevance of this work lies in the importance of controlling cell function and reprogramming cell fate upon external triggering.

2.4. Self-Assembly Methods

The spontaneous formation of non-covalent association of organic molecules in solution is commonly called self-assembly. Scientists are very intrigued by this phenomenon, mainly because of the intrinsic compelling nature of self-ordered structures, but also because these structures naturally occur in living organisms [79]. The formation of hollow carriers is often enabled by the use of

amphiphilic molecules, characterized by both hydrophilic and hydrophobic parts. In the following section, different preparation methods of self-assembled micro- and nanocapsules, based on amphiphilic block copolymers and low molecular weight amphiphiles are reported.

2.4.1. Block Copolymers Self-Assembly

The formation of micelles from self-assembly of block copolymers in a selective solvent has been known since 1970s [80]. Recently, self-assembled polymer capsules have been used to encapsulate drugs and other active agents as well as enzymes and non-biologic catalysts, serving as nanoreactors [81]. Different approaches have been developed to obtain targeted drug delivery via tuning the amphiphilicity of the block copolymers. In particular, Blasco et al. [82] reported a new family of photo-responsive self-assembly formulations based on a series of amphiphilic linear-dendritic block copolymers (LDBC)s containing photochromic azobenzene units and hydrocarbon chains randomly connected to the periphery of the dendron. One of the main drawbacks of this technique is the use of organic solvents and complicated preparation procedures of the block copolymer units. The same authors proposed a simpler synthetic approach compared to the former design, based on an azobenzene-containing miktoarm polymer that formed stable vesicles, able to load and release both hydrophobic and hydrophilic cargo molecules upon UV irradiation [83].

To overcome the problems related to the use of organic solvents, efforts have been done in the development of block copolymer assemblies based on electrostatic interactions [84,85]. Water is a suitable solvent for this novel class of polymeric assemblies, since they are formed by double-hydrophilic block copolymers, containing ionic and nonionic water-soluble segments (block ionomers). A new frontier in ionomer self-assembly was reported by Wang et al. [86]. They introduced stimuli-responsive moieties onto surfactant molecules, so that surfactant aggregates can be tuned toward controllable disassembly. The UV-induced variation of the critical micellar

concentration (CMC) of the trans and cis forms of azobenzene-bearing surfactants is a well-known process, that can be used to induce the destruction/formation of micellar structures. The strategy employed to prepare vesicles based on block ionomer complex is reported in Figure 2.9. UV-vis spectrophotometry tests demonstrated that the molecules of azobenzene-containing surfactant included in the block ionomer complex were able to undergo trans-to-cis isomerization if irradiated with UV light at 365 nm, and reversibly switch back from cis to trans form if irradiated with visible light at 450 nm.

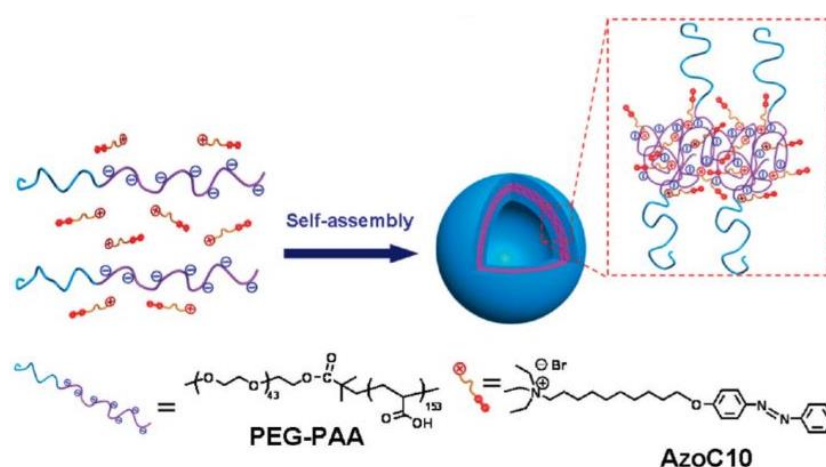


Figure 2.9. - Schematic illustration of the self-assembly of block ionomer complex vesicles as depicted by Wang et al. [86]. Reprinted with permission from [86]. Copyright 2009 American Chemical Society.

2.4.2. Liposomes

Liposomes consist of concentric bilayers of phospholipids and/or other amphiphilic molecules encapsulating an aqueous compartment, resulting in nanosized vesicles. Intensive studies have been carried out on the encapsulation of drugs in liposomes, as they are promising carriers in aqueous fluids [87,88]. Among other drug carriers for cancer treatment, liposomes are the longest-studied nanoparticles and are hence associated with a number of historic milestones [89] Despite improvements in the therapeutic efficacy versus side effects obtained in the dosage of few relevant drugs (e.g., amphotericin B and doxorubicin), the desired drug release from liposomes is still a challenge [90]. One of the main drawbacks of liposome carriers is the passive release by diffusion of

the encapsulated drug. In most cases, diffusion occurs too slowly and the local drug concentrations required for the optimum therapeutic effect are not reached [91]. Rapid and targeted drug delivery can be achieved triggering chemical and physical changes in liposome shell using external light irradiation [92], as illustrated in Figure 2.10.

The mechanism depicted in Figure 2.10A is based on photo-polymerization of membrane lipids. The application of a proper light source induces photo-polymerization of reactive molecules (bearing dienoyl, sorbyl or styryl groups) introduced into the liposome membrane. This leads to the formation of condensed domains in the bilayer; at the same time pores are temporarily formed around the clusters until the surrounding free mobile lipids rearrange to reconstitute the bilayer. Such pores allow drug molecules to diffuse out of the liposome. For example, Bondurant et al. [93] showed that the inclusion of a photo-reactive lipid component in PEG-liposomes membrane did not alter the permeability of liposomes prior to irradiation, while exposure to UV light ($\lambda = 254 \text{ nm}$) for 2 min led to an increased liposome permeability.

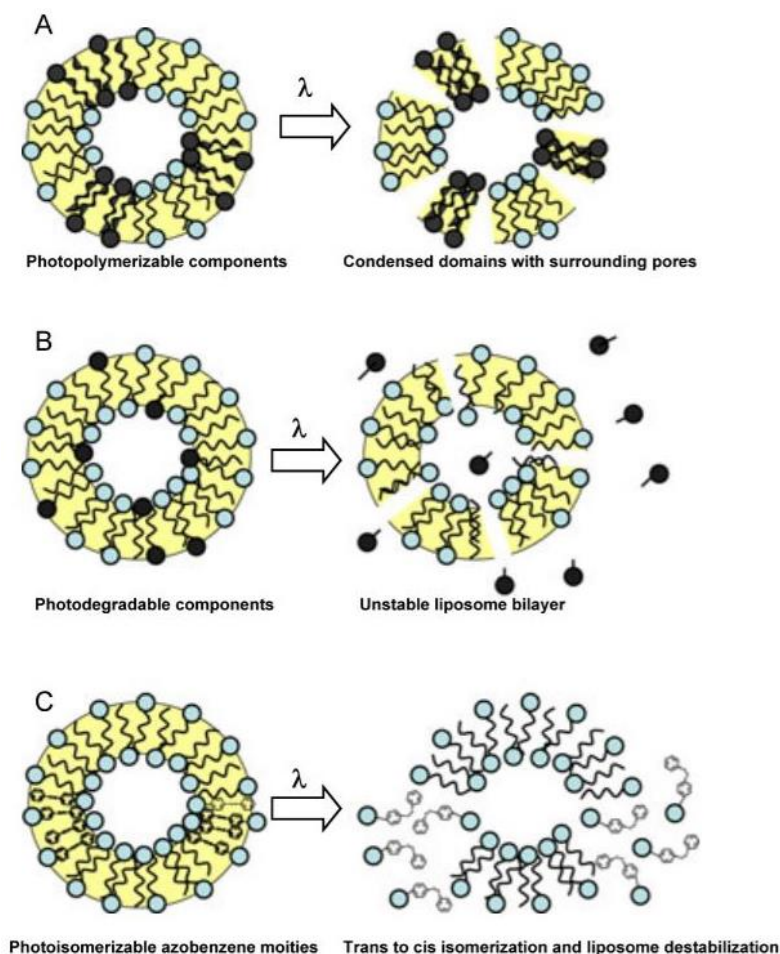


Figure 2.10- Schematization of light-triggered release mechanisms in liposomes by inclusion of: (A) photo-polymerizable components; (B) photodegradable components; or (C) photo-isomerizable azobenzene moieties. Reprinted with permission from [92]. Copyright 2012 Ivyspring International Publisher.

Light-responsiveness of liposomes can also be photo-chemically triggered applying various chemical stimuli responsible for the destabilization or disruption of specific components of the liposome membrane (Figure 2.10B). One of the earliest examples was provided by Thompson et al. [94]. Their approach was based on the photo-cleavage of plasmenylcholine to single chain surfactants via sensitized photooxidation of the plasmalogen vinyl ether linkage (Figure 2.11). The authors presented the photo-triggered behavior of plasmenylcholine liposomes containing three different sensitizers absorbing between 630 and 820 nm.

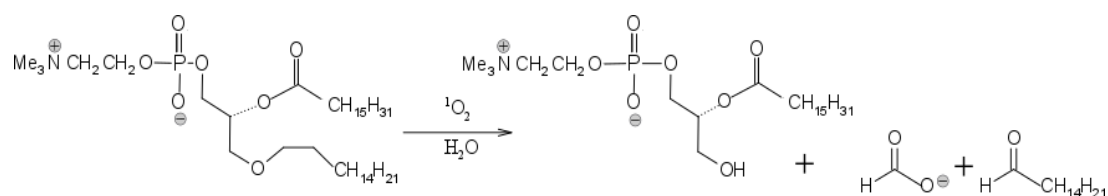


Figure 2.11. Singlet oxygen-mediated photo-oxidation of plasmalogen vinyl ether linkage.

In this frame, Luo et al. [95] demonstrated that the introduction of a small amount of an unsaturated phospholipid accelerates NIR light-triggered doxorubicin release in porphyrin-phospholipid (PoP) liposomes. The mechanism of the enhanced release rate was related to the oxidation of unsaturated phospholipids by singlet oxygen. In vivo studies demonstrated the efficiency of these systems in chemo-photo-therapy. Sine et al. [96] reported in vivo release studies of a novel photo-cleavable liposome system with projected applications for cancer treatment. In this case, the inclusion of a red absorbing photosensitizing agent in the liposome membrane was able to induce destabilization of “pockets” structures, resulting in defects in the liposome bilayer and causing the release of encapsulated drug.

One of the most common approaches for the formation of light-responsive carriers is the introduction of photo-isomerizable lipids in the liposome membrane, as schematized in Figure 2.10C. Azobenzene-modified lipids (Bis-Azo PC) can undergo photo-isomerization, leading to photo-induced conformational changes in the liposomes. The trans to cis isomerization of the azobenzene groups alters the polarity and conformation of the lipids in a rapid and reversible process, as reported in Figure 2.12. This approach can guarantee one of the finest control of drug release by simply adjusting the liposome composition. For example, Bisby et al. [97] reported that an increase in cholesterol content enables to lower the photo-isomerization extent necessary to trigger the release, increasing the light sensitivity of azobenzene-containing liposomes.

More recently, Cui et al. [98] demonstrated the feasibility of fluid-phase photo-sensitive liposomes not based on phospholipids that combine very low passive permeability and good photo-

control of the entrapped payload. The presence of the azobenzene derivative makes these liposomes sensitive to light and allows high-precision control on the release of the encapsulated material. The authors pointed out that the trans form of the azobenzene was compatible with the molecular packing of the bilayer, giving impermeable membranes. On the other hand, the cis form introduced defects in the tightly packed alkyl chains of the bilayer, allowing the photo-induced leakage of the encapsulated material.

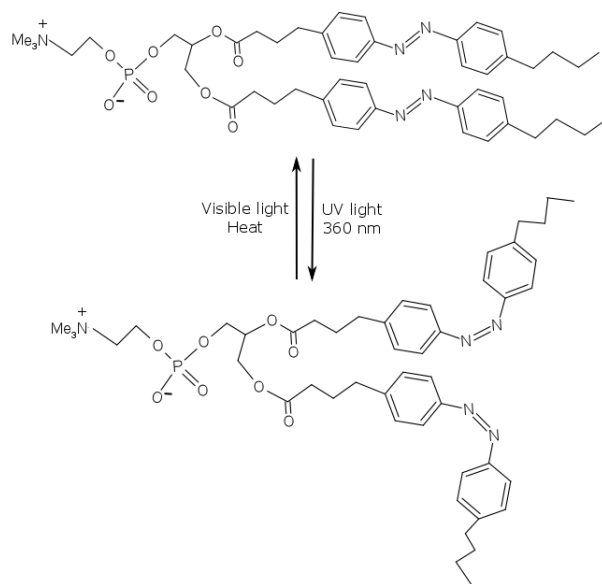


Figure 2.12 - Mechanism of trans-cis isomerization under UV light irradiation of the photochromic lipid, Bis-Azo PC.

Interesting advances in NIR-responsive liposomes consist in a new family of water-in-oil-in-wall (W/O/W) core-shell nanocapsules made from the self-assembly of proteins in a liposome-like double layer intercalated with reduced graphene oxide (rGO) nanosheets [99]. The rGO nanosheets are introduced to minimize unintended drug leakage, but it also serves as the NIR sensor/actuator that triggers drug release.

In a frontier application, multilayer capsule solely based on graphene oxide were tested as controlled drug delivery carriers [100], opening a novel way for NIR-light triggered release in a simple way without addition of nanoparticles or dyes.

2.5. Characterization Methods of Photo-Responsive Capsules

It is worth providing a short outlook on the most used [101–103] methods for collecting valuable data to characterize photo-responsive polymers. In Table 1 the classification of characterization techniques is based on different key capsules properties, namely: shape, size distribution, cross section and surface morphology, surface chemical analysis, thermodynamic properties of shell and encapsulated material, and release and stability of encapsulated material.

Table 2.1. - Characterization techniques of photo-responsive capsules.

Capsules properties	Method
Capsule shape and size	Optical microscopy
	Dynamic Light Scattering (DLS)
	Particle size analyzer
Capsule shape, size and surface/cross-section morphology	Environmental/Scanning Electron Microscopy (ESEM/SEM)
	Transmission Electron Microscopy (TEM)
Capsule surface physical properties	Atomic force microscopy (AFM)
	Contact angle measurement (CA)
	Nanoindentation
Capsule surface chemical properties	SEM + X-Ray microanalysis (EDS)
	X-Ray photoelectron spectroscopy (XPS)
	Nuclear magnetic resonance spectroscopy (NMR)
	Attenuated total reflectance infrared spectroscopy (ATR-IR)
Thermodynamic properties of shell and/or encapsulated materials	Differential scanning calorimetry (DSC)
	Thermogravimetry (TG)
Active material stability and release	Ultraviolet-visible spectrophotometry (UV-Vis)
	Gas chromatography–mass spectrometry (GC-MS)
	High-performance liquid chromatography (HPLC)
	Spectrofluorimetry
	Olfactive Evaluation

2.6. Conclusions

Significant progress in the design and the synthesis of light-responsive polymer micro- and nanocapsules has been made in recent years. Diversification of capsule preparation techniques and fine-tuning of materials chemical design provide an almost infinite number of strategies to obtain a customer-tailored application. However, many challenges need to be addressed, concerning both academic research and industrial application. Understanding the principles of the mechanisms at the basis of these stimuli-responsive materials is essential for developing novel encapsulation, release, and targeting methods.

The ultimate challenge for light-triggered delivery of drugs or other active agents in biological environments is to grant the use of biocompatible materials and un-harmful release process in use. Among the wide variety of photosensitive capsules available, a sensitive factor is the choice of an appropriate size range of delivery systems. Microcapsules, for example, have been widely studied and exploited in commercial applications for their facile preparation and characterization. On the other hand, biological application, such as circulation or cellular uptake experiments, have desperate need of nanocapsules.

Research and development in nano-sized range is currently experiencing a burst development and is in constant need for new carriers to further impact theranostics, nanomedicine and drug delivery.

2.7. References

1. Blume, G.; Cevc, G. Liposomes for the sustained drug release in vivo. *Biochim. Biophys. Acta* 1990, 1029, 91–97.
2. Petcu, S.F.; Oancea, F.; Siciua, O.A.; Constantinescu, F.; Dinu, S. Responsive polymers for crop protection. *Polymers* 2010, 2, 229–251.
3. Hastings, C.J.; Pluth, M.D.; Bergman, R.G.; Raymond, K.N. Enzymelike catalysis of the Nazarov cyclization by supramolecular encapsulation. *J. Am. Chem. Soc.* 2010, 132, 6938–6940.
4. Nguyen, D.; Zondanos, H.S.; Farrugia, J.M.; Serelis, A.K.; Such, C.H.; Hawckett, B.S. Pigment encapsulation by emulsion polymerization using macro-RAFT copolymers. *Langmuir* 2008, 24, 2140–2150.
5. Sanlés-Sobrido, M.; Pérez-Lorenzo, M.; Rodríguez-González, B.; Salgueiriño, V.; Correa-Duarte, M.A. Highly active nanoreactors: Nanomaterial encapsulation based on confined catalysis. *Angew. Chem. Int. Ed.* 2012, 51, 3877–3882.
6. Theato, P.; Sumerlin, B.S.; O'Reilly, R.K.; Epps, T.H., III. Stimuli responsive materials. *Chem. Soc. Rev.* 2013, 42, 7055–7056.
7. Stuart, M.A.C.; Huck, W.T.; Genzer, J.; Müller, M.; Ober, C.; Stamm, M.; Sukhorukov, G.B.; Szleifer, I.; Tsukruk, V.V.; Urban, M.; et al. Emerging applications of stimuli-responsive polymer materials. *Nat. Mater.* 2010, 9, 101–113.
8. Roy, I.; Gupta, M.N. Smart polymeric materials: Emerging biochemical applications. *Chem. Biol.* 2003, 10, 1161–1171.
9. Déjugnat, C.; Sukhorukov, G.B. pH-responsive properties of hollow polyelectrolyte microcapsules templated on various cores. *Langmuir* 2004, 20, 7265–7269.
10. Lawrence, D.B.; Cai, T.; Hu, Z.; Marquez, M.; Dinsmore, A.D. Temperature-responsive semipermeable capsules composed of colloidal microgel spheres. *Langmuir* 2007, 23, 395–398.

11. Jing, Y.; Zhu, Y.; Yang, X.; Shen, J.; Li, C. Ultrasound-triggered smart drug release from multifunctional core-shell capsules one-step fabricated by coaxial electrospray method. *Langmuir* 2010, 27, 1175–1180.
12. Zhu, Y.; Tong, W.; Gao, C. Molecular-engineered polymeric microcapsules assembled from Concanavalin A and glycogen with specific responses to carbohydrates. *Soft Matter* 2011, 7, 5805–5815.
13. Lv, L.P.; Zhao, Y.; Vilbrandt, N.; Gallei, M.; Vimalanandan, A.; Rohwerder, M.; Landfester, K.; Crespy, D. Redox responsive release of hydrophobic self-healing agents from polyaniline capsules. *J. Am. Chem. Soc.* 2013, 135, 14198–14205.
14. Huang, Y.; Dong, R.; Zhu, X.; Yan, D. Photo-responsive polymeric micelles. *Soft Matter* 2014, 10, 6121–6138.
15. Ercole, F.; Davis, T.P.; Evans, R.A. Photo-responsive systems and biomaterials: Photochromic polymers, light-triggered self-assembly, surface modification, fluorescence modulation and beyond. *Polym. Chem.* 2010, 1, 37–54.
16. Yager, K.G.; Barrett, C.J. Azobenzene Polymers for photonic applications. In *Smart Light-Responsive Materials: Azobenzene-Containing Polymers and Liquid Crystals*; Zhao, Y., Ikeda, T., Eds.; John Wiley & Sons, Inc.: Hoboken, NJ, USA, 2009.
17. Görner, H.; Kuhn, H.J. Cis-Trans photoisomerization of stilbenes and stilbene-like molecules. In *Advances in Photochemistry*; Neckers, D.C., Volman, D.H., von Büнау, G., Eds.; John Wiley & Sons, Inc.: Hoboken, NJ, USA, 1994.
18. Klajn, R. Spiropyran-based dynamic materials. *Chem. Soc. Rev.* 2014, 43, 148–184.
19. Zollinger, H. *Color Chemistry: Syntheses, Properties, and Applications of Organic Dyes and Pigments*, 3rd ed.; Wiley-VHCA: Zurich, Switzerland, 2006.
20. El Halabieh, R.H.; Mermut, O.; Barrett, C.J. Using light to control physical properties of polymers and surfaces with azobenzene chromophores. *Pure Appl. Chem.* 2004, 76, 1445–1465.

21. Vauthier, C.; Bouchemal, K. Methods for the preparation and manufacture of polymeric nanoparticles. *Pharm. Res.* 2009, 26, 1025–1058.
22. Anderson, R.R.; Parrish, J.A. The optics of human skin. *J. Investig. Dermatol.* 1981, 77, 13–19.
23. Baumann, E. Ueber eine einfache Methode der Darstellung von Benzoësäureäthern. *Ber. Dtsch. Chem. Ges.* 1886, 19, 3218–3222.
24. Schotten, C. Ueber die Oxydation des Piperidins. *Ber. Dtsch. Chem. Ges.* 1884, 17, 2544–2547.
25. Wittbecker, E.L.; Morgan, P.W. Interfacial polycondensation-I. *J. Polym. Sci.* 1959, 40, 289–297.
26. Torini, L.; Argillier, J.F.; Zydowicz, N. Interfacial polycondensation encapsulation in miniemulsion. *Macromolecules* 2005, 38, 3225–3236.
27. Mora-Huertas, C.E.; Fessi, H.; Elaissari, A. Polymer-based nanocapsules for drug delivery. *Int. J. Pharm.* 2010, 385, 113–142. [
28. Jeong, B.H.; Hoek, E.M.; Yan, Y.; Subramani, A.; Huang, X.; Hurwitz, G.; Ghosh, A.K.; Jawor, A. Interfacial polymerization of thin film nanocomposites: A new concept for reverse osmosis membranes. *J. Membr. Sci.* 2007, 294, 1–7.
29. Gao, H.; Jiang, T.; Han, B.; Wang, Y.; Du, J.; Liu, Z.; Zhang, J. Aqueous/ionic liquid interfacial polymerization for preparing polyaniline nanoparticles. *Polymer* 2004, 45, 3017–3019.
30. Cho, J.S.; Kwon, A.; Cho, C.G. Microencapsulation of octadecane as a phase-change material by interfacial polymerization in an emulsion system. *Colloid Polym. Sci* 2002, 280, 260–266.
31. Asua, J.M. Miniemulsion polymerization. *Prog. Polym. Sci.* 2002, 27, 1283–1346.
32. Landfester, K. Miniemulsions for nanoparticle synthesis. In *Colloid Chemistry II*; Antonietti, M., Ed.; Springer: Berlin, Germany, 2003; pp. 75–123.
33. Tylkowski, B.; Pregowska, M.; Jamowska, E.; Garcia-Valls, R.; Giamberini, M. Preparation of a new lightly cross-linked liquid crystalline polyamide by interfacial polymerization. Application to the obtainment of microcapsules with photo-triggered release. *Eur. Polym. J.* 2009, 45, 1420–1432.

34. Marturano, V.; Cerruti, P.; Carfagna, C.; Giamberini, M.; Tylkowski, B.; Ambrogi, V. Photo-responsive polymer nanocapsules. *Polymer* 2015, 70, 222–230.
35. Bizzarro, V.; Carfagna, C.; Cerruti, P.; Marturano, V.; Ambrogi, V. Light-responsive polymer microcapsules as delivery systems for natural active agents. *AIP Conf. Proc.* 2016, 1736, 020078.
36. Wachtveitl, J.; Zumbusch, A. Azobenzene: An optical switch for in vivo experiments. *ChemBioChem* 2011, 12, 1169–1170.
37. Beharry, A.A.; Sadvski, O.; Woolley, G.A. Azobenzene photoswitching without ultraviolet light. *J. Am. Chem. Soc.* 2011, 133, 19684–19687.
38. Wegner, H.A. Azobenzenes in a new light—Switching in vivo. *Angew. Chem. Int. Ed.* 2012, 51, 4787–4788.
39. Tylkowski, B.; Giamberini, M.; Underiner, T.; Prieto, S.F.; Smets, J. Photo-Triggered Microcapsules. *Macromol. Symp.* 2016, 360, 192–198.
40. Duffy, D.C.; McDonald, J.C.; Schueller, O.J.; Whitesides, G.M. Rapid prototyping of microfluidic systems in poly (dimethylsiloxane). *Anal. Chem.* 1998, 70, 4974–4984.
41. Quevedo, E.; Steinbacher, J.; McQuade, D.T. Interfacial polymerization within a simplified microfluidic device: Capturing capsules. *J. Am. Chem. Soc.* 2005, 127, 10498–10499.
42. Zheng, Y.; Yu, Z.; Parker, R.M.; Wu, Y.; Abell, C.; Scherman, O.A. Interfacial assembly of dendritic microcapsules with host–guest chemistry. *Nat. Commun.* 2014, 5, 1–9.
43. Chen, K.; Zhou, S. Fabrication of ultraviolet-responsive microcapsules via Pickering emulsion polymerization using modified nano-silica/nano-titania as Pickering agents. *RSC Adv.* 2015, 5, 13850–13856.
44. Nakata, K.; Fujishima, A. TiO₂ photocatalysis: Design and applications. *J. Photochem. Photobiol. C Photochem. Rev.* 2012, 13, 169–189.
45. Bogdanowicz, K.A.; Tylkowski, B.; Giamberini, M. Preparation and characterization of light-sensitive microcapsules based on a liquid crystalline polyester. *Langmuir* 2013, 29, 1601–1608.

46. Peña, B.; Panisello, C.; Areste, G.; Garcia-Valls, R.; Gumí, T. Preparation and characterization of polysulfone microcapsules for perfume release. *Chem. Eng. J.* 2012, 179, 394–403.
47. Peyratout, C.S.; Dähne, L. Tailor-made polyelectrolyte microcapsules: From multilayers to smart containers. *Angew. Chem. Int. Ed.* 2004, 43, 3762–3783.
48. Caruso, R.; Susha, L.; Caruso, F. Multilayered Titania, silica and laponite nanoparticle coatings on polystyrene colloidal templates and resulting inorganic hollow spheres. *Chem. Mater.* 2001, 13, 400–409.
49. Caruso, F.; Caruso, R.A.; Möhwald, H. Nanoengineering of inorganic and hybrid hollow spheres by colloidal templating. *Science* 1998, 282, 1111–1114.
50. Yoon, H.J.; Jang, W.D. Polymeric supramolecular systems for drug delivery. *J. Mater. Chem.* 2010, 20, 211–222.
51. Delcea, M.; Möhwald, H.; Skirtach, A.G. Stimuli-responsive LbL capsules and nanoshells for drug delivery. *Adv. Drug Deliv. Rev.* 2011, 63, 730–747.
52. Johnston, A.P.; Cortez, C.; Angelatos, A.S.; Caruso, F. Layer-by-layer engineered capsules and their applications. *Curr. Opin. Colloid Interface Sci.* 2006, 11, 203–209.
53. Tao, X.; Li, J.; Möhwald, H. Self-Assembly, Optical Behavior, and Permeability of a Novel Capsule Based on an Azo Dye and Polyelectrolytes. *Chem. Eur. J.* 2004, 10, 3397–3403.
54. Bédard, M.; Skirtach, A.G.; Sukhorukov, G. Optically driven encapsulation using novel polymeric hollow shells containing an azobenzene polymer. *Macromol. Rapid Commun.* 2007, 28, 1517–1521.
55. Yi, Q.; Sukhorukov, G.B. UV-induced disruption of microcapsules with azobenzene groups. *Soft Matter* 2014, 10, 1384–1391.
56. Yager, K.G.; Barrett, C.J. Novel photo-switching using azobenzene functional materials. *J. Photochem. Photobiol.* 2006, 182, 250–261.
57. Yi, Q.; Sukhorukov, G.B. Photolysis triggered sealing of multilayer capsules to entrap small molecules. *ACS Appl. Mater. Interfaces* 2013, 5, 6723–6731.

58. Yi, Q.; Sukhorukov, G.B. Single component diazo-resin microcapsules for encapsulation and triggered release of small molecules. Part. Part. Syst. Charact. 2013, 30, 989–995.
59. Liu, X.; Gao, C.; Shen, J.; Möhwald, H. Multilayer microcapsules as anti-cancer drug delivery vehicle: deposition, sustained release, and in vitro bioactivity. Macromol. Biosci. 2005, 5, 1209–1219.
60. Sukhorukov, G.L.; Dähne, L.; Hartmann, J.; Donath, E.; Möhwald, H. Controlled precipitation of dyes into hollow polyelectrolyte capsules based on colloids and biocolloids. Adv. Mater. 2000, 12, 112–115.
61. Qu, D.H.; Wang, Q.C.; Zhang, Q.W.; Ma, X.; Tian, H. Photoresponsive host–guest functional systems. Chem. Rev. 2015, 115, 7543–7588.
62. Xiao, W.; Chen, W.H.; Zhang, J.; Li, C.; Zhuo, R.X.; Zhang, X.Z. Design of a photoswitchable hollow microcapsular drug delivery system by using a supramolecular drug-loading approach. J. Phys. Chem. B 2011, 115, 13796–13802.
63. Lin, H.; Xiao, W.; Qin, S.Y.; Cheng, S.X.; Zhang, X.Z. Switch on/off microcapsules for controllable photosensitive drug release in a ‘release-cease-recommence’ mode. Polym. Chem. 2014, 5, 4437–4440.
64. Liu, H.; Zhang, Y.; Hu, J.; Li, C.; Liu, S. Multi-responsive supramolecular double hydrophilic diblock copolymer driven by host-guest inclusion complexation between β -cyclodextrin and adamantyl moieties. Macromol. Chem. Phys. 2009, 210, 2125–2137.
65. Wang, W.; Wang, M.Z. Effect of α -cyclodextrin on the photoisomerization of azobenzene functionalized hydroxypropyl methylcellulose in aqueous solution. Polym. Bull. 2007, 59, 537–544.
66. Achilleos, D.S.; Hatton, T.A.; Vamvakaki, M. Light-regulated supramolecular engineering of polymeric nanocapsules. J. Am. Chem. Soc. 2012, 134, 5726–5729.
67. Minkin, V.I. Photo-, thermo-, solvato-, and electrochromic spiroheterocyclic compounds. Chem. Rev. 2004, 104, 2751–2776.

68. Wajs, E.; Nielsen, T.T.; Larsen, K.L.; Fragoso, A. Preparation of stimuli-responsive nano-sized capsules based on cyclodextrin polymers with redox or light switching properties. *Nano Res.* 2016, 9, 2070–2078.
69. Li, H.; Tong, W.; Gao, C. Photo-responsive polyethyleneimine microcapsules cross-linked by ortho-nitrobenzyl derivatives. *J. Colloid Interface Sci.* 2016, 463, 22–28.
70. Margerum, J.D.; Miller, L.J.; Saito, E.; Brown, M.S.; Mosher, H.S.; Hardwick, R. Phototropism of ortho-NitroBenzyl derivatives. *J. Phys. Chem.* 1962, 66, 2434–2438.
71. Kim, M.S.; Diamond, S.L. Photocleavage of o-nitrobenzyl ether derivatives for rapid biomedical release applications. *Bioorg. Med. Chem. Lett.* 2006, 16, 4007–4010.
72. Roggan, A.; Friebel, M.; Do, K.; Hahn, A.; Mu, G. Optical properties of circulating human blood in the wavelength range 400–2500 nm. *J. Biomed. Opt.* 1999, 4, 36–46.
73. Radt, B.; Smith, T.A.; Caruso, F. Optically addressable nanostructured capsules. *Adv. Mater.* 2004, 16, 2184–2189.
74. Skirtach, A.G.; Muñoz Javier, A.; Kreft, O.; Köhler, K.; Piera Alberola, A.; Möhwald, H.; Parak, W.J.; Sukhorukov, G.B. Laser-induced release of encapsulated materials inside living cells. *Angew. Chem. Int. Ed.* 2006, 45, 4612–4617.
75. Skirtach, A.G.; Karageorgiev, P.; Bédard, M.F.; Sukhorukov, G.B.; Möhwald, H. Reversibly permeable nanomembranes of polymeric microcapsules. *J. Am. Chem. Soc.* 2008, 130, 11572–11573.
76. Angelatos, A.S.; Radt, B.; Caruso, F. Light-responsive polyelectrolyte/gold nanoparticle microcapsules. *J. Phys. Chem.* 2005, 109, 3071–3076.
77. Ishihara, K.; Takai, M. Bioinspired interface for nanobiodevices based on phospholipid polymer chemistry. *J. R. Soc. Interface* 2009, 6, S279–S291.
78. Ambrosone, A.; Marchesano, V.; Carregal-Romero, S.; Intartaglia, D.; Parak, W.J.; Tortiglione, C. Control of Wnt/ β -catenin signaling pathway in vivo via light responsive capsules. *ACS Nano* 2016, 10, 4828–4834.
79. Whitesides, G.M.; Grzybowski, B. Self-assembly at all scales. *Science* 2002, 295, 2418–2421.

80. Tuzar, Z.; Kratochvil, P. Block and graft copolymer micelles in solution. *Adv. Colloid Interface Sci.* 1976, 6, 201–232.
81. Koblenz, T.S.; Wassenaar, J.; Reek, J.N. Reactivity within a confined self-assembled nanospace. *Chem. Soc. Rev.* 2008, 37, 247–262.
82. Blasco, E.; Serrano, J.L.; Piñol, M.; Oriol, L. Light responsive vesicles based on linear–dendritic block copolymers using azobenzene–aliphatic codendrons. *Macromolecules* 2013, 46, 5951–5960.
83. Blasco, E.; Schmidt, B.V.; Barner-Kowollik, C.; Piñol, M.; Oriol, L. A novel photoresponsive azobenzene-containing miktoarm star polymer: Self-assembly and photoresponse properties. *Macromolecules* 2014, 47, 3693–3700.
84. Harada, A.; Kataoka, K. Formation of polyion complex micelles in an aqueous milieu from a pair of oppositely-charged block copolymers with poly(ethylene glycol) segments. *Macromolecules* 1995, 28, 5294–5299.
85. Kabanov, A.V.; Vinogradov, S.V.; Suzdaltseva, Y.G.; Alakhov, V.Y. Water-soluble block polycations as carriers for oligonucleotide delivery. *Bioconjug. Chem.* 1995, 6, 639–643.
86. Wang, Y.; Han, P.; Xu, H.; Wang, Z.; Zhang, X.; Kabanov, A.V. Photocontrolled self-assembly and disassembly of block ionomer complex vesicles: A facile approach toward supramolecular polymer nanocontainers. *Langmuir* 2009, 26, 709–715.
87. Gregoriadis, G. The carrier potential of liposomes in biology and medicine. *N. Engl. J. Med.* 1976, 295, 765–770.
88. Torchilin, V.P. Recent advances with liposomes as pharmaceutical carriers. *Nat. Rev. Drug Discov.* 2005, 4, 145–160.
89. Puri, A. Phototriggerable liposomes: Current research and future perspectives. *Pharmaceutics* 2013, 6, 1–25.
90. Alvarez-Lorenzo, C.; Bromberg, L.; Concheiro, A. Light-sensitive intelligent drug delivery systems. *J. Photochem. Photobiol.* 2009, 85, 848–860.

91. Shum, P.; Kim, J.M.; Thompson, D.H. Phototriggering of liposomal drug delivery systems. *Adv. Drug Deliv. Rev.* 2001, 53, 273–284.
92. Leung, S.J.; Romanowski, M. Light-activated content release from liposomes. *Theranostics* 2012, 2, 1020–1036.
93. Bondurant, B.; Mueller, A.; O'Brien, D.F. Photoinitiated destabilization of sterically stabilized liposomes. *Biochim. Biophys. Acta* 2001, 1511, 113–122.
94. Thompson, D.H.; Gerasimov, O.V.; Wheeler, J.J.; Rui, Y.; Anderson, V.C. Triggerable plasmalogen liposomes: Improvement of system efficiency. *Biochim. Biophys. Acta Biomembr.* 1996, 1279, 25–34.
95. Luo, D.; Li, N.; Carter, K.A.; Lin, C.; Geng, J.; Shao, S.; Huang, W.C.; Qin, Y.; Atilla-Gokcumen, G.E.; Lovell, J.F. Rapid Light-triggered drug release in liposomes containing small amounts of unsaturated and porphyrin–phospholipids. *Small* 2016, 12, 3039–3047.
96. Sine, J.; Urban, C.; Thayer, D.; Charron, H.; Valim, N.; Tata, D.B.; Schiff, R.; Blumenthal, R.; Joshi, A.; Puri, A. Photo activation of HPPH encapsulated in “Pocket” liposomes triggers multiple drug release and tumor cell killing in mouse breast cancer xenografts. *Int. J. Nanomed.* 2015, 10, 125–145.
97. Bisby, R.H.; Mead, C.; Morgan, C.G. Wavelength-programmed solute release from photosensitive liposomes. *Biochem. Biophys. Res. Commun.* 2000, 276, 169–173.
98. Cui, Z.K.; Phoeung, T.; Rousseau, P.A.; Rydzek, G.; Zhang, Q.; Bazuin, C.G.; Lafleur, M. Nonphospholipid fluid liposomes with switchable photocontrolled release. *Langmuir* 2014, 30, 10818–10825.
99. Hu, S.H.; Fang, R.H.; Chen, Y.W.; Liao, B.J.; Chen, I.W.; Chen, S.Y. Photoresponsive protein–graphene–protein hybrid capsules with dual targeted heat-triggered drug delivery approach for enhanced tumor therapy. *Adv. Funct. Mater.* 2014, 24, 4144–4155.

100. Kurapati, R.; Raichur, A.M. Near-infrared light-responsive graphene oxide composite multilayer capsules: A novel route for remote controlled drug delivery. *Chem. Commun.* 2013, 49, 734–736.
101. Smets, J.; Fernández-Prieto, S.; Underiner, T.L.; Wos, J.A.; Huhn, W.E.; Frederick, H.A.; Giamberini, M.; Tylkowski, B. Encapsulates. U.S. Patent 20130039962, 14 February 2013
102. Giamberini, M.; Fernandez Prieto, S.; Tylkowski, B. *Microencapsulation: Innovative Applications*; Walter de Gruyter GmbH & Co KG: Berlin, Germany, 2015.
103. Tylkowski, B.; Tsibranska, I. Overview of main techniques used for membrane characterization. *J. Chem. Technol. Metall.* 2015, 50, 3–12.



CHAPTER 3

Photo-responsive Polymer Nanocapsules

Valentina Marturano, Pierfrancesco Cerruti, Cosimo Carfagna,
Marta Giamberini, Bartosz Tylkowski and Veronica Ambrogi

Polymer, 2015, 70 (23), 222

Abstract

This work reports on the preparation of UV-light responsive nanocapsules based on cross-linked polyamide shell by miniemulsion polymerization. The photo-triggered E-Z transition of azobenzene moieties of the polymer backbone enabled controlled release of encapsulated molecules. Appropriate selection of emulsion conditions allowed tailoring size distribution of the resulting nanocapsules. The light responsiveness of the nanocapsules systems has been evaluated by monitoring size change and release of a fluorescent probe upon UV irradiation, and an unambiguous relationship between capsule size and release kinetics has been highlighted. In particular, the smaller the capsule size, the faster the achieved release. Therefore, the photo-responsiveness of the nanosized capsule systems can be modulated by a proper selection of emulsion and processing parameters. These results are of paramount importance, as the size control of the encapsulating particles enables to tailor their swelling kinetics, and precisely design light-controlled release systems.

3.1. Introduction

Polymeric capsules are vesicular structures [1] of varying size characterized by a polymeric solid shell surrounding a core in which an active substance in liquid, gaseous or solid form is entrapped [2,3]. The main purpose of capsules is to serve as a reservoir for the encapsulated substance and to release it under particular conditions. The concept of sub-millimeter capsule first emerged in 1950s [4]. Since then microencapsulation techniques have been well-established and a wide selection of materials has been encapsulated, among which pharmaceuticals [5], dyes [6], fragrances and flavours [7].

Nanoencapsulation is a more recent approach, which enables producing particles with size ranging from around 5–10 nm up to about 1000 nm, with prevailing dimensions between 100 and 500 nm [8,9,10]. Capsules nanosizing implies a growth in specific area of the single object, resulting in a dramatically increased interfacial area with the surrounding environment, which offers significant advantages in applications where control of release kinetics is needed, such as pharmaceuticals and material science.

In pharmaceutical applications, major benefits of nanosizing can be spotted, as reported in literature. Morey et al [11] have found that the increase in the contact area between drug and scavenging nanoparticles led to a more efficient drug detoxification than their micro counterparts. McClean et al [12] have reported on nanoparticles higher intracellular uptake due to their sub-cellular dimensions. Nanoparticle ability in improving stability of encapsulated active molecules was highlighted by Ourique et al [13]. Moreover, nanoparticles can be biocompatible with tissue and cells when synthesized from materials that are either biocompatible or biodegradable [14]. In materials science, the advantage of high contact surface between capsule and surrounding environment becomes even more significant since nanocapsules can be dispersed in a polymeric matrix, and under certain conditions they can release the encapsulated healing agent [15,16].

One of the challenging aspects of nanocapsules engineering is the achievement of controlled release under particular conditions or stimuli. That is, the polymeric shell, either preformed or synthesized in situ [17,18], is able to “respond” to external forces, such as temperature [19], enzymes [20], pH [21], ionic strength [22], magnetic field [23] or light at different wavelengths, e.g. visible [24,25], near IR [26] or UV [27]. Light induced activation offers an outstanding advantage, since it can be applied externally with high precision and enables the solid-state release even in absence of solvent [28].

Among light-triggered systems, in this work we focused on UV-light responsive polymeric capsules, characterized by the presence of azobenzene moieties as building blocks of a lightly cross-linked polyamide shell. The ability of azo-compounds to undergo reversible E-Z isomerization is widely known [29], and they have been used in a various range of applications [30,31]. Azobenzene E-Z isomerization is achieved under stationary state UV irradiation at 360 nm. Backwards transition to the more stable E form occurs either thermally or under visible light irradiation at 600 nm. This photo-isomerization ability makes azobenzene a suitable element for the synthesis of novel photo-triggered polymers [32,33].

To date, several methods of preparation of azobenzene-based capsules have been reported. In situ polymerization of azobenzene monomers has been exploited to form microcapsules shell [34]. Moreover, layer-by-layer assembly using polyanions such as DNA strands [35] as well as oppositely charged polymers bearing azo-chromophores in the side chains have also been realized [36].

Disclosed herein for the first time is the preparation of UV-responsive nano-sized capsules, based on a lightly cross-linked polyamide containing azobenzene moieties in the main chain. Nanocapsules were synthesized by oil-in-water (o/w) miniemulsion interfacial polycondensation [35,37].

Miniemulsions can be obtained through the application of intense shear forces that leads to fairly stable suspensions of sharply distributed nanosized droplets. Surfactant and co-surfactant type and concentration, along with the processing conditions, i.e. duration and intensity of ultrasonication, are the key parameters in determining capsule size distribution, thus preventing coalescence and Ostwald ripening [38,39]. Nanocapsules size is predicted to be equal to the droplets diameter of the miniemulsion they are generated from [40].

In this work, lightly crosslinked polyamide nanocapsules were prepared by polycondensation reaction that took place at the interface between the aqueous phase containing a diamine and the organic phase in which an azobenzene acyl chloride (acting also as co-surfactant) and a crosslinking agent were dissolved. The reaction rapidly produced a polyamide membrane around the oil droplets. Then, on selected nanocapsule systems, we evaluated the UV light controlled release of a fluorescent probe, paying a particular attention to the relation between capsule size and release kinetics with a view of tailoring the photoresponsiveness of nanosized capsule systems depending on specific timescale requirements.

3.2. Experimental

3.2.1. Materials

1,8-diaminooctane (DAO), 4-nitrobenzoic acid (NBA), D-(+)-glucose, phosphorus pentachloride (PCl₅), 1,3,5-benzenetricarbonyl trichloride (BTC), sodium hydrogenocarbonate, toluene, Mowiol® 18-88 (M18-88, Mw = 130000 Da), Triton® X-100 (TX100, Mn = 625 Da), the fluorescent dye coumarin 6 (C6), were purchased from Sigma-Aldrich and used without any further purification. 4,4'-bis(chlorocarbonyl)azobenzene (CAB) was synthesized according to the procedure reported in literature [41].

3.2.2. Preparation of o/w miniemulsions

Prior to nanocapsule preparation, a systematic study concerning oil-in-water emulsions was carried out to evaluate the effect of emulsion parameters, such as surfactant type and concentration in water solution on droplet size distribution and stability over time. Five formulations containing two different surfactants, M18-88 and TX100, were then chosen as templating systems for the preparation of nanocapsules according to the following general procedure.

100 mL of milliQ water was mixed under magnetic stirring with M18-88 (1.0 or 5.0 g, equivalent to $7.7 \cdot 10^{-2}$ or $3.8 \cdot 10^{-1}$ mM), or TX100 (0.1, 0.5, or 1.0 grams, equivalent to 1.6, 8.0, 16.0 mM), until a clear solution was obtained. Then 2 mL of toluene (corresponding to a 1:50 o/w volume ratio) containing 0.05 g of CAB as co-monomer and co-stabilizer were added dropwise under magnetic stirring at 400 rpm. The obtained dispersion of toluene drops in the aqueous solution was sonicated at 0 °C with a Sonics Vibracell VC505 ultrasonicator, using the following conditions: 3 cycles with 15 s pulse ON, 59s pulse OFF and 65% amplitude. Depending on the type and amount of surfactant, the resulting emulsions were labeled as EM1, EM5, ET01, ET05, ET1.

3.2.3. Synthesis of polyamide nanosized capsules.

Nanocapsules were synthesized by interfacial polymerization in an o/w miniemulsion by the following procedure. Two solutions were prepared separately:

A mother aqueous solution was prepared dissolving varying amounts (0.1, 0.5, 1.0, 5.0 grams) of surfactant (M18-88 or TX-100) in 100 mL of milliQ water. To 2.5 mL of this solution $2.58 \cdot 10^{-2}$ g of DAO ($1.79 \cdot 10^{-4}$ mol) and $3.01 \cdot 10^{-2}$ g of acid quencher NaHCO_3 ($3.58 \cdot 10^{-4}$ mol) were added (Solution 1). The remaining part was labeled as Solution 2.

An organic solution (Solution 3) was obtained by dissolving 0.05 g of CAB ($1.63 \cdot 10^{-4}$ mol), $2.87 \cdot 10^{-3}$ g of BTC ($1.08 \cdot 10^{-5}$ mol) in 2 mL of toluene (1:50 o/w volume ratio). For the evaluation of

the release kinetics, some selected samples were prepared adding to the organic phase 10 mg of fluorescent probe C6.

Solution 3 was added dropwise to Solution 2 under magnetic stirring (800 rpm). The resulting suspension was sonicated at 0 °C, giving rise to a lightly tinted pink miniemulsion. Solution 1 was added dropwise at 0 °C to the obtained suspension under stirring at 400 rpm to initiate polymerization. After 1 h the temperature was raised to ambient, and the mixture was then kept reacting overnight. In Figure 3.1. the polycondensation reaction leading to the formation of capsule shell along with the structure of the obtained nanocapsules is reported.

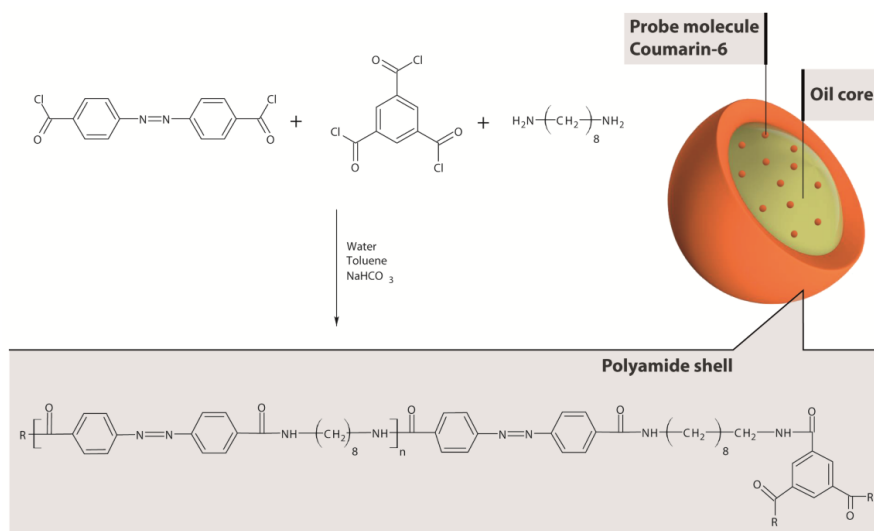


Figure 3.1. - Polycondensation reaction leading to the formation of capsule shell, and structure of the obtained nanocapsules.

The nanocapsules were finally washed using a Vivacell 250 ultrafiltration cell (Sartorius Stedim Biotech). About 4 mL of nanocapsule suspension were dispersed into 200 mL of milliQ water, and the ultrafiltration cell was connected with a flux of air at 2 bar. The cell was then placed on a GFL 3005 orbital shaker and gently stirred at 200-300 rpm. The purification procedure was repeated twice, then the capsules were stored in the aqueous suspension in darkness.

3.2.4. Methods of characterization.

The average size of emulsion droplets and nanocapsules was determined through Dynamic Light Scattering (DLS) analysis using a Zetasizer Nano ZS (Malvern Instruments). The analysis was performed at 25 °C at a scattering angle of 173°. The stability of the emulsions over time was followed by collecting DLS scans every 10 minutes starting from the miniemulsion formation.

Size and morphology of polyamide nanocapsules were characterized by means of electron microscopy. Bright field Transmission Electron Microscopy (TEM) analysis was performed using a TECNAI G12 Spirit-Twin (LaB6 source) microscope equipped with a FEI Eagle 4k CCD camera, operating with an acceleration voltage of 120 kV. Prior to analysis, a drop of the solution containing the nanocapsules was deposited on a 300-mesh copper/carbon grid, and dried overnight at room temperature. Scanning Electron Microscopy (SEM) was carried out using a FEI Quanta 200 FEG instrument in high vacuum mode, equipped with a Large Field Detector (LFD) operating with acceleration voltage ranging between 15 and 20 kV. For SEM analysis, the same grid used for TEM analysis was mounted on an aluminum stub. Prior to observation samples were metallized with an Au-Pd coating. Shell thickness of nanocapsules was determined using Image-Pro Plus Software on TEM images [42].

The kinetics of nanocapsules size change and C6 release was evaluated on nanocapsules dispersed in an aqueous solution containing 20vol % ethanol, in order improve C6 solubility. A quartz cuvette containing the nanocapsules suspension was irradiated by UV light ($\lambda_{\max} = 360$ nm, intensity 5.5 W m⁻²), from a distance of about 10 mm.

DLS and fluorescence data were collected at different irradiation times, and compared with those of an unirradiated sample kept in darkness. In particular, nanocapsules dispersions were constantly irradiated and both DLS and fluorescence data were collected every 12 min up to 72 min. The fluorescence measurements were carried out using a Perkin Elmer LS-55 Fluorescence

Spectrometer, exciting at 400 nm and monitoring the emission at 500 nm. A C6 calibration curve was prepared diluting a 10 mM stock solution of C6 in a 20 vol % ethanol solution up to concentrations of 5–50 μM . Calibration curves were obtained by fitting the fluorophore concentration curve (μM) versus the peak fluorescence intensity.

3.3. Results and discussion

3.3.1. Emulsion characterization

As extensively reported in literature [43,38], miniemulsion interfacial polymerization is sensitive to several parameters, such as processing conditions, disperse phase concentration, type and amount of surfactant and co-surfactant. In particular, the use of surfactant and osmotic pressure agent, i.e. co-surfactant prevents coalescence and Ostwald ripening [38,39]. Co-surfactants, typically dissolved in the organic phase, are molecules with ultra-low solubility in the continuous medium, able to slow down emulsion aging, the so-called Ostwald ripening effect, over a sufficient time to ensure droplet nucleation and polymerization.

Recently, we have described an optimized procedure to prepare micro-sized capsules, with diameters ranging between 30 and 120 μm [34]. In order to downsize these systems to the nanoscale a screening concerning emulsification conditions, nature and amount of stabilizers was carried out. It was found that 1:50 v/v oil-to-water ratio was effective in inhibiting droplets coalescence, whereas 3 ultrasonication cycles with 15 s pulse ON, 59 s pulse OFF and 65% amplitude were necessary to get nanosized droplets. Among different non-ionic surfactants M18-88 and TX100 were selected as more effective. The co-monomer CAB acted also as a co-stabilizer, improving the stability of the emulsions over the time required for completion of the interfacial polymerization. In this regard, Figure 3.2.a illustrates in detail the droplet size variation versus the time as measured by DLS for the selected CAB-free emulsions containing M18-88 and TX100.

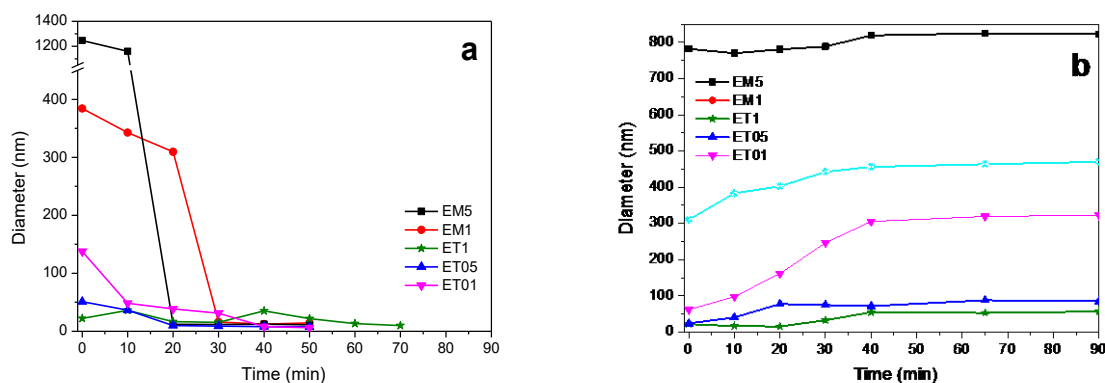


Figure 3.2. – Change of droplet diameters over time of oil-in-water emulsions of M18-88 and TX100 (a) without and (b) with CAB as co-surfactant.

For most of the analyzed systems, a decrease of diameter size in time was observed, due to the migration of toluene out of the droplets and the consequent evaporation from the aqueous continuous phase [44]. This phenomenon was evidenced by the visible change of emulsion appearance from opaque “milky” to transparent liquid. According to Tylkowski et al, interfacial polymerization occurring during microcapsule formation requires up to 90 min to go to completion [34]. Therefore, an amount of CAB equivalent to that used in nanocapsule synthesis was added to the emulsions, to evaluate the effect on the stability over time of the toluene droplets. Long-term stability of emulsions has the potential to enable effective nucleation and growth of polymer shell onto droplet surface, resulting in monodisperse nanocapsules. Size distributions of the as prepared emulsions with CAB and their variation with time up to 90 min are reported in Figure 3.2.b. The droplet diameters of the emulsions containing CAB were comparable to those measured for the emulsions free of co-stabilizer. However, CAB significantly improved the stability over time of the toluene-in-water emulsions.

For most of the analyzed systems, a decrease of diameter size in time was observed, due to the migration of toluene out of the droplets and the consequent evaporation from the aqueous continuous phase [44]. This phenomenon was evidenced by the visible change of emulsion appearance from opaque “milky” to transparent liquid. According to Tylkowski et al, interfacial polymerization occurring during microcapsule formation requires up to 90 min to go to completion [34]. Therefore,

an amount of CAB equivalent to that used in nanocapsules synthesis was added to the emulsions, to evaluate the effect on the stability over time of the toluene droplets. Long-term stability of emulsions has the potential to enable effective nucleation and growth of polymer shell onto droplet surface, resulting in monodisperse nanocapsules. Size distributions of the as prepared emulsions with CAB and their variation with time up to 90 min are reported in Figure 3.2.b. The droplet diameters of the emulsions containing CAB were comparable to those measured for the emulsions free of co-stabilizer. However, CAB significantly improved the stability over time of the toluene-in-water emulsions.

Table 3.1. – Droplet diameter and specific surface area per surfactant molecule of oil-in-water emulsions containing CAB, freshly prepared and after 40 minutes. The diameters of the correspondingly obtained nanocapsules are also reported. The reported size values were obtained through DLS measurements.

O/W Emulsions						Nanocapsules	
Acronym	Surfactant amount (wt.%)	Size (nm) t=0min	A_{surf} (nm ²)	Size (nm) t=40min	A_{surf} (nm ²)	Acronym	Size (nm)
EM5	5.0	782±190	0.67±0.16	820±190	0.64±0.15	NM5	977±268
EM1	1.0	311±90	8.33±2.43	456±210	5.67±2.61	NM1	590±223
ET1	1.0	22±4	0.57±0.10	55±11	0.23±0.04	NT1	4±1 ^a
ET05	0.5	24±10	1.03±0.44	72±46	0.35±0.11	NT05	76±28
ET01	0.1	62±8	2.00±0.25	305±28	0.38±0.03	NT01	261±30

Table 3.1. lists the droplet mean diameter values of oil-in-water emulsions containing CAB at $t = 0$ and after 40 min, along with the respective surface areas per surfactant molecule (A_{surf}) calculated according to Eq 1 [45].

$$A_{surf} = \frac{3V_{tot}}{r \cdot N_{surf}} \quad (1)$$

Where V_{tot} is the total volume of organic phase, r is the average radius of nanocapsules measured by DLS, and N_{surf} is the total number of surfactant molecules dispersed in the aqueous phase. The use of 1.0 and 5.0 wt % of M18-88 led to the formation of submicron sized droplets. Contrary to expectations, the droplet size of the 5.0 wt % emulsion was larger than that of the emulsion with 1.0 wt % M18-88. Moreover, while EM1 displayed A_{surf} values in line with data reported for polymer surfactants in miniemulsion, an unexpectedly low covered surface area value (0.67 nm²) was measured for EM5. As an example, Landfester et al. using an oligomeric surfactant in similar experimental conditions found A_{surf} values > 2.5 nm² [38,45]. These findings suggested that a significant amount of M18-88 was simply dissolved in the aqueous phase and the high viscosity of the solution containing 5 wt % of M18-88 hindered diffusion and adsorption of the emulsifier onto the droplet surface [46,47].

On the other hand, the use of TX100, characterized by a low molecular weight, allowed keeping the solution viscosity low, and facilitated purification and analysis. Depending on the amount of TX100, droplet diameter mean values were in a 10-60 nm range, corresponding to A_{surf} values ranging between 0.57 and 2.00 nm²; a quasi-micellar dispersion was obtained for 1.0 wt % [48].

As for the time stability, it was found that in the early 40 min (see Table 3.1. and Figure 3.2.b), all the emulsions showed an increase of droplet size, driven by the high tendency to reach a low A_{surf} value. In the case of ET01 and ET05, A_{surf} were in the range between 0.3 and 0.4 nm², suggesting the formation of a dense surfactant monolayer, whereas A_{surf} of ET1 reached values close to 0.2 nm² [45] due to the presence of free surfactant micelles. As for EM5, the excess surfactant and the high viscosity of the continuous phase, favored the stability of the emulsion over time. It is worth noticing that for all the emulsions the droplet size reached stability after about 40 min. Therefore, this delay time was

chosen as starting point to initiate the interfacial polycondensation through the addition of the diamine-containing solution.

3.3.2. Nanocapsules characterization

Aliphatic-aromatic polyamide nanocapsules containing either toluene or loaded with a hydrophobic dye solution were obtained via interfacial polymerization in an oil-in-water miniemulsion system as described in the experimental part. Figure 3.3. displays the nanocapsules size distributions as measured by DLS. Particle mean diameters are reported in Table 1.

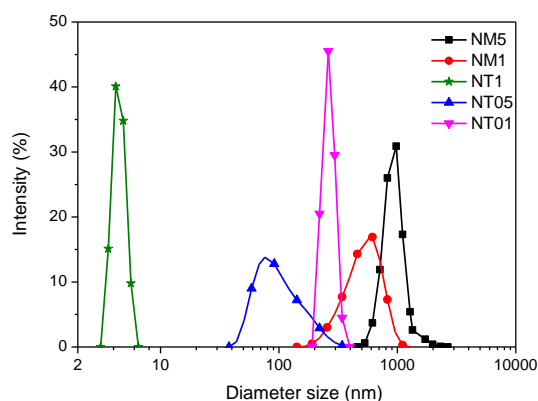


Figure 3.3. – Size distribution of the nanocapsules as measured by DLS.

It is known that for miniemulsion polymerization techniques the nanocapsules diameter is expected to be very close to that of the parent emulsion droplets. Usually the growth of minidroplets is slower than the polymerization time, and a situation very close to a 1:1 copying of the droplets to particles is obtained, freezing the critically stabilized state, being ET1-NT1 system a noticeable exception due to the formation of micellar phases, as discussed hereinafter. In all other cases case, the values of mean diameters were in good agreement with those of the corresponding emulsions, confirming that the delay time of 40 min is a satisfactory compromise between the rate of emulsion

aging and that of polymerization reaction. The resulting nanocapsules were characterized with respect to their size, morphology and release behavior.

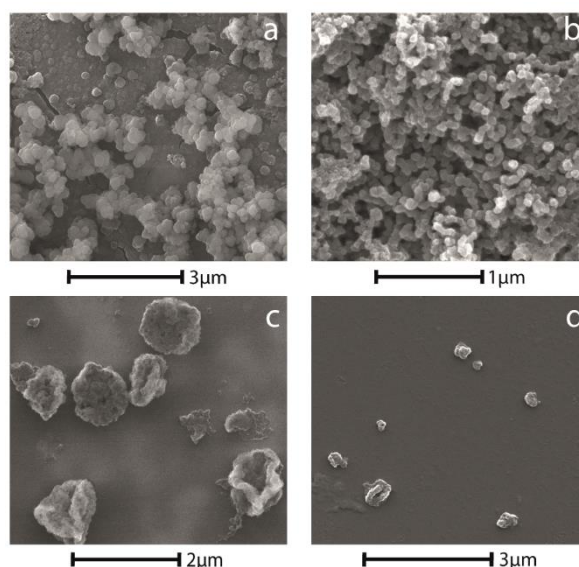


Figure 3.4. – SEM micrographs of NT01 (a), NT05 (b), NM5 (c) and NM1 (d) capsules, respectively.

Representative SEM micrographs of all prepared capsules are displayed in Figure 3.4. It is evident that the morphology of the capsules is strongly dependent on the type and concentration of surfactant used. In particular, the use of TX100 allowed obtaining smaller particles with average hydrodynamic diameter of about 260 and 80 nm (NT01 and NT05 respectively), which showed pseudo-spherical hollow morphology and solid shell structure, as shown by TEM analysis. The presence of TX100 seems to hinder fusion events of adjacent nanodroplets upon polymeric shell formation. On the other hand, nanocapsules obtained with M18-88 exhibit much larger mean diameter values (590 and 980 nm for NM1 and NM5, respectively) with a multi-fold morphology resulting from the collapse of classic hollow structures [49]. These fusion events account for the large size distribution detected through DLS analysis. TEM micrographs (Figure 3.5.) confirm the different morphologies obtained for the two systems. Moreover, by analyzing the images, it was possible to

estimate the mean shell thickness for NT05 (A) and NMI (B), which were 4.2 ± 0.3 and 26.3 ± 5.1 nm, respectively.

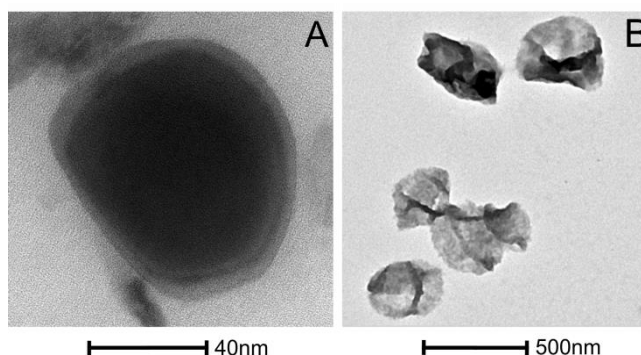


Figure 3.5. – TEM images of (a) NT05 and (b) NMI nanocapsules.

These values are in close agreement with those estimated through a theoretical calculation. In fact, based on DLS and SEM results, and according to simple geometrical considerations, for a fixed amount of starting monomers the overall calculated surface area of NT05 capsules was about 5 times higher than that of NMI (provided that the polymerization yield is the same for both systems). If we assume that NMI and NT05 polymer shells are characterized by a density of 1 g cm^{-3} , the theoretical shell thickness values are actually about 4 and 25 nm for NT05 and NMI, respectively. In particular, the values obtained for NT05 are close to those reported in literature for nanocapsules prepared by emulsion–diffusion method, in which thickness values between 1.5 and 2 nm [14] were calculated.

As previously shown in Table 3.1., considerably smaller diameters for NT1 were measured, consistently with the features of the parent emulsion ET1. Indeed, TEM image of these system reported in Figure 3.6. confirms the generation of micellar structures that inhibited the formation of nanocapsules. Moreover, due to the complete evaporation of toluene, the size of the micellar structures present in the polymerized emulsions was even smaller than that measured in the parent emulsion [50]. As a consequence, NT1 were not characterized in their release behavior.

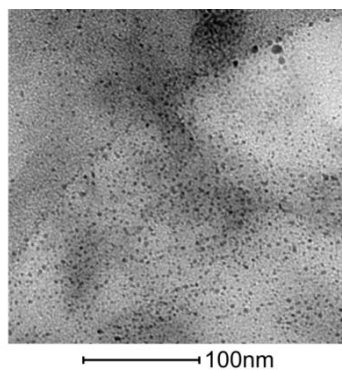


Figure 3.6. – TEM image of the micellar dispersion obtained after polymerizing the emulsion ET1, containing 1.0 wt % TX100.

3.3.3. Photo-responsiveness and release kinetics of the nanocapsules

In order to test their response to UV-irradiation, UV-Vis absorption spectra of NMI and NT05 capsules containing only toluene (i.e. with no C6 added) were measured at different irradiation times. Figure 3.7. displays the absorption peak at 320 nm, which is assigned to the π - π^* transition of the azobenzene electron system of the E form [29].

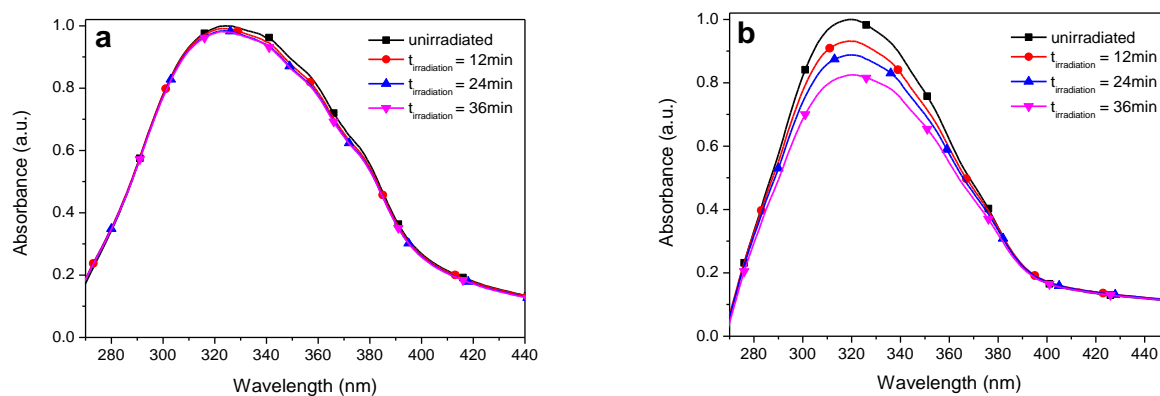


Figure 3.7. – UV-Vis absorption spectra of (a) NMI and (b) NT05 capsules measured at different times of UV irradiation at 360 nm.

The peak absorbance decreased with increasing irradiation time, indicating the occurrence of the E to Z isomerization of the azobenzene moiety. In the case of NT05, a 20% decrease of absorbance occurred in 36 min, while a change of less than 5% was displayed by NMI, indicating a lower

photosensitivity of NMI capsules. This result is related to the different capsule wall dimension characterizing the two systems, since, as discussed before, the higher the size of the capsules, the larger the resulting shell thickness. As a consequence, NMI capsules are less prone to light induced isomerization, likely being more physically constrained because of the gradual stacking of polymerized shell layers. It can be envisaged that the size of the polymeric shell plays also a predominant role in the release profile, as explained hereinafter.

The photo-responsiveness of the nano-sized capsules was evaluated by monitoring the UV-triggered release of the encapsulated fluorescent probe C6 in a 20 vol % ethanolic solution as a continuous phase. NT05 and NMI represented the lowest diameter nanocapsules in each of the two prepared families (TX-100 or M18-88 based): therefore, they were selected as representative systems for the release kinetics study. The nanocapsules suspended in the release medium were irradiated with UV light peaked at 360 nm, and the change in diameter and fluorescence were measured over the course of irradiation time using DLS and spectrofluorimetry, respectively. Figure 3.8. shows the concentration of C6 in the release medium as a function of UV exposure for NMI (a) and NT05 (b), in comparison with unirradiated samples. The same picture also reports the average diameter of the two samples versus irradiation time.

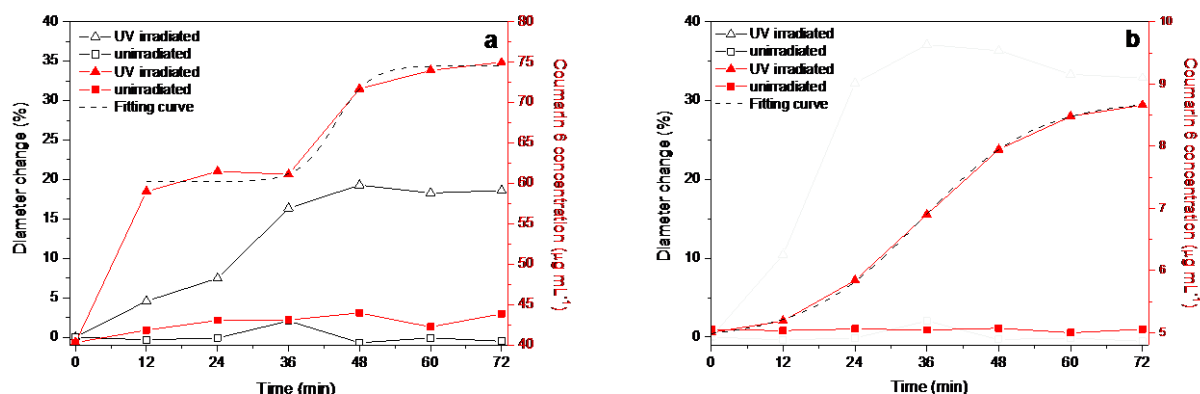


Figure 3.8. – Nanocapsule average diameter changes (empty symbols) and coumarin 6 release kinetics (full symbols) upon UV exposure for (a) NMI and (b) NT05. Values for unirradiated samples are reported as a control. Dashed lines represent fitting curves according to Boltzmann equation.

It can be noticed that the average diameter of the particles significantly increased on UV exposure, reaching in both cases a plateau value after 48 minutes of irradiation. In particular, NT05 exhibited a size increase of about 35% with respect to the initial value, whereas the NMI capsules swelled by about 20%. In addition, in the case of NMI the C6 concentration was significantly larger compared to NT05 even prior to irradiation. This result suggests that NMI had higher encapsulation efficiency. This was likely due to the ability of TX100 water solutions to dissolve C6, preventing its encapsulation during the interfacial polymerization reaction. This hypothesis was confirmed by spectrofluorometric titration of free C6 in the polymerization water solution, after centrifugation of the suspended nanocapsules. In fact, concentration of C6 was 2.8 and 78.0 $\mu\text{g mL}^{-1}$ for NMI and NT05 water solution, corresponding to an encapsulation efficiency of about 97 and 20%, respectively.

As far as the release of C6 is concerned, Figure 3.8. shows that for NT05 nanocapsules a constant value of about 5 $\mu\text{g mL}^{-1}$ was observed in absence of irradiation, attributable to the dye extracted by the ethanolic medium from the capsule surface. On the other hand, under continuous UV irradiation the dye concentration curve exhibited a sigmoidal shape, with an induction period of about 12 min, and a plateau value of about 9 $\mu\text{g mL}^{-1}$ attained after 60 min. The observed induction time suggests that a critical swelling threshold for the triggered release is about 10%. As a matter of fact, Tylkowski et al. observed similar release kinetics of β -carotene from polyamide microsized capsules as a consequence of photo-isomerization [34]. A different time-dependent release behaviour was exhibited by NMI capsules, since 12 min UV-irradiation caused a quick release of about 50% of the dye. Subsequently, the kinetic curve showed a sigmoidal shape, similarly to that observed for NT05, with a plateau value of about 75 $\mu\text{g mL}^{-1}$ after 60 min of irradiation. It is likely that a significant amount of dye was entrapped within the capsule wall, and it was released as soon as the polymer shell underwent rearrangement as a consequence of photo-isomerization. Further irradiation allowed the diffusion of the dye entrapped in the capsule core, characterized by a sigmoidal release trend. For irradiation times longer than 72 min, a slight decrease of C6 concentration was observed, suggesting

the onset of fluorophore photobleaching. In terms of release efficiency, the percentage of UV-triggered release of C6 was about 87% and 74% for NM1 and NT05, respectively. If one considers that in the case of NM1 almost 50% of dye was actually released from the capsule shell, the release efficiency of NT05 is remarkably higher, because of a greater swelling rate. The shielding effect against UV light due to the higher shell thickness can explain the reduced photo-responsiveness observed for NM1.

As reported in literature, sigmoidal fitting of the release data from a nanocarrier can be performed by means of the Boltzmann equation (Eq. 2) [51].

$$C_t = \frac{C_0 - C_f}{1 + e^{(t-t_{1/2})/d\tau}} + C_f \quad (2)$$

Where C_t represents C6 concentration measured by means of spectrofluorometry throughout the experiment, C_0 and C_f are the initial and final values of C6 concentration, respectively, $t_{1/2}$ is the time corresponding to the inflection point, at which the maximum change rate of concentration occurs, and the steepness factor $d\tau$ relates to the slope of the tangent line at $t_{1/2}$. The fitting curves according to Boltzmann equation for NT05 and NM1 are represented in Figure 3.8, and the corresponding calculated parameters are listed in Table 3.2.

Table 3.2. – Fitting parameters to Boltzman equation for the release curves in Fig. 8.

Sample	Fitting parameters			
	$t_{1/2}$ (min)	$d\tau$ (min)	C_0 ($\mu\text{g mL}^{-1}$)	C_f ($\mu\text{g mL}^{-1}$)
NM1	43.8 \pm 2,3	3.0 \pm 1.4	0.060 \pm 0.001	0.075 \pm 0.001
NT05	35.0 \pm 0.3	9.7 \pm 0.3	0.0050 \pm 0.0001	0.0087 \pm 0.0001

Interpreting the kinetic parameters is helpful in understanding the corresponding release behavior, as they can be utilized as indicators in evaluating the efficiency of an active agent. In particular, the steepness factor represents the maximum rate of released dose, whereas $t_{1/2}$ gives information on the time required for the release to occur [52]. From a design standpoint, these values can be used to predict active agent release rates, and to purposely construct a new delivery route by proper, simultaneous variation of specifically selected experimental conditions.

Quantitative values derived from Boltzmann equation applied to the kinetics of nanocapsule-mediated delivery of C6 reveal time constants $t_{1/2} = 44$ and 35 min for NMI and NT05 capsules, respectively, indicating that the smaller the capsule size, the faster the release. Furthermore, the slope $d\tau$ of the tangent line for the smaller sized capsules was about three times higher than that of the larger particles. For the latter sample a constant, sustained release spanned over a longer time, whereas a quick release was observed for NT05. The differences observed in the kinetic parameters are ascribed to different capsule size and shell thickness, which affect the response rate of the particles to the UV-light trigger in terms of swelling and release rate. These results demonstrate that a proper design of synthesis and processing parameters enables obtaining nanocarriers with tailored light-activated release profiles.

3.4. Conclusions

We have reported for the first time a straightforward route for the preparation of solid shell nanocapsules with controlled UV-triggered release. A miniemulsion interfacial polymerization technique has been employed to prepare lightly cross-linked polyamide capsules with a hydrophobic liquid core. Appropriate selection of surfactant type and concentration, as well as processing conditions allowed tailoring the size of the resulting nanocapsules. The light responsiveness of the nanocapsules systems has been evaluated by monitoring the capsule size increase and the release over

time of a fluorescent probe upon UV irradiation. The kinetics of release has been fitted to a Boltzmann equation whose parameters can be utilized as indicators in evaluating the release efficiency. It has been found that smaller capsules achieve faster release profiles, and the photo-responsiveness of the capsule systems can be modulated by proper selection of emulsion and processing parameters. Collectively, these findings outline the potential of the proposed approach in view of engineering the delivery of active agents according to specific applications.

3.5. References

- (1) Quintanar-Guerrero, D.; Allémann, E.; Fessi, H.; Doelker, E. Preparation Techniques and Mechanisms of Formation of Biodegradable Nanoparticles from Preformed Polymers. *Drug Dev. Ind. Pharm.* 1998, 24, 1113–1128.
- (2) Soppimath, K. S.; Aminabhavi, T. M.; Kulkarni, A. R.; Rudzinski, W. E. Biodegradable Polymeric Nanoparticles as Drug Delivery Devices. *J. Control. Release* 2001, 70, 1–20.
- (3) Radtchenko, I. L.; Sukhorukov, G. B.; Möhwald, H. A Novel Method for Encapsulation of Poorly Water-Soluble Drugs: Precipitation in Polyelectrolyte Multilayer Shells. *Int. J. Pharm.* 2002, 242, 219–223.
- (4) Green, B. K. Oil-Containing Microscopic Capsules and Method of Making Them, 1957.
- (5) Biju, S. S.; Saisivam, S.; Rajan, N. S. M. G.; Mishra, P. R. Dual Coated Erodible Microcapsules for Modified Release of Diclofenac Sodium. *Eur. J. Pharm. Biopharm.* 2004, 58, 61–67.
- (6) Auger, A.; Samuel, J.; Poncelet, O.; Raccurt, O. A Comparative Study of Non-Covalent Encapsulation Methods for Organic Dyes into Silica Nanoparticles. 2011, 1–12.
- (7) Ciriminna, R.; Pagliaro, M. Sol-Gel Microencapsulation of Odorants and Flavors: Opening the Route to Sustainable Fragrances and Aromas. *Chem. Soc. Rev.* 2013, 42, 9243–9250.
- (8) Quintanar-Guerrero, D.; Allémann, E.; Doelker, E.; Fessi, H. Preparation and Characterization of Nanocapsules from Preformed Polymers by a New Process Based on Emulsification-Diffusion Technique. *Pharm. Res.* 1998, 15, 1056–1062.
- (9) Mora-Huertas, C. E.; Fessi, H.; Elaissari, a. Polymer-Based Nanocapsules for Drug Delivery. *Int. J. Pharm.* 2010, 385, 113–142.
- (10) Cao, Z.; Ziener, U. Synthesis of Nanostructured Materials in Inverse Miniemulsions and Their Applications. *Nanoscale* 2013, 5, 10093–10107.

- (11) Morey, T. E.; Varshney, M.; Flint, J. A.; Rajasekaran, S.; Shah, D. O.; Dennis, D. M. Treatment of Local Anesthetic-Induced Cardiotoxicity Using Drug Scavenging Nanoparticles. *Nano Lett.* 2004, 4, 757–759.
- (12) McClean, S.; Prosser, E.; Meehan, E.; Malley, D. O.; Clarke, N.; Ramtoola, Z.; Brayden, D. Binding and Uptake of Biodegradable Poly- DL -Lactide Micro- and Nanoparticles in Intestinal Epithelia. *Eur. J. Pharm. Sci.* 1998, 6, 153–163.
- (13) Ourique, A. F.; Pohlmann, A. R.; Guterres, S. S.; Beck, R. C. R. Tretinoin-Loaded Nanocapsules: Preparation, Physicochemical Characterization, and Photostability Study. *Int. J. Pharm.* 2008, 352, 1–4.
- (14) Guinebretière, S.; Briançon, S.; Fessi, H.; Teodorescu, V. .; Blanchin, M. . Nanocapsules of Biodegradable Polymers: Preparation and Characterization by Direct High Resolution Electron Microscopy. *Mater. Sci. Eng. C* 2002, 21, 137–142.
- (15) Caruso, M. M.; Blaiszik, B. J.; Jin, H.; Schelkopf, S. R.; Stradley, D. S.; Sottos, N. R.; White, S. R.; Moore, J. S. Robust, Double-Walled Microcapsules for Self-Healing Polymeric Materials. *ACS Appl. Mater. Interfaces* 2010, 2, 1195–1199.
- (16) Borisova, D.; Möhwald, H.; Shchukin, D. G. Mesoporous Silica Nanoparticles for Active Corrosion Protection. *ACS Nano* 2011, 5, 1939–1946.
- (17) Fattal, E., Vauthier, C. Nanoparticles as Drug Delivery Systems. *Encyclopedia of Pharmaceutical Technology.*, 2002, pp. 1864–1882.
- (18) Vauthier, C.; Bouchemal, K. Methods for the Preparation and Manufacture of Polymeric Nanoparticles.pdf. *Pharm. Res.* 2009, 26.

- (19) Liu, P.; Dong, Y.; Du, P.; Mu, B. Superparamagnetic Temperature-Responsive Ionic-Cross-Linked Polymeric Hybrid Nanocapsules via Self-Templating Approach. *Ind. Eng. Chem. Res.* 2012, 51, 3350–3355.
- (20) Chen, J.; Liu, M.; Chen, C.; Gong, H.; Gao, C. Synthesis and Characterization of Silica Nanoparticles with Well-Defined Thermoresponsive PNIPAM via a Combination of RAFT and Click Chemistry. *ACS Appl. Mater. Interfaces* 2011, 3, 3215–3223.
- (21) Feng, W.; Nie, W.; He, C.; Zhou, X.; Chen, L.; Qiu, K.; Wang, W.; Yin, Z. Effect of pH-Responsive Alginate/Chitosan Multilayers Coating on Delivery Efficiency, Cellular Uptake and Biodistribution of Mesoporous Silica Nanoparticles Based Nanocarriers. *ACS Appl. Mater. Interfaces* 2014.
- (22) Antipov, A. A.; Sukhorukov, G. B.; Möhwald, H. Influence of the Ionic Strength on the Polyelectrolyte Multilayers' Permeability. *Langmuir* 2003, 19, 2444–2448.
- (23) Katagiri, K.; Nakamura, M.; Koumoto, K. Magneto-responsive Smart Capsules Formed with Polyelectrolytes, Lipid Bilayers and Magnetic Nanoparticles. *ACS Appl. Mater. Interfaces* 2010, 2, 768–773.
- (24) Nayak, S.; Lyon, L. A. Photoinduced Phase Transitions in Poly(N-Isopropylacrylamide) Microgels. *Chem. Mater.* 2004, 16, 2623–2627.
- (25) Niikura, K.; Iyo, N.; Matsuo, Y.; Mitomo, H.; Ijiri, K. Sub-100 Nm Gold Nanoparticle Vesicles as a Drug Delivery Carrier Enabling Rapid Drug Release upon Light Irradiation. *ACS Appl. Mater. Interfaces* 2013, 5, 3900–3907.
- (26) Wu, G.; Mikhailovsky, A.; Khant, H. a; Fu, C.; Chiu, W.; Zasadzinski, J. a. Remotely Triggered Liposome Release by near-Infrared Light Absorption via Hollow Gold Nanoshells. *J. Am. Chem. Soc.* 2008, 130, 8175–8177.

- (27) Bédard, M. F.; De Geest, B. G.; Skirtach, A. G.; Möhwald, H.; Sukhorukov, G. B. Polymeric Microcapsules with Light Responsive Properties for Encapsulation and Release. *Adv. Colloid Interface Sci.* 2010, 158, 2–14.
- (28) Dispinar, T.; Colard, C. a. L.; Du Prez, F. E. Polyurea Microcapsules with a Photocleavable Shell: UV-Triggered Release. *Polym. Chem.* 2013, 4, 763.
- (29) Mita, I.; Horie, K.; Hirao, K. *Photochemistry in Polymer Solids*. 9. Photoisomerization. 1989, 558–563.
- (30) Tseng, C.-W.; Huang, D.-C.; Tao, Y.-T. Electric Bistability Induced by Incorporating Self-Assembled Monolayers/aggregated Clusters of Azobenzene Derivatives in Pentacene-Based Thin-Film Transistors. *ACS Appl. Mater. Interfaces* 2012, 4, 5483–5491.
- (31) Akiyama, H.; Kanazawa, S.; Okuyama, Y.; Yoshida, M.; Kihara, H.; Nagai, H.; Norikane, Y.; Azumi, R. Photochemically Reversible Liquefaction and Solidification of Multiazobenzene Sugar-Alcohol Derivatives and Application to Reworkable Adhesives. *ACS Appl. Mater. Interfaces* 2014.
- (32) Peris, S.; Reina, A.; Tylkowski, B.; Ronda, J. C.; Garcia-valls, R.; Giamberini, M.; Rovira, U.; Marcel, C. Synthesis, Characterization, and Photoresponsiveness of New Azobenzene-Containing Polyethers. *Polym. Chem.* 2009, 47, 5426–5436.
- (33) Tylkowski, B.; Peris, S.; Giamberini, M.; Garcia-Valls, R.; Reina, J. A.; Ronda, J. C. Light-Induced Switching of the Wettability of Novel Asymmetrical Poly(vinyl Alcohol)-Co-Ethylene Membranes Blended with Azobenzene Polymers. *Langmuir* 2010, 26, 14821–14829.
- (34) Tylkowski, B.; Pregowska, M.; Jamowska, E.; Garcia-Valls, R.; Giamberini, M. Preparation of a New Lightly Cross-Linked Liquid Crystalline Polyamide by Interfacial Polymerization. Application to the Obtainment of Microcapsules with Photo-Triggered Release. *Eur. Polym. J.* 2009, 45, 1420–1432.

- (35) Tanaka, F.; Mochizuki, T.; Liang, X.; Asanuma, H.; Tanaka, S.; Suzuki, K.; Kitamura, S.; Nishikawa, A. Robust and Photocontrollable DNA Capsules Using Azobenzenes. *Nano Lett.* 2010, 10, 3560–3565.
- (36) Yi, Q.; Sukhorukov, G. B. UV-Induced Disruption of Microcapsules with Azobenzene Groups. *Soft Matter* 2014, 10, 1384–1391.
- (37) Perignon, C.; Ongmayeb, G.; Neufeld, R.; Frere, Y.; Poncelet, D. Microencapsulation by Interfacial Polymerisation: Membrane Formation and Structure. *J. Microencapsul.* 0, 1–15.
- (38) Landfester, K. Polyreactions in Miniemulsions. *Macromol. Rapid Commun.* 2001, 22, 896–936.
- (39) Tadros, T. F. *Emulsion Science and Technology*; 2009.
- (40) Landfester, K. Quantitative Considerations for the Formulation of Miniemulsions. In *Adsorption and Nanostructure SE - 18*; Dékány, I., Ed.; Springer Berlin Heidelberg, 2002; Vol. 117, pp. 101–103.
- (41) Ameerunisha, S.; Zacharias, P. S. Characterization of Simple Photoresponsive Systems and Their Application to Metal Ion Transport. *J. Chem. Soc.* 1995, 2–5.
- (42) Chen, T.; Du, B.; Zhang, X.; Fan, Z. Fabrication of Polymer Nanocapsules with Controllable Oligo (Ethylene Glycol) Densities , Permeation Properties and Robustly Crosslinked Walls. *ACS Appl. Mater. Interfaces* 2013, 5, 3748–3756.
- (43) Schork, J.; Luo, Y.; Smulders, W.; Russum, J. P. .; Buttè, A.; Fontenot, K. Miniemulsion Polymerization. *Adv Polym Sci* 2005, 129–225.
- (44) Fryd, M. M.; Mason, T. G. Time-Dependent Nanoemulsion Droplet Size Reduction By Evaporative Ripening. *J. Phys. Chem. Lett.* 2010, 1, 3349–3353.

- (45) Landfester, K.; Bechthold, N.; Tiarks, F.; Antonietti, M. Miniemulsion Polymerization with Cationic and Nonionic Surfactants: A Very Efficient Use of Surfactants for Heterophase Polymerization. *Macromolecules* 1999, 32, 2679–2683.
- (46) Jafari, S. M.; He, Y.; Bhandari, B. Optimization of Nano-Emulsions Production by Microfluidization. *Eur. Food Res. Technol.* 2006, 225, 733–741.
- (47) Troncoso, E.; Aguilera, J. M.; McClements, D. J. Influence of Particle Size on the in Vitro Digestibility of Protein-Coated Lipid Nanoparticles. *J. Colloid Interface Sci.* 2012, 382, 110–116.
- (48) Khakpay, A.; Abolghasemi, H.; Salimi-Khorshidi, A. The Effects of a Surfactant on Mean Drop Size in a Mixer-Settler Extractor. *Chem. Eng. Process. Process Intensif.* 2009, 48, 1105–1111.
- (49) Chen, T.; Du, B.; Fan, Z. Facile Fabrication of Polymer Nanocapsules with Cross-Linked Organic - Inorganic Hybrid Walls. *Langmuir* 2012, 28, 11225–11231.
- (50) Mishael, Y. G.; Dubin, P. L. Toluene Solubilization Induces Different Modes of Mixed Micelle Growth. *Langmuir* 2005, 21, 9803–9808.
- (51) Koffie, R. M.; Farrar, C. T.; Saidi, L.-J.; William, C. M.; Hyman, B. T.; Spires-Jones, T. L. Nanoparticles Enhance Brain Delivery of Blood–brain Barrier-Impermeable Probes for in Vivo Optical and Magnetic Resonance Imaging. *Proc. Natl. Acad. Sci.* 2011, 108, 18837–18842.
- (52) Wang, X.; Li, S.; Wang, L.; Yi, X.; Hui, Y. S.; Qin, J.; Wen, W. Microfluidic Device for Controllable Chemical Release via Field-Actuated Membrane Incorporating Nanoparticles. *J. Nanomater.* 2013, 2013, 1–6.



CHAPTER 4

Light-induced Release of Essential Oils from Polymer Nanocapsules

Valentina Marturano, Valentina Bizzarro, Anna Calarco, Pierfrancesco Cerruti, Marta Giamberini,

Bartosz Tylkowski, Veronica Ambrogi.

In preparation for submission

ACS Sustainable Chemistry and Engineering

Abstract

The present work reports the preparation of light-responsive Polyamide nanosized capsules containing azobenzene moieties in the main chain via interfacial polycondensation in oil-in-water miniemulsion. Noticeably, the potentially toxic organic solvent traditionally used in this class of reactions was replaced with natural essential oils, also employed for their powerful antimicrobial effect, resulting in a more sustainable and green functional system. The presence of azobenzene segments in the capsule shell is the cause for the capsule photo-responsive behavior, since trans-to-cis isomerization of azobenzene, triggered by UV light irradiation (360nm) leads to major rearrangements in the polymer shell and consequent release of the encapsulated core material. Release kinetics of essential oils and fluorescent probe molecule, coumarin-6, were evaluated via UV-vis spectrometry and spectrofluorimetry respectively, proving the efficiency of the release mechanism. Capsules size and morphology were evaluated via dynamic light scattering (DLS) and electron microscopy (SEM and TEM). The cytotoxicity of the nanocapsules was also evaluated via trypan blue exclusion assays and the results proved that the nanocapsules were non-toxic and could be used in environmentally friendly applications.

4.1. Introduction

Stimuli-responsive micro and nanocapsules are recently attracting a growing interest of academic and industrial research and have found application as smart carriers for active agents. Numerous examples of *stimuli*-triggered release of drugs [1], self-healing agents [2] or fragrances [3] are reported in the literature of the latest years. Higher quality storage, minimized reactivity and custom-designed release of core materials, are only some of the advantages of dealing with encapsulated substances rather than pristine ones. The design of highly performing stimuli-responsive systems includes the quest for appropriate triggering factors. In this frame, light (infrared, visible or ultraviolet) represents the best option as one of the few remote control and one of the least harmful triggering factors available [4].

The photo-responsive behavior of polymers is generally provided by photo-sensitive moieties introduced in the polymeric backbone or in the side chains. Some of the most performing photo-sensitive molecules are based on azobenzene [5], stilbene [6] or spiroiranes [7]. In particular, azobenzene is recognized as the most reliable and versatile molecular switch. The photoactivity of azo-groups is exhibited as a result of the existence of two interconvertible geometrical isomers. Upon irradiation at a certain wavelength, generally ultraviolet light, the di-azo bond undergoes a conformational transition, changing the symmetry of the molecule from a thermally stable *trans* orientation to a less favorable *cis* orientation [8].

One of the most sensitive factors involved in this process is the choice of the organic phase, that needs to meet two requirements: it must serve as good solvent for the acyl chloride monomer, and it should not react with the monomers involved in the process. Until now organic solvents, such as toluene or chloroform have been employed [4, 5]. However, they have the remarkable disadvantage of being potentially toxic [9].

The search for viable alternatives to organic solvents is indeed one of the key points in the trending concept of “green” chemistry. Among the vast variety of substances available, the class of natural oils (NOs) emerged as the most valuable alternative to traditional organic solvents. NOs are aromatic hydrophobic liquids obtained from plant material (seeds, leaves, fruits and roots) [10], their antioxidant and antimicrobial properties are well known and vastly reported in literature [11, 12].

Photo-responsive NOs-loaded nanocapsules can potentially be applied in a wide range of applications, such as food packaging [13], pesticides [14] and health-care [15] applications. For example, in the last decades the food packaging industry showed interest in innovative materials technology and in the concept of “active” packaging [16], upgrading the traditional container with new features that help preserving freshness, quality and safety and in general extend shelf life of perishable foodstuff. Natural oils, with their antimicrobial activity, can be introduced in packaging materials in different forms: dispersed films and coatings [17, 18], entrapped in nanoparticles [19] or encapsulated [20].

The use of nanocapsules and nanocarriers also constitute a strong asset in the biomedical field, where controlled delivery of drugs is a necessary feature for therapeutics and imaging in many diseases [21, 22]. In healthcare applications light-responsive materials can be employed wherever light is available, which means that the use of UV and visible light in triggered release is suitable for topical application, while IR light, characterized by higher penetration depth, can also be used in internal applications [23].

The aim of this work was to investigate encapsulation and UV-induced release of NOs and C6 from polymeric nanocapsules obtained via interfacial polycondensation in miniemulsion. Many NOs have been tested as suitable core phase, that can be classified in three main groups, on the basis of their chemical composition, namely terpenoids, aldehydes and phenolic compounds. Each of the tested compounds have been reviewed as powerful biological active agents, characterized by antimicrobial, anti-inflammatory and antioxidant activity [24, 25]. Taking all into account, the

reported nanocapsules system can find promising application in a broad range of technological fields, thanks to the photo-responsive behavior of the capsule shell, the use of green alternatives to potentially harmful organic solvent and the multitasking features of NOs as active agents and cargo solvents for other active molecules.

In this paper, following the procedure reported in a previous work [4], light-responsive polymeric nanocapsules were prepared by oil-in-water interfacial polycondensation in miniemulsion, one of the most employed methods to obtain hollow capsules with a solid shell [26] Accordingly, the polycondensation reaction takes place at the interface between the organic phase, containing the azobenzene acyl chloride and a crosslinking agent, and the continuous aqueous phase, containing a diamine. When these three monomers meet at the interface of each oil droplet, they react to form the lightly cross-linked polyamide membrane, that forms the polymeric shell of the capsules. The obtained nanocapsules were able to release the encapsulated core material when irradiated with UV light at 360 nm. At this specific wavelength, the *trans*-to-*cis* photo-isomerization of azobenzene is triggered, resulting in a massive rearrangement of the shell, from a “closed” conformation to a more “open” one allowing the release of the encapsulated molecule.

4.2. Experimental

4.2.1. Materials

1,8-diaminooctane (DAO), 1,3,5-benzenetricarbonyl trichloride (BTC), sodium hydrogenocarbonate, Mowiol 18-88 (M18-88, $M_w = 130$ kDa), the fluorescent dye Coumarin-6 (C6), were purchased from Sigma-Aldrich and used without any further purification. 4,4'-bis(chlorocarbonyl)azobenzene (CAB) was synthesized according to the procedure reported in literature [5]. All NOs were used without any further purification: (-)- menthone (90% pure), (+)- carvone (96% pure), citronellal (>95% pure), benzaldehyde (99.5% pure), *trans*- cinnamaldehyde

(99% pure), linalool (97% pure), thymol (99% pure), eugenol (99% pure) and carvacrol (90% pure) were purchased from Sigma-Aldrich; basil, thyme and turpentine essential oils were purchased from Pharmalab, orange terpenes were purchased from Visalli.

4.2.2. Choice of natural oils as organic phase

The NO selection was initially carried out screening three main classes of compounds as summarized in Figure 4.1.: terpenoids, aldehydes and phenolic compounds. The compounds under study are both essential oils, constituted by a mixture of molecules, and their single-component extracts. For example, thymol is extracted from thyme essential oil being its most abundant component (see Table 1).

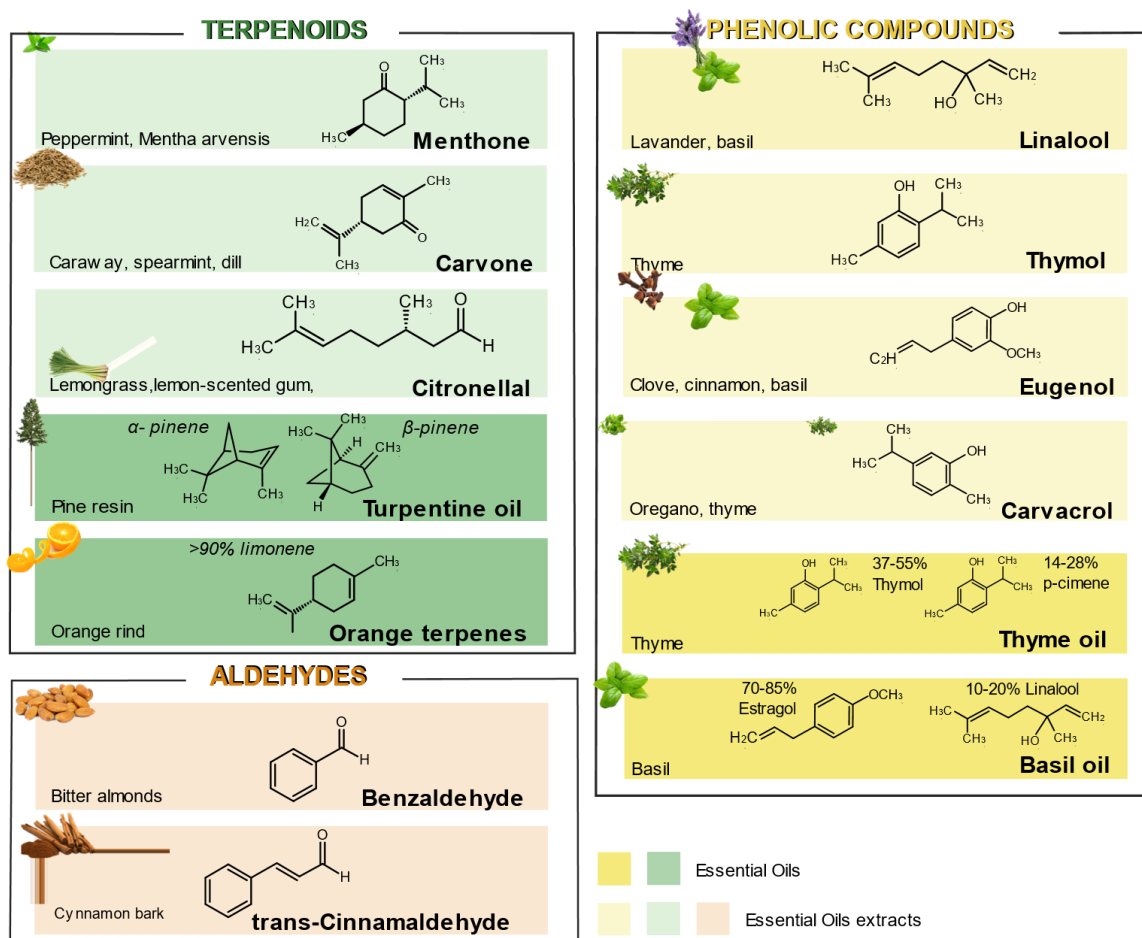


Figure 4.1. – Classification of NOs based on their chemical composition.

To be selected as a suitable organic phase for the miniemulsion interfacial polycondensation procedure, the thirteen natural oils needed to meet two criteria: each had to be a good solvent for CAB monomer and at the same time chemically inert toward CAB and DAO monomers involved in the reaction. Solubility tests were carried out dispersing 5 mg of CAB in 200 μ L of each NO and leaving the solution under magnetic stirring for 20 min, both at room temperature and at 50°C. The presence of a solid residue labeled each NO as unsuitable to be a good solvent for CAB and relieved it from further investigations. To exclude any reaction between CAB or DAO with NOs, reactivity tests were performed for each essential oil on CAB/EO and DAO/EO solutions, using Thin Layer Chromatography (TLC). Silica gel TLC plates coated with fluorescent indicator F254 (Millipore) and a toluene/methanol 80:20 mixture was used as stationary phase and eluent respectively. The stains on the silica gel substrate were observed using a UV lamp with maximum emission wavelength equal to 254 nm. To detect any reaction between NO and monomer, three samples were deposited and analyzed:

(a) CAB reference: 5 mg of CAB were dissolved in 200 μ L of chloroform (CHCl_3), and added to 2 mL of CHCl_3 .

(b) NO reference: 200 μ L of essential oil were dissolved in 2 mL CHCl_3

(c) CAB in NO sample: 5 mg of CAB were dissolved in 200 μ L of essential oil, and added to 2 mL of CHCl_3 .

The same procedure was repeated using DAO monomer instead of CAB.

4.2.3. Preparation of Nanocapsules from o/w emulsion

Nanocapsules were obtained by interfacial polycondensation in o/w miniemulsion. The organic phase, containing the CAB monomer and a small percentage of the crosslinking agent, was dispersed in a water phase containing a fixed amount of surfactant. High shear homogenization

(IKA Ultraturrax) was chosen to obtain a stable nano-sized emulsion. Once the miniemulsion was formed, a second aqueous solution, containing the second monomer, DAO, was added dropwise. The lightly cross linked polymer, resulted from the polycondensation reaction between DAO and CAB, quickly precipitates at the interface of the emulsion droplets. The reaction proceeds by diffusion of one of the monomers through the already formed shell (Figure 4.2).

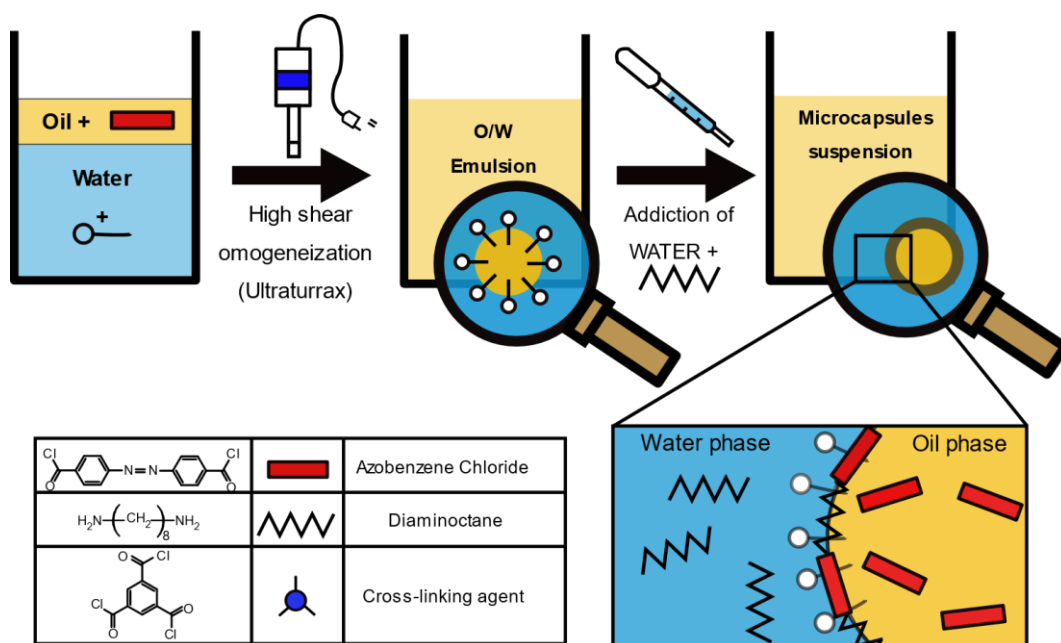


Figure 4.2. – Schematic representation of the interfacial polycondensation reaction in miniemulsion.

Nanocapsules containing thyme (NCT) and basil (NCB) oils were prepared according to the following detailed procedure: two solutions were separately prepared, an aqueous phase and an organic phase, respectively:

Aqueous phase (Mother solution)

Mother solution was prepared dissolving, in 100 mL of milliQ water, 1 g (1 wt.%) of surfactants (Mowiol 18-88). From mother solution two different solutions were obtained: Solution

1 consisted of 30 mL of mother solution. Solution 3 was prepared by dissolving 0.061 g of 1,8-diaminooctane and 0.071 g of acid quencher NaHCO₃ in 6 mL of mother solution.

Organic phase:

Solution 2 was obtained dissolving in 6 mL of thyme or basil essential oils (EO) (1:6 v/v o/W ratio) 0.125 g of 4,4'-bis(chlorocarbonyl)azobenzene, 0.00335g of benzene tricarbonyl trichloride (crosslinker) and 4 mg of Coumarin-6. To dissolve azobenzene in the EO, the solution was kept under magnetic stirring (500 rpm) until the solid was dissolved and the red solution appeared clear.

Solution2 was then added drop-wise to Solution 1 under magnetic stirring (800 rpm) for 15 min. In these conditions an unstable system prone to phase separation was obtained, afterwards it was ultraturaxed in ice bath (0°C) at 8000 rpm for 15 min, giving rise to a lightly tinted yellow emulsion. Solution 3 was then added drop-wise to the Solution 1+2 for 20 min, under magnetic stirring at 400 rpm.

4.2.4. Methods of characterization

4.2.4.1. Size and morphology

The nanocapsules average size was determined via Dynamic Light Scattering (DLS) analysis using a Zetasizer Nano ZS (Malvern Instruments). The analysis was performed at 25 °C at a scattering angle of 173°.

Size and morphology of nanocapsules were characterized by means of electron microscopy. Bright field Transmission Electron Microscopy (TEM) analysis was performed using a TECNAI G12 Spirit-Twin (LaB₆ source) microscope equipped with a FEI Eagle 4k CCD camera, operating with an acceleration voltage of 120 kV. Prior to analysis, a drop of the solution containing the nanocapsules

was deposited on a 300 mesh copper/carbon grid, and dried overnight at room temperature. Scanning Electron Microscopy (SEM) was carried out using a FEI Quanta 200 FEG instrument in high vacuum mode, equipped with a Large Field Detector (LFD) operating with acceleration voltage ranging between 15 and 20 kV. For SEM sample preparation, a drop of washed nanocapsules solution was deposited on an aluminum stub and metallized with an Au-Pd coating.

4.2.4.2. EOs Encapsulation efficiency

The encapsulation efficiency was evaluated via UV-vis spectroscopy, thanks to the absorbance peak of basil and thyme EOs at around 278 nm. The evaluation of the encapsulation efficiency (EE) were performed using both indirect and direct methods.

The *indirect method* involves the evaluation of encapsulated EO as the difference between the theoretical EO content involved in the procedure and the free oil detected in the supernatant. Accordingly, 100 μ L of nanocapsules suspension containing thyme or basil EO (NCT and NCB, respectively) were mixed with 25 mL of 80% ethanol solution and placed on an orbital shaker at 200 rpm for 20 min. The so obtained suspension was then filtered with a CA filter with 0.2 μ m cutoff, removing all the nanocapsules. 1 mL of the so obtained solution was diluted with 6 mL 80% EtOH solution and analyzed via UV-vis spectroscopy. The procedure was repeated 3 times and the absorbance values were then converted into concentration values using calibration line of the thyme or basil EO in 80% EtOH. The encapsulation efficiency (EE') was calculated using the following equation:

$$EE' = (C_0 - C_0^F) / C_0 \quad (1)$$

Where C_0 is the theoretical concentration of the oil and C_0^F is the free oil concentration evaluated as reported above.

The *direct method* for the encapsulation efficiency (EE) evaluation is based on the quantification of the EO extracted from nanocapsules. 200 mL of NCT or NCB were mixed with 6 mL of DMSO and placed in a sealed flask under magnetic stirring at 200 rpm at 70°C for 24h. 200 mL of the obtained suspension were then diluted in 5 mL of DMSO and observed via UV-vis spectroscopy. The procedure was again repeated three times and the absorbance values were converted in concentration values using the calibration line of thyme and basil oil in DMSO. The encapsulation efficiency obtained via the direct method (EE) was calculated using the following formula:

$$EE = [C_0 - C_0^* (1 - EE')] / C_0 \quad (2)$$

Where C_0 is the theoretical concentration of the oil, C_0^* is the concentration of oil extracted by DMSO and measured as reported above and EE' is the encapsulation efficiency calculated using the indirect method.

4.2.4.3. EOs release kinetics

Basil and thyme EOs both show a defined absorption peak in the UV-vis spectra, therefore UV-vis spectrometry can be exploited to evaluate the increase in the oil concentration as a function of irradiation time. Variations in thyme and basil EOs concentration were analyzed via UV-vis spectroscopy, using an 80 vol % ethanolic solution as release media, in order improve EOs solubility. In a typical experiment, 200 μ L of nanocapsules were dispersed in 10 mL 80% EtOH solution and stirred at room temperature for 5 min at 200 rpm. The dispersion was then placed in two quartz testing tubes, containing approximately 5 mL each. One testing tube containing the nanocapsules was irradiated by UV light ($\lambda_{max} = 360$ nm, intensity 5.5 W m^{-2}) from a distance of about 2 cm, the other was kept in darkness. Two different release experiments were performed, one with continuous irradiation of the sample and the other with three irradiation cycles of 15 min each. Periodically, 100

μL of each sample were collected, dispersed in 3 mL EtOH solution, filtered with a PTFE filter with 0.2 μm cut-off and analyzed via UV-vis spectroscopy.

4.2.4.4. C6 release kinetics

Further analysis on the photo-triggered release were performed via spectrofluorimetry on NCT capsules, loaded with the fluorescent probe molecule Coumarin-6 (C6). In a typical experiment, 50 μL of NCT sample was dispersed in 50 mL aqueous solution containing 80 vol% ethanol (EtOH 80%), to improve C6 solubility in the release media. A quartz cuvette containing the (25 times) diluted nanocapsules suspension was then irradiated with UV light ($\lambda_{\text{max}} = 360 \text{ nm}$, intensity 5.5 W m^{-2}) from about 2 cm. The samples underwent two different irradiation procedures: a continuous irradiation and a sequence of three 15-min long irradiation. Fluorescence data of the irradiated samples were collected periodically, until a plateau value was reached, and compared to the spectra of an un-irradiated sample, kept in darkness between two measurements. All fluorescence measurements were carried out using a Perkin Elmer LS-55 Fluorescence Spectrometer, exciting at 390 nm and monitoring the emission at 500 nm.

4.2.4.5. Cytotoxicity and Uptake tests

Cytotoxicity test were performed by means of Trypan blue exclusion assay using Normal Rat Kidney Epithelial Cells (NRK). Cells were seeded in 24-well plates at the density of 1×10^4 cells/ml in Dulbecco's Modified Eagle Medium (DMEM) supplemented with 10% fetal bovine serum (FBS), 1% penicillin and streptomycin, 1% glutamine and allow to adhere. NRK were grown for 24-48-72 h in presence of 10, 25, 50, 100 and 250 $\mu\text{g/ml}$ nanocapsules solution. Then, a half mL aliquot of cell suspension was mixed with 0.5 mL of 0.4% trypan blue dye and left for 5 min at room temperature.

Cell number was counted on a hemocytometer and the proliferation indexes (N/N_0 , where N is the total number of cells at $T=24, 48$ or 72 h and N_0 is the number at $T=0$) was determined.

Concerning cellular uptake, Normal Rat Kidney Epithelial Cells (NRK) were seeded in 24-well plates at the density of $1,5 \times 10^4$ cells/ml, and treated with 10 and 50 $\mu\text{g/ml}$ of nanocapsules samples. After 24 h cells were fixed with paraformaldehyde and stained with 4',6-diamidin-2-fenilindolo (DAPI). Nanoparticles uptake were visualized by fluorescent microscope (Leica fluorescence microscope model ax70) at an excitation wavelengths of 450 nm for DAPI.

4.3. Results and discussion

4.3.1. Selection of essential oils

As mentioned above, the use of natural oils in nanocapsules preparation has different advantages concerning both the encapsulation procedure, since NOs can substitute traditional unhealthy organic solvents, and the final application, because of their beneficial effects on human health. However, prior to their use it was necessary to evaluate their suitability for the protocol adopted for nanocapsules synthesis. In particular, they had to be good solvents for the acyl chloride monomer, and inert towards the monomers involved in the encapsulation process. Accordingly, solubility and reactivity tests were carried out to select the NOs possessing the needed requirements.

As shown in Table 4.1., this procedure highlighted advantages and drawbacks of each compound. For example, aldehydes were excellent solvents for CAB but they were too reactive, terpenoids were not able to dissolve CAB even at high temperature ($T = 50$ °C), while phenolic compounds were good solvents at high temperature, and were generally less prone to react. Therefore, among thirteen NOs tested, thyme and basil essential oils (EOs) were considered suitable alternatives as organic phase for the miniemulsion polycondensation reaction. Basil and thyme EOs are reported to have powerful antimicrobial, antifungal and antimould effect [26-28]. Antioxidant activity of basil

and thyme oil have also been studied [29]. It is worth noticing that thymol and carvacrol, the main active components of thyme and basil oil, respectively are volatile. This feature makes them suitable for a variety of non-contact mode applications, such as household [30], healthcare [31] and active packaging [32].

Table 4.1. – NOs behavior as CAB solvents and their reactivity toward CAB and DAO monomers.

Essential Oil (EO)		CAB Solubility		Reactivity	
Name	Composition	25°C	20 min at 50°C	CAB	DAO
Terpenoids	(-)- Menthone	No	Solid residue	-	-
	(+)- Carvone	Yes	Yes	Ok	Reacts
	Citronellal	No	Solid residue	-	-
	Turpentine	No	No	-	-
	Orange terpenes	No	No	-	-
Aldehydes	Benzaldehyde	Yes	Yes	n.d.	n.d.
	Trans- cinnamaldehyde	Yes	Yes	Reacts	Reacts
Phenolic compounds	Linalool	No	Solid residue	-	-
	Thymol	No	Solid residue	-	-
	Eugenol	No	Solid residue	-	-
	Carvacrol	Yes	Yes	Reacts	ok
	Thyme oil	No	Yes	ok	ok
	Basil oil	No	Yes	ok	ok

4.3.2. Nanocapsules characterization

4.3.2.1 Nanocapsules size and morphology

On the basis of the results discussed above, NCB and NCT samples were prepared following the procedure reported in section 2.2, using basil and thyme oil, respectively, as organic phase for the

interfacial polycondensation in miniemulsion. SEM (Figure 4.3.a,b) and TEM (Figure 4.3.c,d) micrographs allowed the evaluation of capsules shape and morphology. For both systems, pseudo-spherical particles formed. However, NCB exhibited a multi-fold, lobate morphology, whereas NCT were more regularly shaped and prone to agglomerate [4].

Measurements of NC mean diameter obtained via Dynamic Light Scattering were compared with data gathered from dimensional analysis of SEM micrographs carried out by means of ImageProPlus6 software (Figure 4.3.e-f).

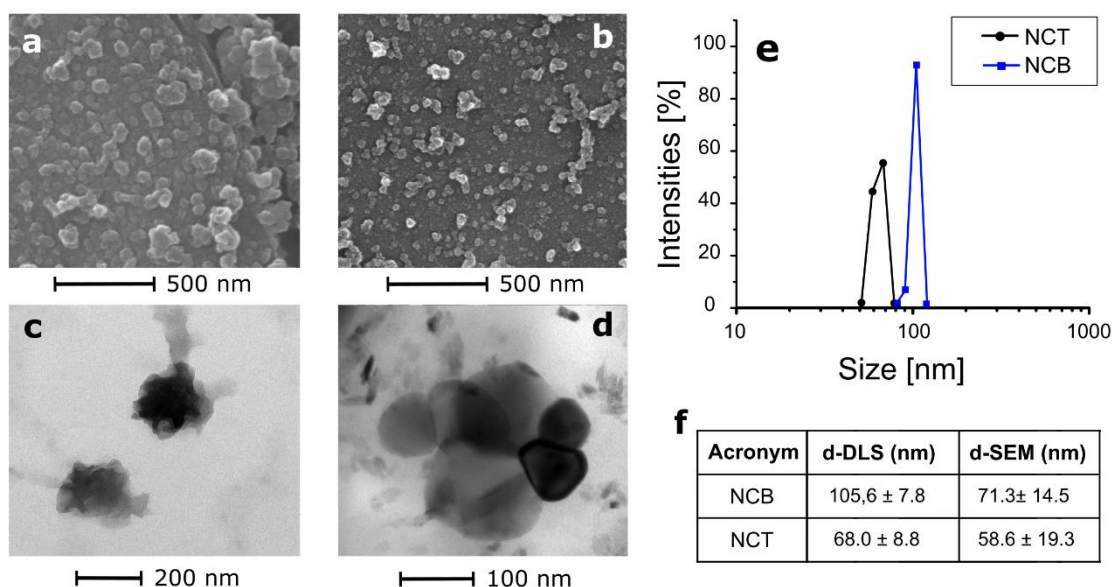


Figure 4.3. – SEM micrographs of (a) NCB and (b) NCT, TEM micrographs of (c) NCB and (d) NCT. (e) Scattering intensity vs. particle diameter (nm) of both nanocapsules samples, and (f) comparison of DLS and SEM analysis data.

As shown in Figure 4.3., both nanocapsules systems were characterized by a narrow particle size distribution. Diameter values calculated through DLS were 68 and 106 nm for NCT and NCB, respectively, while SEM analysis yielded values of 58.6 and 71.3 nm. If one considers the two different measurement conditions, the two methods provided consistent results, demonstrating that, on

average, NCT capsules were slightly smaller than NCB. Most probably, in the conditions used, thyme oil was more efficiently emulsified in the aqueous phase giving rise to smaller droplets.

4.3.2.2 Encapsulation efficiency

The determination of the encapsulation efficiency was carried out using two methods, according to the procedure reported in the experimental section 2.4.2. An *indirect* measurement involved the dilution on the nanocapsules suspension with 80% EtOH solution that, at room temperature and for reduced contact times (20 min), was able to dissolve the un-encapsulated EOs present on the external surface of capsules and in the aqueous phase. The average value of *indirect* encapsulation efficiency (EE') was calculated by UV-vis spectroscopy of filtered diluted NC suspension, using Equation 1. EE' values of $87.3 \pm 3.5\%$ and 94.2 ± 2.3 were obtained for NCB and NCT, respectively. To confirm these results, a *direct* method involving quantitative evaluation of the encapsulated EOs by DMSO extraction was also employed. Indeed, the use of DMSO at 70 °C for 24h resulted in a complete extraction of encapsulated EOs from the core. The direct encapsulation efficiency (EE) values obtained using equation 2 were $86.0 \pm 2.0\%$ and $95.7 \pm 0.3\%$ for NCB and NCT, respectively. It is worth to notice that, for both NCB and NCT, EE' and EE values were consistent, confirming the reliability of the two methods. These data can be correlated with the different reported solubility of the two EO in water. In fact, a theoretical calculation based on the average composition of the employed EOs demonstrated that thyme oil was more soluble than basil oil in water (Table X in Supporting Information).

As reported by Mora-Huertas et al. [33] nanoprecipitation, emulsion–diffusion and layer-by-layer methods currently provide the best results for encapsulation efficiency (80% or more). In this work, a high encapsulation efficiency was achieved via EOs emulsion in water, since each oil droplet serves as a reservoir of CAB monomer as well as a template for nanocapsules formation.

4.3.3. Photo-responsiveness and release kinetics

The UV-responsiveness of nanocapsules is due to the presence of CAB in the polyamide main chain. The release study was carried out on systems encapsulating EOs and the fluorescent probe C6, employed as a model drug. The UV-induced release behavior was evaluated by diluting NC suspension in 80% EtOH solution and following two different experimental protocols [34].

The release kinetics of EOs were studied by evaluating the concentration of EOs in the release medium via UV-vis spectrophotometry. In a first experiment, the NC suspensions were continuously irradiated for 180 minutes and UV-vis spectra collected every 15-30 min. In a second experiment, NCs underwent pulsed UV irradiation (2 cycles of 15 min) and the EOs concentration was monitored for a total period of 1000 min under dark conditions. Unirradiated samples were also tested and used as control experiments.

In Figure 4.4., release kinetics of NCB and NCT samples are reported, showing the oil concentration as a function of the irradiation time as a result of the two described procedures. In Figure 4.4.A it can be observed that for both unirradiated NCT and NCB, the EOs concentration values are constantly low. On the other hand, when irradiated the EOs concentration increased with time, reaching a plateau value after about 120 minutes, indicating the efficiency of the UV light stimulus in triggering the release.

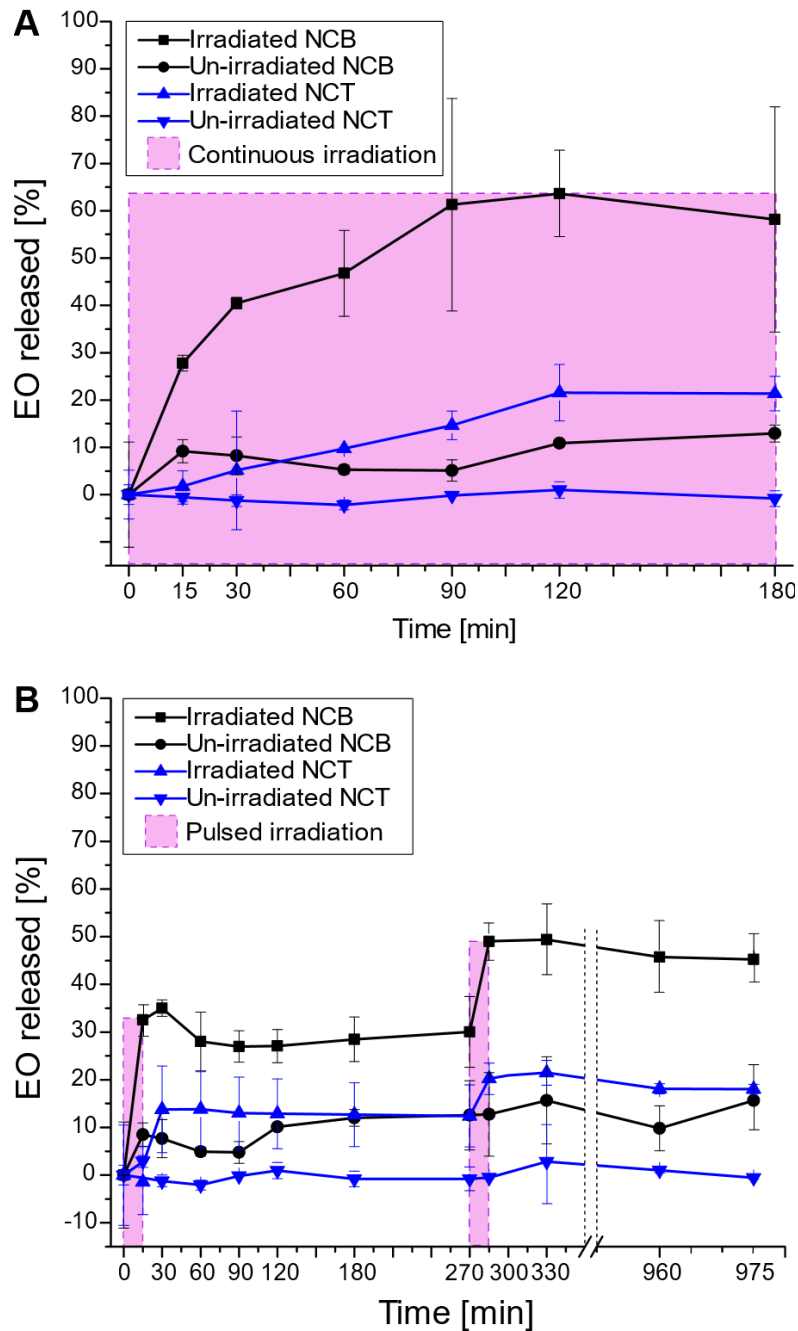


Figure 4.4. - Release kinetics of encapsulated EOs from NCB and NCT samples under (a) continuous UV irradiation and (b) pulsed UV irradiation (2 cycles of 15 min each).

It should be mentioned that before irradiation, the oil concentration values were 1.0 and 1.2 $\mu\text{L}/\text{mL}$, for NCB and NCT respectively, suggesting that a small amount of EOs entrapped in the capsule shell was partially dissolved in the ethanol solution used as media. As a consequence, the release behavior of NCB and NCT capsules was found to strongly diverge. In the case of NCB, about 60% of EO release was observed after 180 min of UV irradiation, while a total release of 20% was found

in NCT sample. The different values of total EO released can be attributed to the different solubility of the EO in the release media.

It has been reported that thyme oil has a solubility of 1 part oil in 3 parts 80% EtOH solution, while for basil oil solubility increases to 1-2 parts of oil in 3 parts 80% EtOH [35]. It is worth noticing that the release kinetics also differed. Basil-loaded capsules exhibited a faster and quantitatively more efficient release than those containing thyme oil. In NCB, 63% of the total released EO diffused in the medium within 30 min, while in the same time interval NCT released less than 25% of the total. Probably the multi-fold morphology, associated with a larger surface to volume ratio, makes the NCB release kinetics faster.

Considering the potentially harmful nature of UV light, a short irradiation time is desirable for active release applications involving biological systems. For this reason, nanocapsules systems were subjected to two cycles of 15 min irradiation to inquire about the possibility of achieving a cease-recommence release mechanism [36]. As expected, the release behavior exhibits a “step-like” trend, proving that 15 min of irradiation provide limited energy to the photo-isomerization. Nonetheless, 15 min irradiation is sufficient to induce in NCB and NCT samples respectively the release of 28 and 13% of encapsulated EO after 60 min. By the end of the experiment, 49% and 20% of the total released core material was found outside of the capsules. For NCB, the amount of EO released by the end of the experiment was approximately the same, independently from the irradiation history that the sample underwent. This was not true for NCT capsules, where a greater amount of EO was released when non-continuous irradiation is applied. This result can be attributed to the higher photo-sensitivity of thyme oil, while basil oil is more resistant to continuous UV irradiation.

Encapsulated EOs can also be employed as cargo solvents for other small active molecules to be employed in different applications, where the photo-responsiveness of NC systems can be exploited, such as pesticides for crop protection [37], anticancer agents for in-cell delivery and photo-

dynamic therapy [38], antimicrobials for food packaging applications [39] and antioxidants and photo-protective agents for cosmetics and solar protection [40].

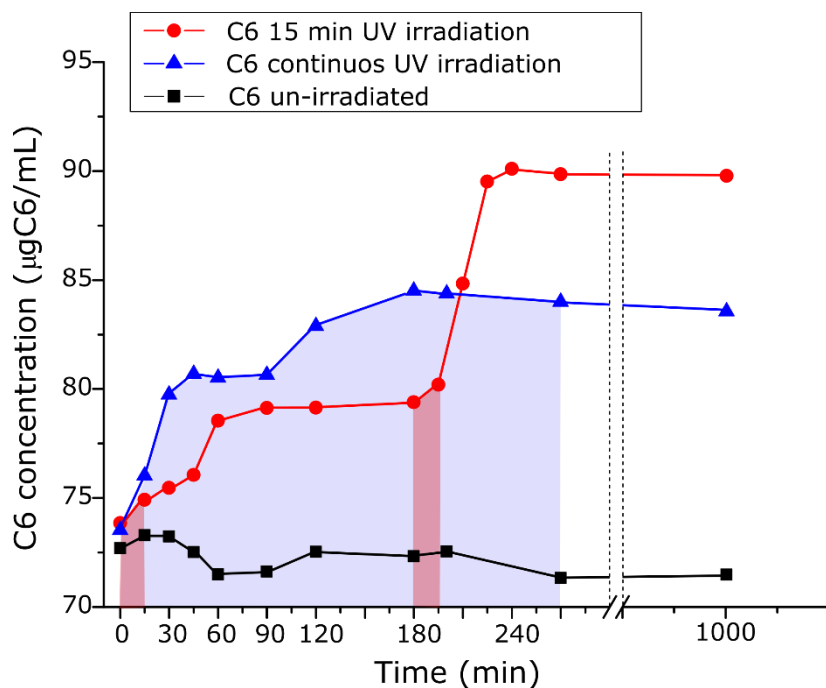


Figure 4.5. – Release of fluorescent probe molecule C6 from NCT sample after continuous (blue triangle) and 15 min (red circle) UV light irradiation.

In this study Coumarin-6 was used as model drug and loaded in the preparation process in the oil core of NCT capsules, selected for their higher encapsulation efficiency. Release experiments were performed via spectrofluorimetry, to study the release of C6 from NCT under UV irradiation. Similarly to EOs release studies, two different UV irradiation experiments were performed: continuous irradiation (blue triangle in Fig. 4.5.) and 3 cycles consisting in 15 min irradiation each (red circle in Fig 4.5.). The results were confronted with a non-irradiated sample. As reported in Figure 4.5., C6 release experiments kinetics are characterized by a burst release that occurs in the first 30 min, followed by a *sigmoidal shape* release, after 180 min the release kinetics reaches a plateau value. This NCs behavior has already been studied in a previous work [4], where the initial burst release has been

attributed to the C6 that is entrapped in the polymeric shell of the nanocapsules. Upon light irradiation, the molecular movements of the polymer chains primarily promote the release of superficial C6, while subsequently, the capsules start to release the C6 that is loaded in the oil core.

4.3.4. Cellular uptake and cytotoxicity

In view of potential healthcare applications involving light activated release of drugs, the cell toxicity of the nanocapsules was studied. Due to the potential harmful reported effects of EOs *in vitro*, cytotoxicity tests were performed on neat nanocapsules which were produced using a volatile organic solvent (toluene). Prior to the experiment, the solvent was completely stripped under reduced pressure, then cells proliferation was assessed by trypan blue exclusion assays. In control conditions, the cell number increased at 24, 48 and 72 hours. The treatment of cells with low concentrations of both nanoparticles did not alter significantly cell proliferation rate. However, with higher nanoparticles concentrations (250 µg/ml), cell proliferation decreased significantly. Trypan blue exclusion test on NRK cells after 24-48-72h confirmed that nanoparticles were not toxic even when cells were treated with 250 µg/ml (Figure 4.6.).

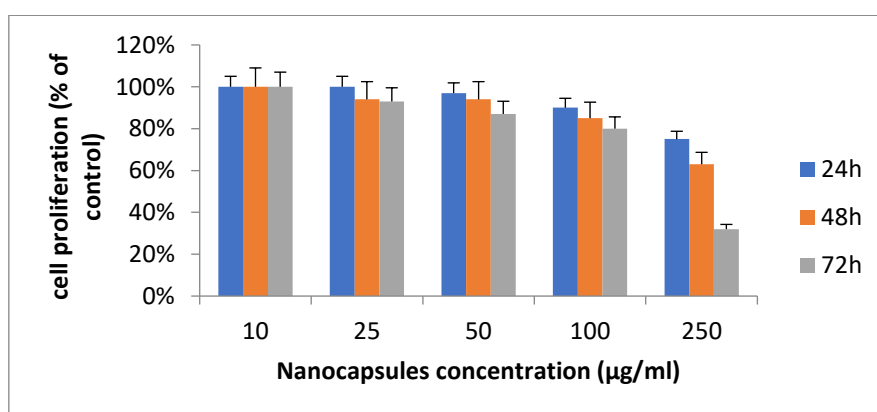


Figure 4.6. – Trypan blue exclusion histograms reporting the variations in cell proliferation as a dependence of NCs concentration.

As reported in Figure 4.7., nanoparticles were internalized and accumulated within NRK in a concentration-dependent way. In particular, nanoparticles showed a perinuclear localization at all tested concentrations as early as 24h. As the fluorescent probe molecule C6 is proved to be insoluble in water environment.

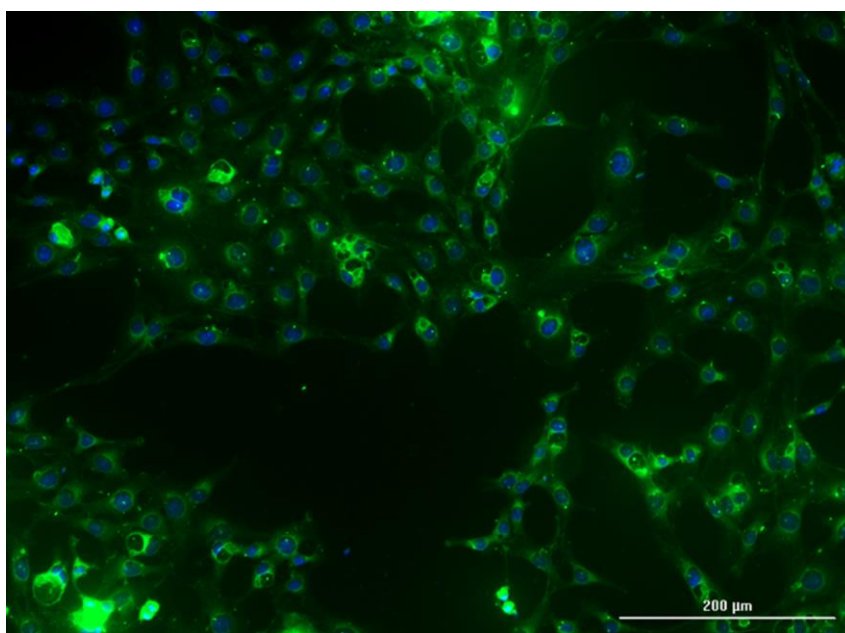


Figure 4.7. – Internalization and accumulation of NCs within NRK cells

4.4. Conclusions

This work presents, for the first time, the encapsulation and light-triggered release of basil and thyme essential oils via interfacial polycondensation in miniemulsion, providing multiple benefits to nanoencapsulation technology. First of all, the essential oils have the dual role of active core material and solvent for the azo-monomer in the miniemulsion reaction, thus implying the elimination of potentially toxic organic solvents from the procedure. The versatility and reliability of the photo-

induced release mechanism in azo-polymers makes these capsules promising candidate for a wide variety of applications, such as food-packaging, agriculture, household and cosmetics. Moreover, the study regarding Coumarin-6 encapsulation and release, as a model drug, strongly hints at future application in biological environments.

UV-light is poorly available and pose threats to human health as well. Therefore, a red-shift of the azobenzene *trans-cis* photo-isomerization wavelength towards visible range in the radiation spectrum would be preferable. Overcoming this problem is of key interest of our forthcoming research.

4.5. References.

1. Mura, S., Nicolas, J. and Couvreur, P., 2013. Stimuli-responsive nanocarriers for drug delivery. *Nature materials*, 12(11), pp.991-1003.
2. Wei, H., Wang, Y., Guo, J., Shen, N.Z., Jiang, D., Zhang, X., Yan, X., Zhu, J., Wang, Q., Shao, L. and Lin, H., 2015. Advanced micro/nanocapsules for self-healing smart anticorrosion coatings. *Journal of Materials Chemistry A*, 3(2), pp.469-480.
3. Hofmeister, I., Landfester, K. and Taden, A., 2014. pH-sensitive nanocapsules with barrier properties: fragrance encapsulation and controlled release. *Macromolecules*, 47(16), pp.5768-5773.
4. Marturano, V., Cerruti, P., Carfagna, C., Giamberini, M., Tylkowski, B. and Ambroggi, V., 2015. Photo-responsive polymer nanocapsules. *Polymer*, 70, pp.222-230
5. Tylkowski, B., Pregowska, M., Jamowska, E., Garcia-Valls, R. and Giamberini, M., 2009. Preparation of a new lightly cross-linked liquid crystalline polyamide by interfacial polymerization. Application to the obtainment of microcapsules with photo-triggered release. *European Polymer Journal*, 45(5), pp.1420-1432.
6. Bogdanowicz, K.A., Tylkowski, B. and Giamberini, M., 2013. Preparation and characterization of light-sensitive microcapsules based on a liquid crystalline polyester. *Langmuir*, 29(5), pp.1601-1608.
7. Jiang, F., Chen, S., Cao, Z. and Wang, G., 2016. A photo, temperature, and pH responsive spiropyran-functionalized polymer: Synthesis, self-assembly and controlled release. *Polymer*, 83, pp.85-91.
8. Bédard, M., Skirtach, A.G. and Sukhorukov, G., 2007. Optically driven encapsulation using novel polymeric hollow shells containing an azobenzene polymer. *Macromolecular rapid communications*, 28(15), pp.1517-1521.

9. Kimura ET, Ebert DM, Dodge PW. Acute toxicity and limits of solvent residue for sixteen organic solvents. *Toxicol Appl Pharmacol* 1971;19:699–704.
10. Burt, S., 2004. Essential oils: their antibacterial properties and potential applications in foods—a review. *International journal of food microbiology*, 94(3), pp.223-253.
11. Hammer KA, Carson CF, Riley TV. Antimicrobial activity of of essential oils and other plant extract. *J Appl Microbiol* 1999; 86:985–90.
12. Dorman HJD, Deans SG, Merr L, Myrtaceae P. Antimicrobial agents from plants : antibacterial activity of plant volatile oils 2000:308–16.
13. Licciardello, F., Muratore, G., Suma, P., Russo, A. and Nerín, C., 2013. Effectiveness of a novel insect-repellent food packaging incorporating essential oils against the red flour beetle (*Tribolium castaneum*). *Innovative Food Science & Emerging Technologies*, 19, pp.173-180.
14. Isman, Murray B. "Pesticides Based on Plant Essential Oils: Phytochemical and Practical Considerations." In *Medicinal and Aromatic Crops: Production, Phytochemistry, and Utilization*, pp. 13-26. American Chemical Society, 2016.
15. Langeveld, Wendy T., Edwin JA Veldhuizen, and Sara A. Burt. "Synergy between essential oil components and antibiotics: a review." *Critical reviews in microbiology* 40, no. 1 (2014): 76-94.
16. Gómez-Estaca, J., López-de-Dicastillo, C., Hernández-Muñoz, P., Catalá, R. and Gavara, R., 2014. Advances in antioxidant active food packaging. *Trends in Food Science & Technology*, 35(1), pp.42-5.
17. Campos C. A., Gerschenson L. N., Flores S. K. Development of Edible Films and Coatings with Antimicrobial Activity. *Food Bioprocess Technol* 2010;4:849–75.
18. Persico, P., Ambrogi, V., Carfagna, C., Cerruti, P., Ferrocino, I. and Mauriello, G., 2009. Nanocomposite polymer films containing carvacrol for antimicrobial active packaging. *Polymer Engineering & Science*, 49(7), pp.1447-1455.

19. Gomes C, Moreira RG, Castell-Perez E. Poly (DL-lactide-co-glycolide) (PLGA) nanoparticles with entrapped trans-cinnamaldehyde and eugenol for antimicrobial delivery applications. *J Food Sci* 2011; 76: N16–24.
20. Pan K, Chen H, Davidson PM, Zhong Q. Thymol nanoencapsulated by sodium caseinate: physical and antilisterial properties. *J Agric Food Chem* 2014; 62: 1649–57.
21. Davis, M.E. and Shin, D.M., 2008. Nanoparticle therapeutics: an emerging treatment modality for cancer. *Nature reviews Drug discovery*, 7(9), pp.771-782.
22. Fleige, E., Quadir, M.A. and Haag, R., 2012. Stimuli-responsive polymeric nanocarriers for the controlled transport of active compounds: concepts and applications. *Advanced drug delivery reviews*, 64(9), pp.866-884.
23. Marturano, V., Cerruti, P., Giamberini, M., Tylkowski, B. and Ambrogi, V., 2016. Light-Responsive Polymer Micro-and Nano-Capsules. *Polymers*, 9(1), p.8
24. Bakkali, F., Averbeck, S., Averbeck, D. and Idaomar, M., 2008. Biological effects of essential oils—a review. *Food and chemical toxicology*, 46(2), pp.446-475.
25. Kalemba, D. and Kunicka, A., 2003. Antibacterial and antifungal properties of essential oils. *Current medicinal chemistry*, 10(10), pp.813-829.
26. Torini, L., Argillier, J.F. and Zydowicz, N., 2005. Interfacial polycondensation encapsulation in miniemulsion. *Macromolecules*, 38(8), pp.3225-3236.
- 27.
28. Paster, N., Juven, B.J., Shaaya, E., Menasherov, M., Nitzan, R., Weisslowicz, H. and Ravid, U., 1990. Inhibitory effect of oregano and thyme essential oils on moulds and foodborne bacteria. *Letters in Applied Microbiology*, 11(1), pp.33-37.
29. Wilson, C.L., Solar, J.M., El Ghaouth, A. and Wisniewski, M.E., 1997. Rapid evaluation of plant extracts and essential oils for antifungal activity against *Botrytis cinerea*. *Plant disease*, 81(2), pp.204-210.

30. Herrmann, A., Debonneville, C., Laubscher, V. and Aymard, L. (2000), Dynamic headspace analysis of the light-induced controlled release of perfumery aldehydes and ketones from α -keto esters in bodycare and household applications. *Flavour Fragr. J.*, 15: 415–420.
31. Lee, S.J., Umamo, K., Shibamoto, T. and Lee, K.G., 2005. Identification of volatile components in basil (*Ocimum basilicum* L.) and thyme leaves (*Thymus vulgaris* L.) and their antioxidant properties. *Food Chemistry*, 91(1), pp.131-137.
32. Persico, P., Ambrogi, V., Carfagna, C., Cerruti, P., Ferrocino, I. and Mauriello, G., 2009. Nanocomposite polymer films containing carvacrol for antimicrobial active packaging. *Polymer Engineering & Science*, 49(7), pp.1447-1455.
33. Mora-Huertas, C.E., Fessi, H. and Elaissari, A., 2010. Polymer-based nanocapsules for drug delivery. *International journal of pharmaceutics*, 385(1), pp.113-142.
34. Dispinar, T., Colard, C.A. and Du Prez, F.E., 2013. Polyurea microcapsules with a photocleavable shell: UV-triggered release. *Polymer Chemistry*, 4(3), pp.763-772.
35. Ziegler, H. ed., 2007. *Flavourings: production, composition, applications, regulations*. John Wiley & Sons.
36. Lin, H., Xiao, W., Qin, S.Y., Cheng, S.X. and Zhang, X.Z., 2014. Switch on/off microcapsules for controllable photosensitive drug release in a 'release-cease-recommence' mode. *Polymer Chemistry*, 5(15), pp.4437-4440.
37. Peteu, S.F.; Oancea, F.; Siciua, O.A.; Constantinescu, F.; Dinu, S. Responsive polymers for crop protection. *Polymers* 2010, 2, 229–251.
38. Son, K.J., Yoon, H.J., Kim, J.H., Jang, W.D., Lee, Y. and Koh, W.G., 2011. Photosensitizing hollow nanocapsules for combination cancer therapy. *Angewandte Chemie International Edition*, 50(50), pp.11968-11971.
39. Mastromatteo, M., Mastromatteo, M., Conte, A. and Del Nobile, M.A., 2010. Advances in controlled release devices for food packaging applications. *Trends in Food Science & Technology*, 21(12), pp.591-598.

40. Hanno, I., Anselmi, C. and Bouchemal, K., 2012. Polyamide nanocapsules and nano-emulsions containing Parsol® MCX and Parsol® 1789: in vitro release, ex vivo skin penetration and photo-stability studies. *Pharmaceutical research*, 29(2), pp.559-573.



CHAPTER 5

Photo-triggered Polymer Capsules Loaded with Antimicrobial Essential Oils: An Application in Active Food Packaging

Valentina Marturano, Valentina Bizzarro, Anna Calarco,
Pierfrancesco Cerruti, Adele Cutignano, Veronica Ambrogi.

In preparation for submission:

Journal of Food Engineering

Abstract

This work reports on the preparation and characterization of photo-responsive capsules loaded with antimicrobial essential oils and employed as a coating for commercial polymers, such as polyethylene (PE) and polylactic acid (PLA). Photo-responsive capsules, having a shell of polyamide with azobenzene moiety in the main chain, were synthesized *in-situ* via interfacial polycondensation in *o/w* emulsion, employing basil and thyme essential oils as the organic phase. PE and PLA films were surface modified through corona or plasma treatments to increase their wettability and improve the microcapsules dispersion during coating. Morphology of both capsules and coated films were analyzed via optical microscopy and electron microscopy (SEM, TEM). The UV-induced release of the volatile components of essential oils from coated polymeric films was studied via gas chromatography and antimicrobial activity of the encapsulated essential oils against *e-coli* was also evaluated. The antimicrobial packaging showed good efficiency in confirming its promising application as a food packaging system.

5.1. Introduction

Modern society, where consumer goods are readily available, is increasingly inclined to favor waste, especially of food. Over the last few decades, the necessity to address feeding issues related to increasing world population has pushed scientific efforts towards a more aware food industry [1]. Materials technology can help minimize food losses and improve quality, freshness, and safety of food products. [2] In fact, a wide variety of “active” packaging technologies have been developed to meet these requirements. Important examples of active packaging include oxygen scavengers, carbon dioxide emitters/absorbers, moisture absorbers, ethylene absorbers, ethanol emitters, flavor releasing/absorbing systems, time-temperature indicators, and antimicrobial-containing films. [3]. Active, or *smart*, packaging has often been described as any kind of packaging that provides specific functionality beyond the role of physical barrier between the food product and the surrounding environment [4]. More recently, a novel concept of packaging has been introduced: *Responsive* packaging has been defined as any packaging that elicits a response as a result of a specific trigger or change occurring in the food product, food package headspace, or the outside environment [5].

Antimicrobial (AM) packaging systems incorporate antimicrobials into the packaging to prevent microbial growth on the surface of solid foods and to reduce the need for larger quantities of antimicrobials in liquid foods. AM packaging can play an important role in reducing the risk of pathogen contamination as well as in extending the shelf life of minimally processed foods [6]. Different mechanisms of action of AM food packaging are proposed in literature [7] and schematized in Figure 5.1. For instance, AM agents can diffuse via headspace in a non-contact mode or migrate in the food via direct contact from the packaging material to the food. For some food products, such as fresh meat, in which the microbial contamination occurs primarily at the surface, direct surface application of AM has limited benefits, because the AM rapidly migrate in the food mass. On the other hand, the non-contact and prolonged release of AM from packaging, coatings or sachets can help maintain high AM concentrations when needed [8].

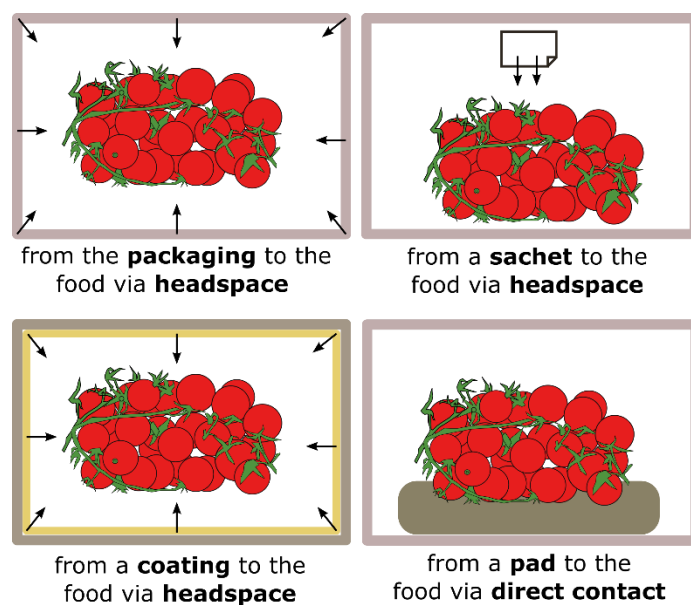


Figure 5.1– Methods for the release of antimicrobial agents in food packaging technologies.

However, food application of an antimicrobial packaging system is limited due to the availability of suitable antimicrobials, new polymer materials, regulatory concerns, and appropriate testing methods. [9, 10]

In this work, we present a novel responsive packaging system obtained by coating commercial packaging films, such as PE and PLA, with photo-responsive nanocapsules loaded with antimicrobial basil and thyme essential oils (EOs) prepared as reported elsewhere [11]. The coating process was promoted by surface modification of PE and PLA films by plasma and corona treatment. The antimicrobial properties of basil and thyme EOs are vastly acknowledged, moreover their highly volatile components make them very suitable for non-contact antimicrobial food packaging applications [12, 13].

5.2. Experimental

5.2.1. Materials

An unstabilized grade of a butene-copolymer linear low-density polyethylene (PE), DJM1826, with a melt flow index (MFI) of 2.5 g 10 min⁻¹ was supplied as a powder by Versalis (Italy). Polylactic acid (PLA) grade 4042D (94% L-lactic acid) was obtained from NatureWorks LLC (U.S.A.). Basil and thyme EOs were purchased from Pharmalab and used without further purification. Polymer nanocapsules, loaded with basil and thyme EOs, were synthesized as reported elsewhere [11]. Basil and thyme-loaded nanocapsules were coded as NCB and NCT respectively.

5.2.2. Preparation and surface treatments of PE and PLA films

PLA pellets were oven-dried for 24h at 65 °C under vacuum, prior to extrusion. PLA films were prepared using a Collin E 20T single screw extruder equipped with a Collin CR 72T calendaring unit, using the following temperature profile (from hopper to die): 165, 170, 170, 170, 170 °C. The thickness of the film obtained was on average 60±10 μm. PE films were obtained using the same equipment, with the following temperature profile: 150, 170, 180, 180, 170 °C. PE film thickness was 68±12 μm.

Both PE and PLA films were then subjected to surface treatments (corona and plasma) to increase their wettability and promote the adhesion of the nanocapsules coating. Plasma treatment was performed on square polymer films (surface area of 2 cm²) employing a Tucano medium plasma reactor 600 (Gambetti KENOLOGIA S.R.L.) for 12 min. Alternatively, corona treatment was performed on other polymer films employing a Tantec corona effect machinery at 150 W for 10 min. In order to verify the efficiency of the two surface treatments, contact angle measurements were performed using an OCA/Dataphysics/SCA20 Contact Angle System. In a typical experiment, 2 μl of

water or 1 μl of diiodomethane are deposited on the surface of the film under study, the contact angles formed by the droplets of the two liquids on the substrate are then measured by optical microscopy.

5.2.3. Coating of PE and PLA films with nanocapsules.

The coating of surface-activated PE and PLA substrates with NC suspensions was performed employing an aqueous nanocapsules suspension and two different deposition methods, dip-coating and spraying. Both techniques mimic an industrial process and can be easily scaled up. In both cases, prior to characterization, the coated polymer films were left to dry for 12 h under the hood at room temperature. Surface morphology of nanocapsules-coated films was observed via scanning electron microscopy (SEM) using a FEI Quanta 200 FEG instrument in high vacuum mode, equipped with a Large Field Detector (LFD) operating with acceleration voltage ranging between 15 and 20 kV. For SEM sample preparation, a 25 mm² film specimen was deposited on an aluminum stub and metallized with an Au-Pd coating.

5.2.4. Release of EO from nanocapsules-coated films

Thyme and basil EOs are composed by a mixture of volatile components (Figure 5.2.), therefore gas chromatography (GC) can be used to evaluate the release kinetics of one or more of the chemical compounds. To perform these measurements, 2 mL of nanocapsules solution were deposited on a PE thin film (2x4 cm²) and left to dry for 15 h. The film was then introduced in a quartz testing tube that was sealed with a gas-tight stopper with a pierceable septum. The sample was kept at a constant temperature of 15 °C and 0.5 mL of the headspace was collected and introduced in the GC to be analyzed. The sample was tested at time 0 and, after a 15-min irradiation with UV light at 365 nm, further analyzed at t= 3, 24 and 27 h. The EO release from a non-irradiated sample was also evaluated to exclude any factor other than light affecting the release mechanism.

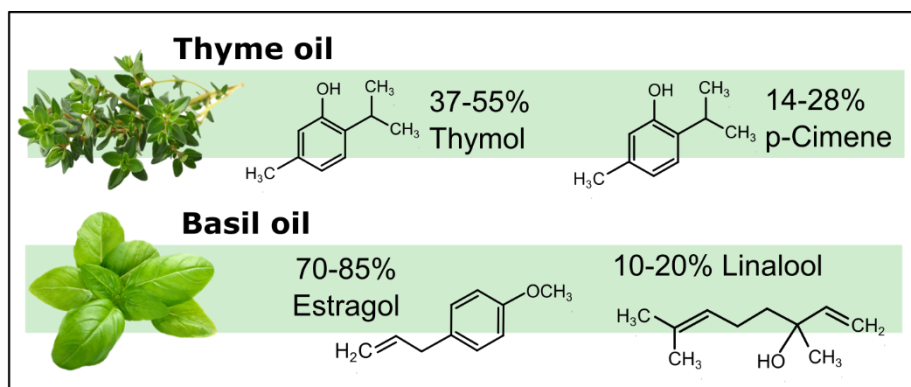
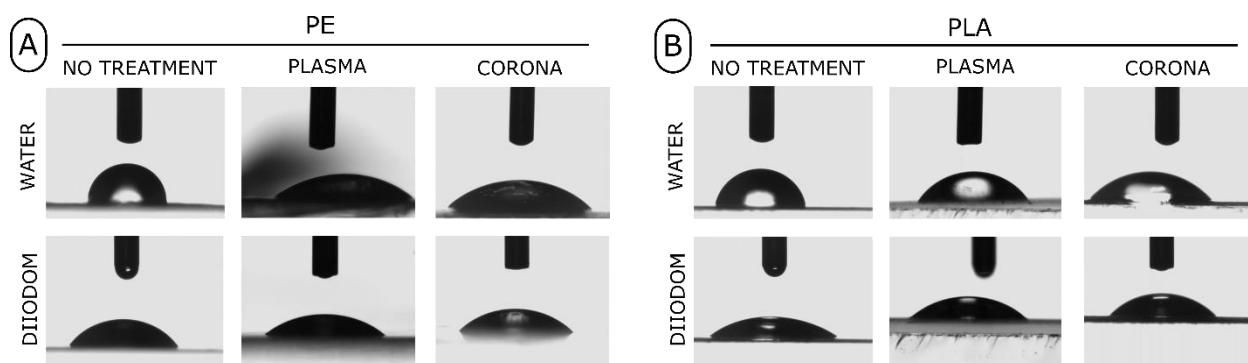


Figure 5.2. – Chemical composition of basil and thyme essential oils.

5.3. Results and discussion

5.3.2. Characterization of the treated polymer films

To promote the deposition of the EO-loaded capsules aqueous solution, surface treatments such as plasma and corona were applied to polymer films to improve their wettability. To assess and compare the effects on PE and PLA films of the plasma and corona treatments used, contact angle measurements were performed. The smaller the contact angle, the higher is the affinity of the surface towards the reference liquids, resulting in a higher wettability. In Figure 5.3. the contact angle measurements of water and diiodomethane on PE (Fig. 5.3.A) and PLA (Fig. 5.3.B) films are reported as well as the associated values of surface energy (SE) (Fig. 5.3.C). Figure 5.3. shows that, depending on the surface treatment applied, a different response was observed for the two analysed materials. In particular, PE films exhibited higher wettability upon plasma treatment, while in the biodegradable polymer PLA corona treatment resulted more effective. These latter were selected for further investigation.



(C)		CA water [°]	CA diiodomethane [°]	SE [mN/m]
PE	No treatment	91.5 ± 3.7	47.9 ± 4.3	34.3
	Plasma	40.6 ± 2.2	38.5 ± 1.7	63.5
	Corona	47.4 ± 3.2	54.9 ± 0.9	57.6
PLA	No treatment	74.5 ± 2.1	38.7 ± 7.5	47.0
	Plasma	57.5 ± 1.0	45.2 ± 1.2	51.8
	Corona	46.9 ± 0.7	46.3 ± 0.1	57.8

Figure 5.3. –(top) Contact angle micrographs performed on untreated and plasma and corona-treated PE (A) and PLA (B). (bottom) surface energy values (SE) calculated from contact angle measurements (CA) using water or diiodomethane as reference liquids.

5.3.4. Characterization of nanocapsules-coated films

EO-loaded capsules were deposited on PE or PLA films by either spray or immersion techniques. The quality of the deposition method was assessed via optical and SEM microscopy. Figure 5.4. shows the effect of the deposition method of NCT capsules suspension on corona-treated PLA films in comparison with neat PLA (Fig. 5.4. a and d). As expected, spray deposition did not provide a well dispersed layer of capsules on the film surface (Fig. 5.4. c and f). On the contrary, dip-coating seemed to grant a uniform distribution at all scales of magnification (Fig. 5.4. b and e).

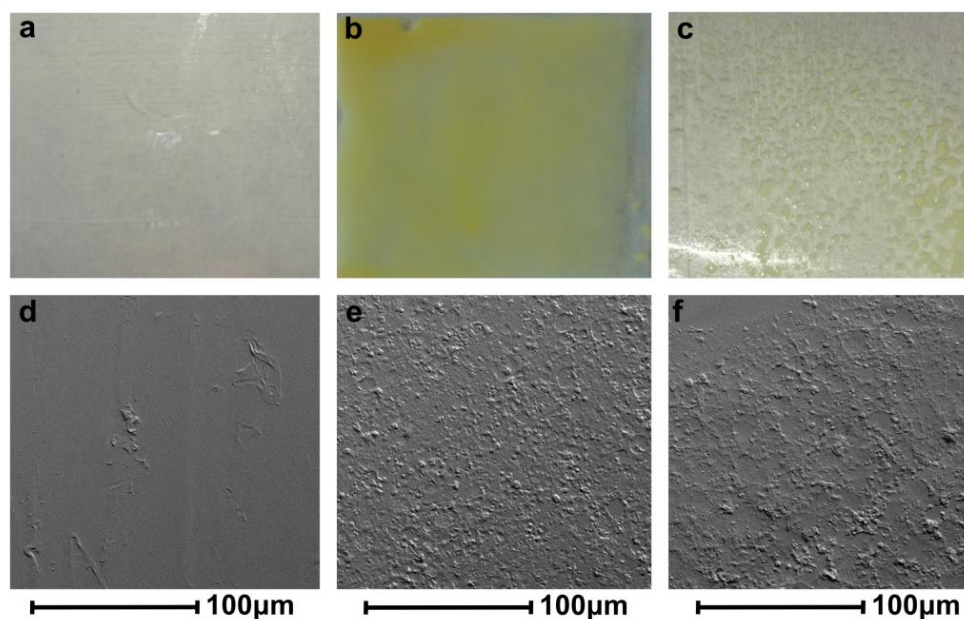


Figure 5.4. - Optical images and SEM micrographs of the surface of a pure PLA film (a, d), upon dip-coating (b, e) and after spraying (c, f) with an aqueous nanocapsules suspension.

A good deposition method results in a more uniform layer of EO-loaded capsules, thus providing a greater surface area for the release of the encapsulated essential oil. For this reason, SEM measurements were performed on PE and PLA films treated with plasma and corona, respectively, and coated with NCB and NCT. Results are reported in Figure 5.5. As expected, untreated polymers exhibited poor compatibility with nanocapsules suspensions as evidenced by the appearance of inhomogeneous areas which are particularly evident in PLA samples. As mentioned above, plasma treatment improved PE wettability providing uniform coatings upon deposition of both NCT and NCB suspensions. In the case of corona-treated PLA comparable results were gathered from SEM analysis although some impurities were still identified on the coated surface. As a consequence, NCT-coated PE samples were selected as representative for the successive analysis on the release behavior.

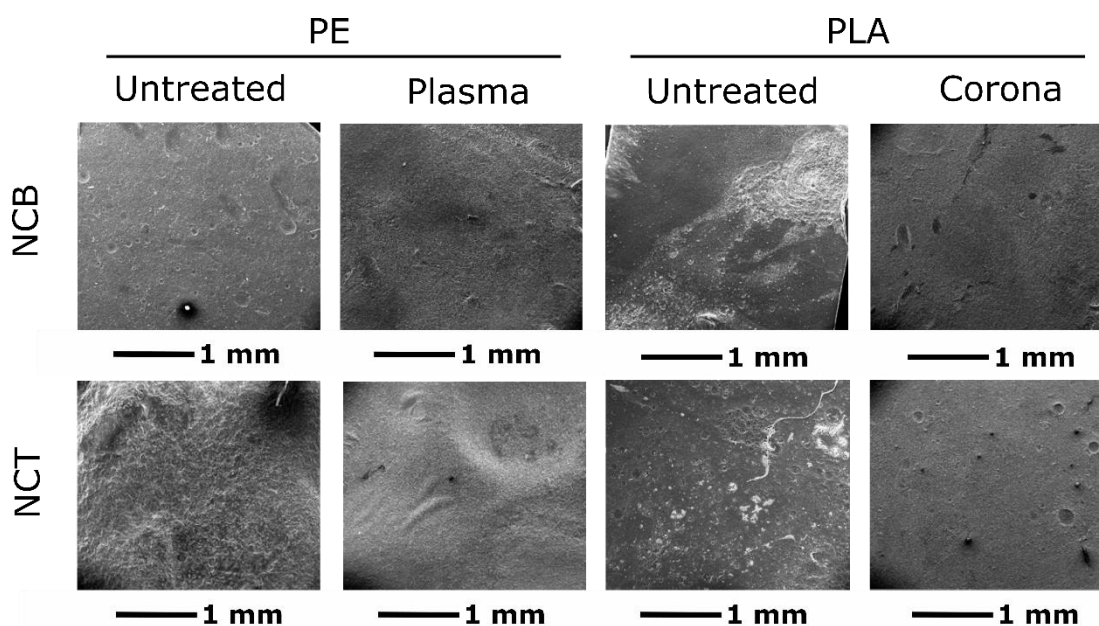


Figure 5.5. – SEM micrographs of treated PE and PLA films coated with NCT and NCB.

5.3.5. Release from nanocapsules-coated films

As discussed above, non-contact food packaging applications require the use of volatile AM agents. Therefore, the release of thymol, an extremely volatile component of thyme EO, was evaluated via gas chromatography (GC) measurements on NCT-coated PE films. To this purpose, two NCT-coated PE films were placed in two quartz testing tubes, one was kept in darkness while the other was irradiated for 15 min with a UV lamp (360 nm) to trigger the EO release from the photo-responsive capsules. The headspace of each tube was withdrawn several times with a gas syringe and was analyzed via GC. The results, reported in Figure 5.6., show that prior to irradiation (t=0) the thymol concentration in both samples was comparable. After 3 h from irradiation, thymol concentration increased in the irradiated sample, while it remained constant in the non-irradiated one, proving the reliability of the release mechanism. After 48 h from irradiation, the thymol concentration increased more than tenfold with respect to the initial value.

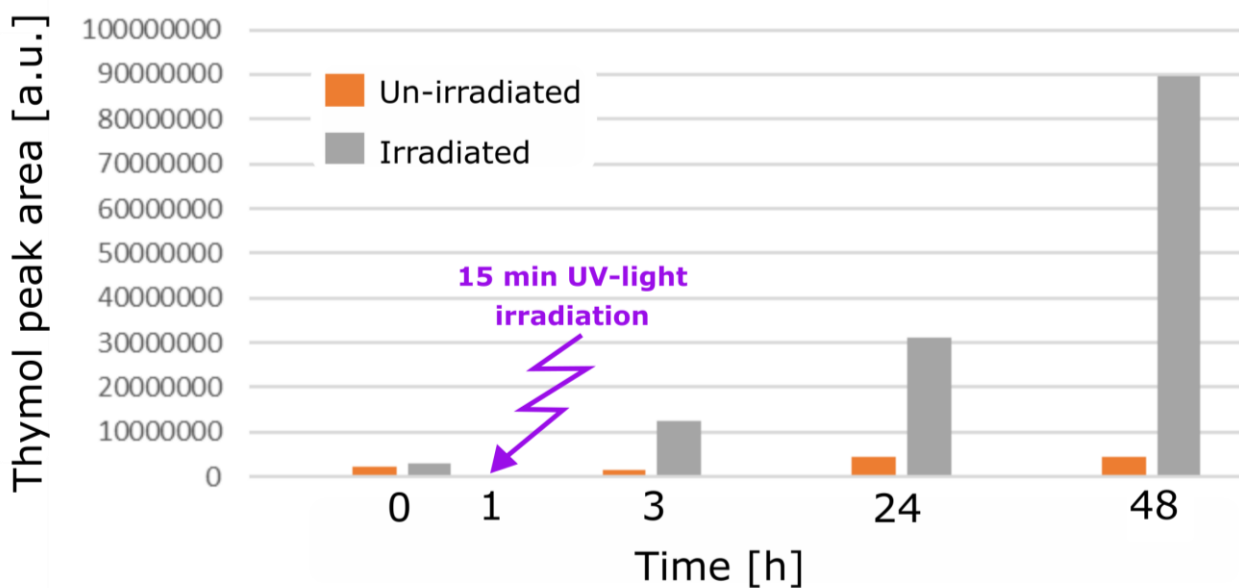


Figure 5.6– Evaluation of the thymol release via GC for: ■ un-irradiated and ■ irradiated NCT samples

5.3.6. Antibacterial properties

A preliminary study on the effectiveness of basil and thyme as antimicrobial active agents was conducted on essential oils in contact with a bacterial culture of Escherichia Coli (E. Coli) and calculating the Minimum Inhibitory Concentration (MIC). The data reported in Figure 5.7. shows that thyme and basil EOs are effective against the E. Coli at concentrations of 1 and 5 mg / ml respectively.

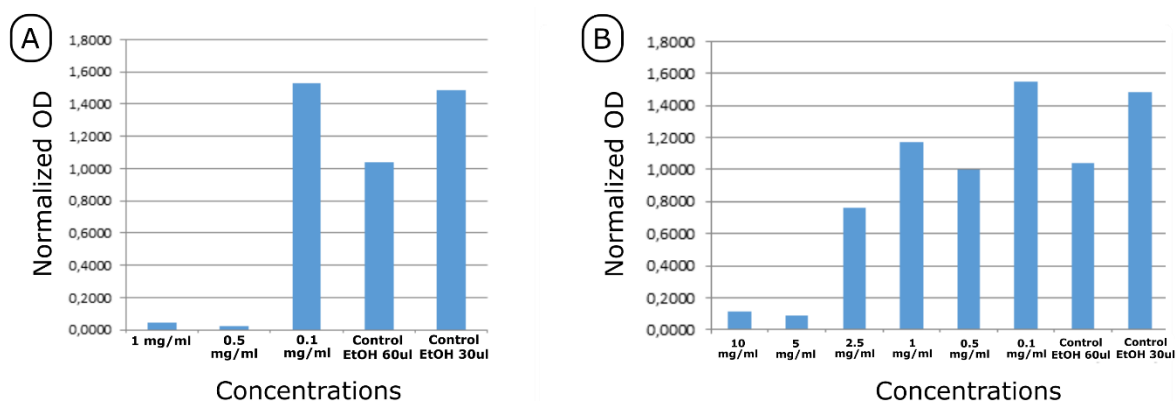


Figure 5.7.- Antimicrobial activity of thyme (A), and basil (B) essential oils.

The antimicrobial and antifungal power of Thyme EO was also tested on wholemeal breadcrumbs. Three bread crumbs of the same weight were placed inside three quartz tubes with a drop of water, subsequently, a PE film coated NCT capsules was introduced in two of the three tubes. The three samples were left in a climatic chamber (25 ° C and 50% humidity) for 7 days. Only one of the two tubes containing the AM photoactivable film underwent daily 15 min irradiations (several layers of aluminum foil shielded the breadcrumb from UV radiation – that possess and intrinsic AM effect), while the other was used as a control. As can be observed in Figure 5.8., both the sample containing solely bread and the one containing non-activated AM film, are characterized by the growth of different microorganisms: white mold fungus, respectively. In the sample with photo-activated release of thyme antimicrobial EO the growth of harmful microorganisms seemed hindered.

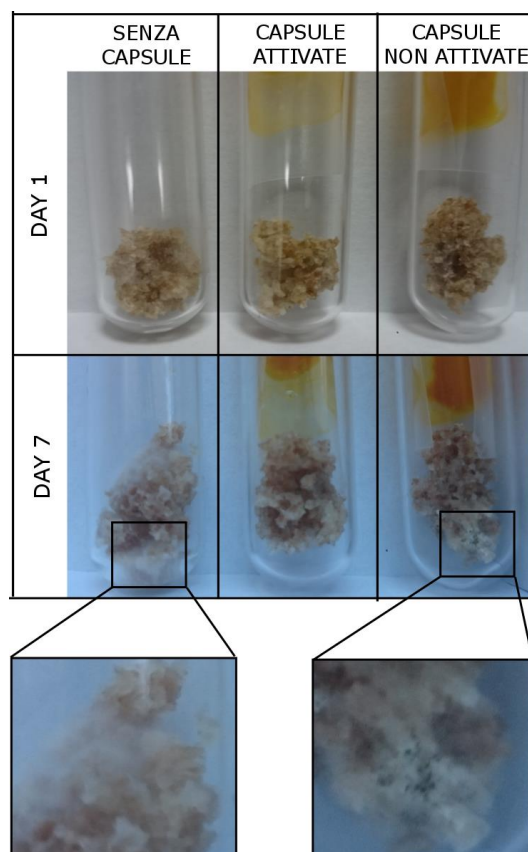


Figure 5.8. - Antimicrobial activity tests on PE film coated with NCT capsules on a sample of whole-wheat bread.

5.4. Conclusions

Thyme and basil essential oils are renowned antimicrobial agents, used in many food packaging applications. However, to our knowledge this is the first time in literature that the two EO have been incorporated in a packaging material in capsules formulations. The coating process of PE and PLA with EO-loaded capsules was carefully assessed, determining that a surface treatment is necessary to increase the wettability of the polymeric materials and that the immersion of the film in a NCs suspension could promote a better dispersion in comparison to spray coating. Both release experiments and antimicrobial tests were performed to confirm the feasibility of the active packaging system.

A possible application of the presented active packaging system is schematized in Figure 5.9. A closed compartment, equipped with a LED UV lamp (360 nm), would be included in the lower

part of the refrigerator in which most perishable foods, such as meat and vegetables, would be stored. To prevent an excessive power consumption, the UV lamp would be set to power on for just 15 min per day or after every usage. The nanocapsules-coated packaging could be disposable, to be changed when exhausted.

The applications of this promising release technology go far beyond the food packaging industry, since it results appealing also for drug delivery, agriculture, household and cosmetics.

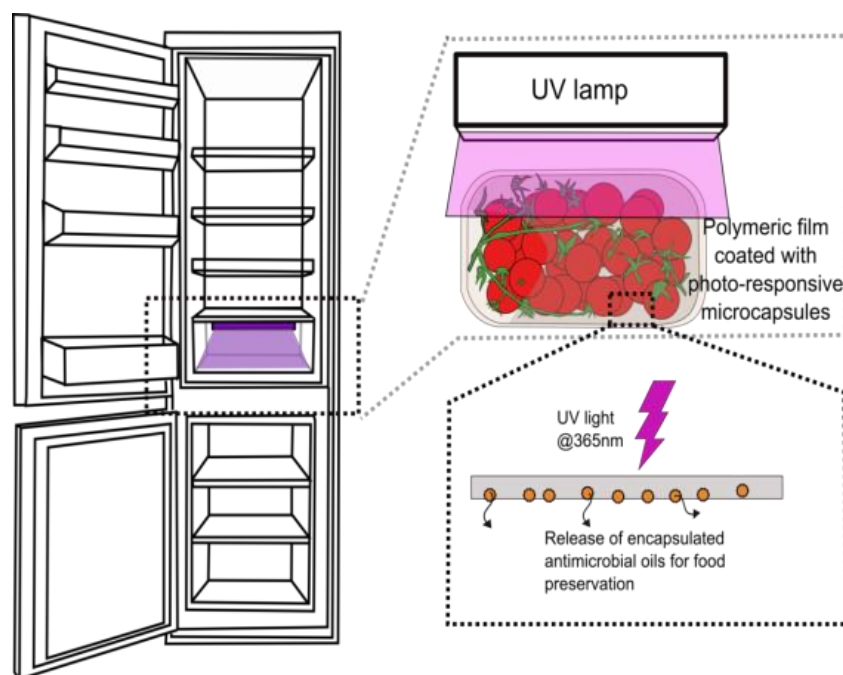


Figure 5.9– Schematization of a possible setup for the AM active packaging based on photo-responsive polymer nanocapsules.

5.5. References:

1. Godfray, H.C.J., Beddington, J.R., Crute, I.R., Haddad, L., Lawrence, D., Muir, J.F., Pretty, J., Robinson, S., Thomas, S.M. and Toulmin, C., 2010. Food security: the challenge of feeding 9 billion people. *science*, 327(5967), pp.812-818.
2. Labuza, T. P. and Breene, W. M.1989. Applications of “Active Packaging” for improvement of shelf-life and nutritional quality of fresh and extended shelf-life foods. *J. Food Proc. Preserv.*, 13: 1–69.
3. Ozdemir, M. and Floros, J.D., 2004. Active food packaging technologies. *Critical Reviews in Food Science and Nutrition*, 44(3), pp.185-193.
4. Butler P. 2001. Smart packaging–intelligent packaging for food, beverages, pharmaceuticals and household products. *Mater World* 9(3):11–3.
5. Brockgreitens, J. and Abbas, A., 2016. Responsive food packaging: recent progress and technological prospects. *Comprehensive Reviews in Food Science and Food Safety*, 15(1), pp.3-15.
6. Jin, T. and Zhang, H., 2008. Biodegradable polylactic acid polymer with nisin for use in antimicrobial food packaging. *Journal of Food Science*, 73(3), pp.M127-M134.
7. Han, J.H., 2003. Antimicrobial food packaging. *Novel food packaging techniques*, pp.50-70.
8. Quintavalla, S. and Vicini, L., 2002. Antimicrobial food packaging in meat industry. *Meat science*, 62(3), pp.373-380
9. Malhotra, B., Keshwani, A. and Kharkwal, H., 2015. Antimicrobial food packaging: potential and pitfalls. *Frontiers in microbiology*, 6.
10. Becerril, R., Gómez-Lus, R., Goni, P., López, P. and Nerín, C., 2007. Combination of analytical and microbiological techniques to study the antimicrobial activity of a new active food packaging containing cinnamon or oregano against *E. coli* and *S. aureus*. *Analytical and bioanalytical chemistry*, 388(5-6), pp.1003-1011.

11. Bizzarro, V., Carfagna, C., Cerruti, P., Marturano, V. and Ambrogi, V., 2016, May. Light-responsive polymer microcapsules as delivery systems for natural active agents. In A. D'Amore, D. Acierno and L. Grassia eds., *AIP Conference Proceedings* (Vol. 1736, No. 1, p. 020078). AIP Publishing.
12. Beier, R.C., Byrd, J.A., Kubena, L.F., Hume, M.E., McReynolds, J.L., Anderson, R.C. and Nisbet, D.J., 2014. Evaluation of linalool, a natural antimicrobial and insecticidal essential oil from basil: Effects on poultry. *Poultry science*, 93(2), pp.267-272.
13. Guarda, A., Rubilar, J.F., Miltz, J. and Galotto, M.J., 2011. The antimicrobial activity of microencapsulated thymol and carvacrol. *International journal of food microbiology*, 146(2), pp.144-150.



CHAPTER 6

Visible-light Responsive Azobenzene and Future Applications

6.1. Introduction

Azobenzene and its derivatives are fascinating and widely studied molecules that display a reversible photo-isomerization between the more stable *trans* to the less stable *cis* isomers. As described before, the introduction of azobenzene in polymers or liquids can enable the use of light as a powerful external stimulus to control or trigger changes in the properties of such materials [1]. Azobenzene-based systems are vastly employed in many advanced fields, such as photonics [2], organic electronics [3] and waveguides [4].

However, the limited range of switching wavelengths in the UV region limits the applicability of such materials in biological and clinical applications [5, 6]. While commonly applied in the above mentioned applications, UV-light still poses a threat to living organisms and its carcinogenic effect has been vastly reported in literature [7].

Recently, many groups have addressed this issue [8-10], demonstrating that incorporation of electron-donating groups in *ortho* or *para* position to the azo moiety can dramatically red-shift the photo-switching wavelength. A large number of azobenzene derivatives are known in which enhanced electron-donating nature of ring substituents increases both the wavelength of absorption of the *trans* isomer and the rate of thermal back-isomerization from *cis* to *trans*. On the basis of the above-mentioned results in this work the preliminary results of the synthesis of a visible light-responsive azobenzene monomer was carried out, in a view of preparing polymer capsules for the visible light-induced release [11]

6.2. Experimental

6.2.1. Materials

3-methoxy-4-nitrobenzoic acid were purchased from Alfa Aesar and NaOH and D-glucose were purchased from Sigma-aldrich. All reagents were used without further purification.

6.2.2. Synthesis of 4,4'-bis(carboxy)-2,2'-dimethoxyazobenzene

4,4'-bis(carboxy)-2,2'-dimethoxyazobenzene was synthesized according to a modified procedure previously reported by Thylkowski et al. [11]. In a typical experiment, 3.55 g (18.00 mmol) of 3-methoxy-4-nitrobenzoic acid and 10 g (25 mmol) of NaOH were mixed in 60 ml of water and heated until the solid dissolved. Then, a hot aqueous glucose solution, containing 20 g of glucose in 30 ml water, was slowly added at 80°C. The mixture was left for 24h under a bubbling air flux. Then the solution was diluted with 200 mL milli-Q water and acidified with 25 ml acetic acid, thus yielding the ortho-substituted azobenzene-4,4'-dicarboxylic acid as a light pink precipitate. The latter was filtered, washed with 900 ml of distilled water and dried in oven at 80°C. (yield 26 %).

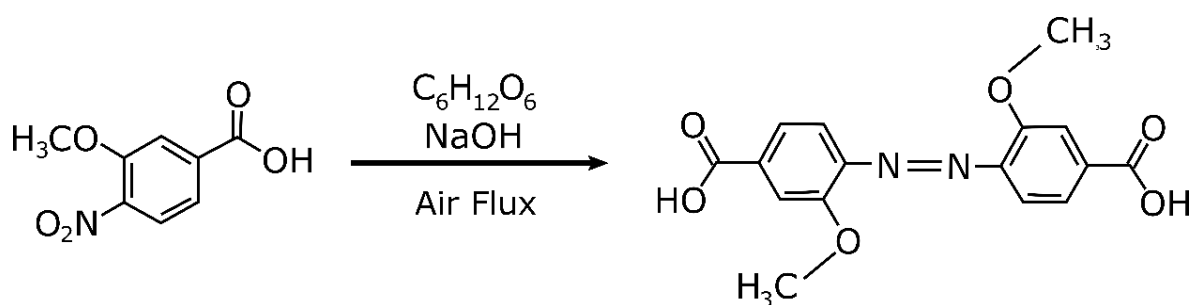


Figure 6.1. – Reaction scheme for the synthesis of 4,4'-bis(carboxy)-2,2'-dimethoxyazobenzene

6.2.3. Characterization of visible light-sensitive azobenzene monomer

In order to follow the occurrence of the *trans* to *cis* isomerization, NMR spectra were recorded in DMSO- d_6 by a Ultrashield TM 300 Bruker spectrometer before and after 30 min of visible light irradiation.

The light-responsive behavior of the prepared monomer was studied using a simple desk lamp with tunable colors. The optical signal output of white, red, green, yellow and blue light, was recorded by an Ocean Optics USB2000 Miniature Fiber Optic Spectrometer, in a dark room at room temperature $23.0 \pm 0.5^\circ\text{C}$.

The photo-isomerization of the modified azo was studied on a DMSO diluted solution via UV-vis spectrophotometry. The sample was placed in a 1 cm quartz cuvette and the changes in absorbance upon light irradiation was detected using a V-570 (Jasco Easton - USA) spectrophotometer (equipped with double beam system, single monochromator, and scanning wavelengths between 800 and 200 nm with a speed of 400 nm min^{-1}). The spectrophotometric data were collected before and after irradiation with white, blue, yellow and red light as well as natural sunlight and compared to identify the wavelength that triggers the photo-isomerization of the modified azo.

6.3. Results and Discussion

Figure 6.2. reports $^1\text{H-NMR}$ spectra of 4,4'-bis(carboxy)-2,2'-dimethoxyazobenzene before and after visible light irradiation. Before irradiation (blue line) the spectral pattern includes four distinct resonance bands. The first is a singlet at 4.02 ppm, due to the methoxy protons on the phenyl ring. A doublet at 7.50 ppm stems from the proton adjacent to the azo group, while the multiplet at 7.62 is due to the proton adjacent to the carboxyl and *para* to the methoxy. Finally, the singlet at 7.74 ppm is due to the hydrogen proton adjacent to the methoxy group. From the observed pattern, it is deduced that before irradiation, the azo compound exists almost exclusively in the *trans* conformation,

as the two symmetrical phenyl rings give rise to the same NMR signals. After irradiation, the proton NMR spectrum shows the appearance of three further resonances, at 3.72, 6.70 and 7.40 ppm, confirming the partial isomerization of the azobenzene in the *cis* conformation.

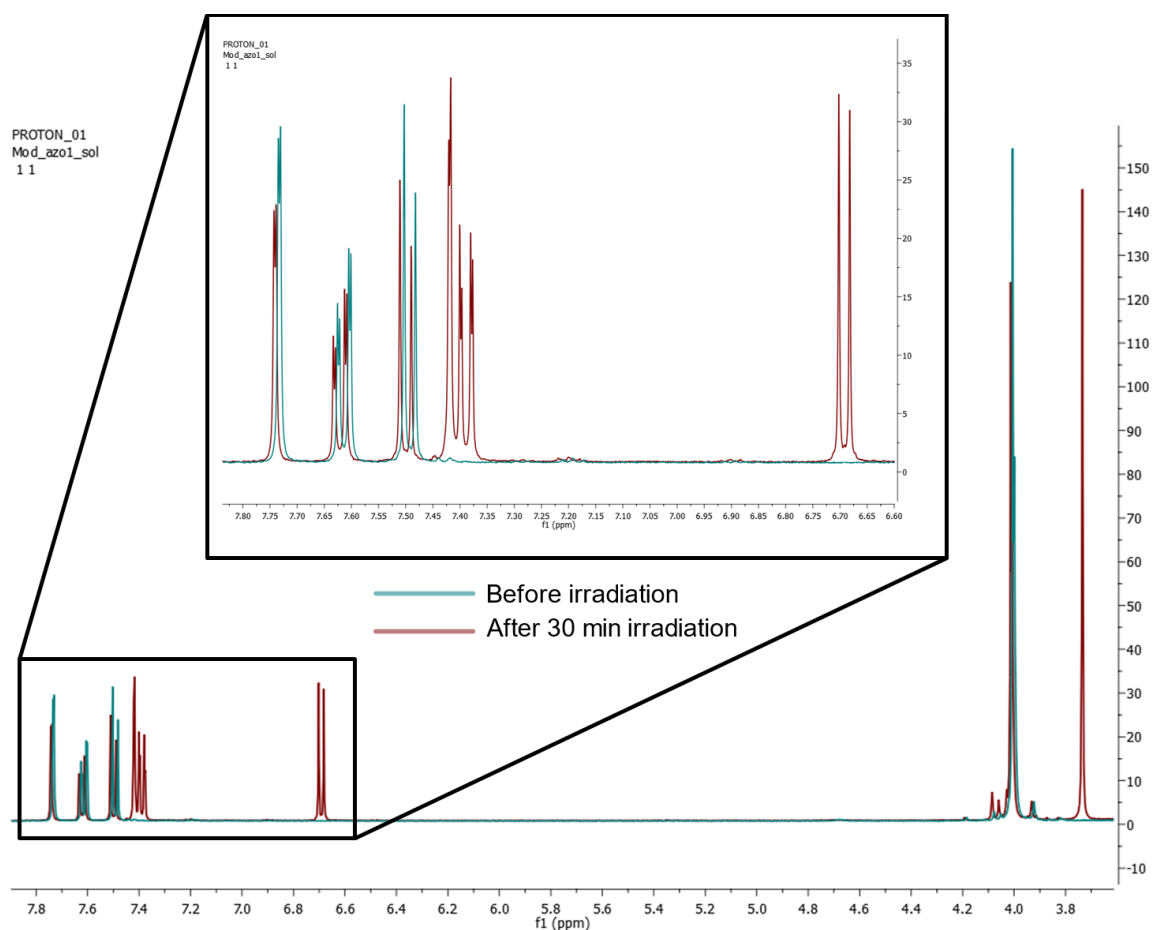


Figure 6.2. – NMR of 4,4'-bis(carboxy)-2,2'-dimethoxyazobenzene, before (blue line) and after 30 min of white-light irradiation (red line).

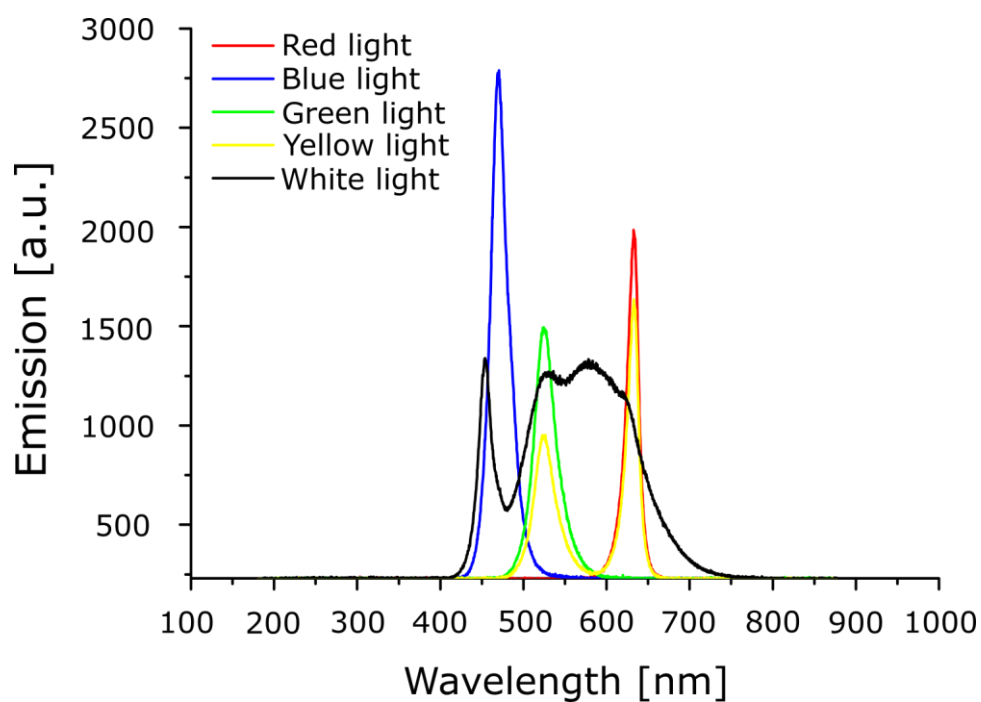


Figure 6.3. – Emission spectra of different optical signal output of the commercial tunable lamp.

The emission spectra relative to the different optical radiations of the tunable lamp used to irradiate the azo compound are reported in Figure 6.3. It can be seen that blue, green and red light emission are achieved using single LED sources, with maxima centered at about 480, 530, 640 nm, respectively. On the other hand, yellow light is obtained as a combination of green and red light, while white light is a combination of the three main light sources.

In order to characterize the wavelength sensitivity of the azo compound, a DMSO diluted solution of *ortho*-modified azobenzene was than irradiated with light at different wavelengths available on the desk lab. The results, reported in Figure 6.4., show that even after 30-min irradiation, red (B) and blue (C) light do not modify the spectra of the azobenzene, suggesting that the latter retained its conformation. On the other hand, azobenzene *trans-cis* photo-isomerization is triggered by white (D) and yellow light (E) as well as sunlight (F). The absorbance spectra show that

irradiation causes a decrease in the *trans* peak (around 400 nm) and an increase in the *cis* peak (below 300 nm) proving that the photo-isomerization is taking place.

In the case of sunlight-triggered isomerization (Fig.6.4.F), a reversed thermal *cis-trans* isomerization has been observed placing the testing tube containing the DMSO solution of the monomer in the dark in an oil bath at 80°C for 10 min. This allowed to the monomer to recover its *trans* conformation.

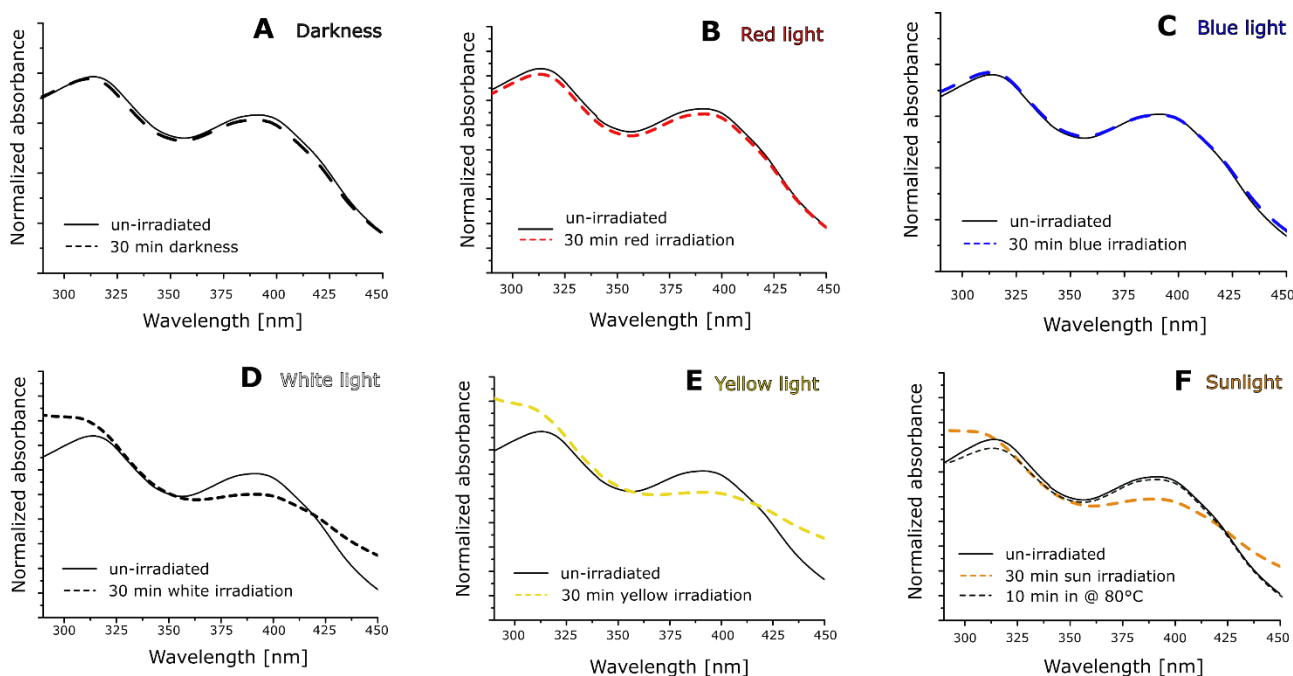


Figure 6.4. – Normalized absorbance of the azobenzene before and after 30 min under: (A) dark; (B) red light irradiation; (C) blue light irradiation; (D) white light irradiation; (E) yellow light irradiation; (F) sunlight irradiation.

6.4. Conclusions and future applications

This preliminary study represents promising foundations for future applications of photo-responsive polymer capsules. The applications involving UV or IR capsules require expensive and poorly available light sources, therefore visible light in the wavelength range of 500-600 nm represent a valid alternative since it is readily provided by natural sunlight or any white desk lamp. These

capsules could be employed in encapsulation of a wide variety of active agents, such as pesticides for crop protection, fragrances for household products and flavors for food engineering, as well as active molecules for cosmetics and medicine.

6.5. References

1. Zhao, Y. and Ikeda, T. eds., 2009. Smart light-responsive materials: azobenzene-containing polymers and liquid crystals. John Wiley & Sons.
2. Priimagi, A. and Shevchenko, A., 2014. Azopolymer-based micro-and nanopatterning for photonic applications. *Journal of Polymer Science Part B: Polymer Physics*, 52(3), pp.163-182.
3. Nakanishi, T., 2011. Supramolecular soft matter: applications in materials and organic electronics. John Wiley & Sons.
4. Bang, C.U., Shishido, A. and Ikeda, T., 2007. Azobenzene Liquid-Crystalline Polymer for Optical Switching of Grating Waveguide Couplers with a Flat Surface. *Macromolecular rapid communications*, 28(9), pp.1040-1044.
5. R. H.Kramer, J. J.Chambers, D.Trauner, *Nat.Chem.Biol.* 2005, 1, 360–365
6. C. Boulègue, M. Lowenack, C. Renner, L. Moroder, *ChemBioChem* 2007, 8, 591–594.
7. Mancebo, S.E. and Wang, S.Q., 2014. Skin cancer: role of ultraviolet radiation in carcinogenesis. *Reviews on environmental health*, 29(3), pp.265-273.
8. Samanta, S., Beharry, A.A., Sadovski, O., McCormick, T.M., Babalhavaeji, A., Tropepe, V. and Woolley, G.A., 2013. Photoswitching azo compounds in vivo with red light. *Journal of the American Chemical Society*, 135(26), pp.9777-9784.
9. Dong, M., Babalhavaeji, A., Samanta, S., Beharry, A.A. and Woolley, G.A., 2015. Red-shifting azobenzene photoswitches for in vivo use. *Accounts of chemical research*, 48(10), pp.2662-2670.
10. Helmy, S., Leibfarth, F.A., Oh, S., Poelma, J.E., Hawker, C.J. and Read de Alaniz, J., 2014. Photoswitching using visible light: a new class of organic photochromic molecules. *Journal of the American Chemical Society*, 136(23), pp.8169-8172.
11. Tylkowski, B., Giamberini, M., Underiner, T., Prieto, S.F. and Smets, J., 2016, February. Photo-Triggered Microcapsules. In *Macromolecular Symposia* (Vol. 360, No. 1, pp. 192-198).



CHAPTER 7

General Conclusions

Considerable progress in the design and the synthesis of light-responsive polymer micro- and nanocapsules has been made in recent decades. Diversification of capsule preparation techniques and fine-tuning of materials chemical design provide a wide an almost infinite number of strategies to obtain customer-tailored products. In particular, research and development in nano-sized range is currently experiencing a burst development and is in constant need for new carriers to further impact frontier applications such as theranostics, nanomedicine and drug delivery.

We have reported a straightforward route for the preparation of solid shell nanocapsules with controlled UV-triggered release. A miniemulsion interfacial polymerization technique has been employed to synthesize *in-situ* a polyamide shell containing azobenzene segments in the main chain. The *trans* to *cis* photo-isomerization of azobenzene, occurring upon UV-light irradiation (360 nm), leads to major rearrangements in the capsules shell inducing the release of encapsulated materials. The feasibility and reliability of the release mechanism has been assessed by monitoring the UV-induced release of a fluorescent probe molecule, Coumarin 6, dispersed in the toluene core. Collectively, these findings outline the efficacy of the proposed approach in view of engineering the delivery of active agents according to specific applications.

Moreover, encapsulation and light-triggered release of basil and thyme essential oils was also studied in detail proving the versatility and reliability of the miniemulsion interfacial polycondensation in the preparation of stimuli responsive capsules. The essential oils have the dual role of active core material and solvent for the azo-monomer in the miniemulsion reaction, thus implying the elimination of potentially toxic organic solvents from the procedure. The photo-induced release mechanism in azo-polymers makes these capsules promising candidate for a wide variety of applications, such as food-packaging, agriculture, household and cosmetics. Moreover, the study regarding Coumarin-6 encapsulation and release, as a model drug, strongly hints at future application in biological environments.

Thyme and basil essential oils are renowned antimicrobial agents, used in many food packaging applications. Herein, for the first time to our knowledge, the encapsulation of these essential oils in a packaging material was reported. The coating process of PE and PLA with EO-loaded capsules was efficiently assessed. Both release experiments and antimicrobial tests confirmed the feasibility of the active packaging system.

UV-light is poorly available and pose threats to human health as well. Therefore, a red-shift of the azobenzene *trans-cis* photo-isomerization wavelength towards visible range in the radiation spectrum would be preferable. Visible light in the wavelength range of 500-600 nm represent a valid alternative since it is readily provided by natural sunlight or any white desk lamp. We report on the synthesis and characterization of a modified azobenzene, where photo-isomerization is triggered by visible-light. This monomer could be employed in encapsulation of a wide variety of active agents, such as pesticides for crop protection, fragrances for household products and flavors for food engineering, as well as active molecules for cosmetics and medicine.

Appendix A

List of Figures and Tables

Figures.

Figure 1.1. - Schematic representation of different types of colloidal nanoparticles.

Figure 1.2. - Schematization of the application of micro and nanocapsules.

Figure 1.3. - Schematization of a two-sheet copying paper.

Figure 1.4. - Schematization of microcapsules-based e-ink.

Figure 1.5. - Internal structure of a microcapsules based self-healing material.

Figure 1.6. - Release mechanisms of core-shell capsules.

Figure 2.1. - Photo-isomerization mechanism of photochromic molecules: (a) azobenzene; (b) stilbene; and (c) spiropyrane.

Figure 2.2. - Schematization of the C6 release from photo-responsive polymer nanocapsules as depicted by Marturano et al. [34]. Reproduced with permission from Elsevier.

Figure 2.3. - Formation of polyelectrolyte based layer-by-layer nanocapsule as schematized by Yoon et al. [50]. Reprinted with permission from [50].

Figure 2.4. - Schematic illustration of (PDADMAC/PAZO) microcapsule disruption induced by UV irradiation [55]: (a) LbL assembly of the polyelectrolytes on the capsule shell surface; (b) formation of J aggregates under UV irradiation; (c,d) extended aggregates act as stress raisers, triggering capsule breakage. Reprinted with permission from [55]. Copyright 2014 Royal Society of Chemistry.

Figure 2.5. – Photolysis-induced small molecule encapsulation in: (a) Nafion/DAR; and (b) DAR single component multilayer capsules as depicted in [57]. Reprinted with permission from [57]. Copyright 2013 American Chemical Society.

Figure 2.6. – Capsules structure and release mechanism of α -CD/Azo LbL microcapsules as depicted by Xiao et al. [62]. Reprinted with permission from [62]. Copyright 2011 American Chemical Society.

Figure 2.7. – On/off photo-responsive switch in the LbL microcapsules designed by Lin et al. [63]. Reprinted with permission from [63]. Copyright 2014 Royal Society of Chemistry.

Figure 2.8. – Schematic illustration of the various colloidal systems investigated by Angelatos et al. [76]. Reprinted with permission from [76]. Copyright 2005 American Chemical Society.

Figure 2.9. – Schematic illustration of the self-assembly of block ionomer complex vesicles as depicted by Wang et al. [86]. Reprinted with permission from [86]. Copyright 2009 American Chemical Society.

Figure 2.10. – Schematization of light-triggered release mechanisms in liposomes by inclusion of: (A) photo-polymerizable components; (B) photodegradable components; or (C) photo-isomerizable azobenzene moieties. Reprinted with permission from [92]. Copyright 2012 Ivyspring International Publisher.

Figure 2.11. – Singlet oxygen-mediated photo-oxidation of plasmalogen vinyl ether linkage.

Figure 3.1. – Polycondensation reaction leading to the formation of capsule shell, and structure of the obtained nanocapsules.

Figure 3.2. – Change of droplet diameters over time of oil-in-water emulsions of M18-88 and TX100 (a) without and (b) with CAB as co-surfactant.

Figure 3.3. – Size distribution of the nanocapsules as measured by DLS.

Figure 3.4. – SEM micrographs of NT01 (a), NT05 (b), NM5 (c) and NM1 (d) capsules, respectively.

Figure 3.5. – TEM images of (a) NT05 and (b) NM1 nanocapsules.

Figure 3.6. – TEM image of the micellar dispersion obtained after polymerizing the emulsion ET1, containing 1.0 wt % TX100.

Figure 3.7. – UV-Vis absorption spectra of (a) NM1 and (b) NT05 capsules measured at different times of UV irradiation at 360 nm.

Figure 3.8. – Nanocapsule average diameter changes (empty symbols) and coumarin 6 release kinetics (full symbols) upon UV exposure for (a) NM1 and (b) NT05. Values for unirradiated samples are reported as a control. Dashed lines represent fitting curves according to Boltzmann equation.

Figure 4.1. – Classification of NOs based on their chemical composition.

Figure 4.2. – Schematic representation of the interfacial polycondensation reaction in miniemulsion.

Figure 4.3. – SEM micrographs of (a) NCB and (b) NCT, TEM micrographs of (c) NCB and (d) NCT. (e) Scattering intensity vs. particle diameter (nm) of both nanocapsules samples, and (f) comparison of DLS and SEM analysis data.

Figure 4.4. – Release kinetics of encapsulated EOs from NCB and NCT samples under (a) continuous UV irradiation and (b) pulsed UV irradiation (2 cycles of 15 min each).

Figure 4.5. – Release of fluorescent probe molecule C6 from NCT sample after continuous (blue triangle) and 15 min (red circle) UV light irradiation.

Figure 4.6. – Trypan blue exclusion histograms reporting the variations in cell proliferation as a dependence of NCs concentration.

Figure 4.7. – Internalization and accumulation of NCs within NRK cells

Figure 5.1 – Methods for the release of antimicrobial agents in food packaging technologies.

Figure 5.2. – Chemical composition of basil and thyme essential oils.

Figure 5.3. – (top) Contact angle micrographs performed on untreated and plasma and corona-treated PE (A) and PLA (B). (bottom) surface energy values (SE) calculated from contact angle measurements (CA) using water or diiodomethane as reference liquids.

Figure 5.4. – Optical images and SEM micrographs of the surface of a pure PLA film (a, d), upon dip-coating (b, e) and after spraying (c, f) with an aqueous nanocapsules suspension.

Figure 5.5. – SEM micrographs of treated PE and PLA films coated with NCT and NCB.

Figure 5.6 – Evaluation of the thymol release via GC for ■ un-irradiated and ■ irradiated NCT samples.

Figure 5.7. – Antimicrobial activity of the thyme (A) and basil (B) essential oils.

Figure 5.8. – Antimicrobial activity tests on PE film coated with NCT capsules.

Figure 5.9 – Schematization of a possible setup for the AM active packaging based on photo-responsive polymer nanocapsules.

Figure 6.1. – Reaction scheme for the synthesis of 4,4'-bis(carboxy)-2,2'-dimethoxyazobenzene.

Figure 6.2. – NMR of 4,4'-bis(carboxy)-2,2'-dimethoxyazobenzene, before (blue line) and after 30 min of white-light irradiation (red line).

Figure 6.3. – Emission spectra of different optical signal output of the commercial tunable lamp.

Figure 6.4. – Normalized absorbance of the azobenzene before and after 30 min under: (A) dark; (B) red light irradiation; (C) blue light irradiation; (D) white light irradiation; (E) yellow light irradiation; (F) sunlight irradiation.

Tables

Table 2.1. – Characterization techniques of photo-responsive capsules.

Table 3.1. – Droplet diameter and specific surface area per surfactant molecule of oil-in-water emulsions containing CAB, freshly prepared and after 40 minutes. The diameters of the correspondingly obtained nanocapsules are also reported. The reported size values were obtained through DLS measurements.

Table 3.2. – Fitting parameters to Boltzman equation for the release curves in Fig. 8.

Table 4.1. – NOs behavior as CAB solvents and their reactivity toward CAB and DAO monomers.

Appendix B

List of Publications

Directly related with the thesis

Photo-triggered release in polyamide nanosized capsules, *AIP Conference Proceedings* 2014, 234. V. Marturano, V. Ambrogi, P. Cerruti, M. Giamberini, B. Tylkowski.

Photo-responsive polymer nanocapsules, *Polymer*. 2015 70, p 222. V. Marturano, P. Cerruti, C. Carfagna, M. Giamberini, B. Tylkowski, V. Ambrogi.

Light-responsive polymer microcapsules as delivery systems for natural active agents, *AIP Conference Proceedings*. 2016, 1736. V. Bizzarro, C. Cosimo, P. Cerruti, V. Marturano, V. Ambrogi.

Light-Responsive Polymer Micro-and Nano-Capsules. *Polymers*. 2016 9(8). V. Marturano, P. Cerruti, M. Giamberini, B. Tylkowski, V. Ambrogi.

Other publications:

Recent advances in nanoparticle-mediated delivery of anti-inflammatory natural molecules. *International Journal of Molecular Science*. 2017. 18(4), p.709. R. Conte, V. Marturano, G. Peluso, A. Calarco, P. Cerruti.

Power of light – functional complexes based on azobenzene molecules. Submitted to *Coordination Chemistry Reviews* (Under review). B. Tylkowskil, A. Trojanowska, V. Marturano, M. Nowak, L. Marciniak, M. Giamberini, V. Ambrogi, P. Cerruti.

Appendix C

Congresses and Contributions

Congresses

"Synthesis of photo-responsive polyamide nanocapsules through miniemulsion polymerization".
Poster. "EPF 2013". Pisa, Italia. 21-26 giugno 2013.

"Photo-triggered release in Polyamide Nanosized Capsules". Oral presentation "TOP conference 2014". Ischia, Italia 22-26 giugno 2014.

"Activated Food Packaging Systems: Microcapsule coatings with anti-microbial photo-triggered release to extend the shelf life of perishable food". Oral presentation. "Forum Italiano per l'Ambient Assisted Living". Lecco, Italia, 19-22 maggio 2015.

"UV-induced release of antimicrobial oils from polymeric nanocapsules". Oral presentation. "EPF 2015". Dresda, Germania, 21-26 giugno 2015.

"Photo-triggered release of anti-microbial agents from microcapsule coatings for food packaging applications". Oral presentation. "Shelf life International Meeting". Monza, Italia, 21-23 ottobre 2015.

"Agri-food industry wastes as additives for polymer stabilization". Oral presentation. "Solid Urban Waste Management IUPAC 2016". Roma, Italia, 6-8 aprile 2016.

“*Agri-food industry wastes as additives for polymer stabilization*”. Oral presentation. “Macrogiovani 2016”. Catania, Italia, 12-13 maggio 2016.

“*Light-Responsive Polymer Microcapsules as Delivery Systems for Natural Active Agents*”. Oral presentation “TOP conference 2016”. Ischia, Italia, 19-23 giugno 2016.

Chapters in Books

Additives in Polymers V. Ambrogi, C. Carfagna, P. Cerruti and V. Marturano. In “*Modification of Polymer Properties*”, edited by C. F. Jasso-Gastinel and J. M. Kenny. William Andrew Publishing, 2017, Pages 87-108. ISBN: 978-0-323-44353-1

Additives for Polymers P. Cerruti, V. Marturano, V. Ambrogi. In “*Polymer Engineering*”, edited by B. Tylkowski, K. Wieszczycka, G. Palumbo, R. Jastrzab. ISBN: 978-3-11-046974-5. (Under revision)

Modeling of Azobenzene-based compounds. V. Marturano, V. Ambrogi, N. A. G. Bandeira, B. Tylkowski, M. Giamberini, P. Cerruti. In “*Chemical Synergies*”, edited by N. A. G. Bandeira, B. Tylkowski. ISBN: 978-3-11-048206-5. (Under revision)

